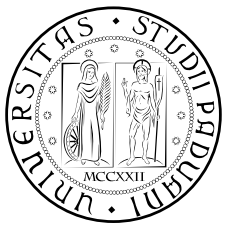

UNIVERSITÀ DEGLI STUDI DI PADOVA

Dipartimento di Tecnica e Gestione dei Sistemi Industriali

SCUOLA DI DOTTORATO IN INGEGNERIA MECCATRONICA E DELL'INNOVAZIONE DEL PRODOTTO
CICLO XXVII

STUDY OF THE INTERACTION BETWEEN HUMAN MUSCULOSKELETAL SYSTEM AND ROBOTIC ASSISTIVE DEVICES

PhD Advisor: Monica Reggiani

PhD Candidate: Michele Vivian
Matricola: 1039958

This research has been partially supported by
Fondazioni Studi Iniversitari di Vicenza.

ABSTRACT

In the latest years, robotic technologies have been increasingly introduced in rehabilitation with the main purpose of reducing the costs and speeding up the recovery process of patients. However, most of the commercial devices impose a pre-programmed trajectory to the limbs of the patients, who therefore behave in a passive way. Another current major limitation is the inability to accurately evaluate the dynamics of the interaction between the patient and the robotic device. This interaction plays a central role in the mutual modulation of human and robot system behavior with respect of their standalone behavior. In particular, the prediction of the interaction can provide useful information to better design the exoskeleton as well as the rehabilitation treatment.

This thesis presents my proposed solution for the development of a simulator able to dynamically simulate at the same time the actuated robot device, the human body, and their emerging physical interaction during the movement cooperation. The main idea behind this solution is to decompose the main system in different levels. I called the proposed solution *Multi-Level modeling approach*, which is the main topic of this thesis.

I proposed the following decomposition: Human, Robot, and Boundary Level. The levels are integrated into a whole system in which each of them addresses specific challenges. The Human Level represents the subject who is wearing, for example, an exoskeleton for the lower limbs. To reach a symbiotic collaboration between the subject and the exoskeleton, the proposed approach has to include the subject's intentions and efforts. Moreover, user's internal transformations provide important information about the internal dynamic parameters modulation due to the external device. The Robot Level consists of the wearable robot system which supports the movements. Our proposed approach includes models of both device mechanics and control strategies. This allows to test different control strategies and find the one that better fits each specific patient's needs and characteristics. The last level is the Boundary Level, which has the main objective to model the human-robot mechanical power transfer, including also the non-idealities (such as dissipative forces), in order to accurately estimate interactions.

Challenges emerged during the development of the simulator system were faced, investigating different solutions, and selecting and validating the most promising one. First, I selected a common software platform, able to simultaneously reproduce the dynamic behavior of the three levels. The common software platform allows to build a quite

flexible system where different solution could be evaluated simply modifying model parameters. Among different available software, OpenSim was selected because it is well known and used for the dynamic study of human movement. Although OpenSim was well tested in biomechanics, it required a further evaluation as simulator for Robot and Boudary Levels. Performed tests and their motivations are reported in this work.

Human internal dynamics parameters are modulated by the influence of the external device. I proposed to monitor this variation, taking into consideration the neural drive sent to the muscles. This can be done by measuring the muscles' electromyographic (EMG) signals, which are the electrical potential generated by muscle cells when they are activated, prior to muscle contraction. These signals can be used as input for a physiologically accurate human musculoskeletal model, to calculate the subject contribution to the movement. As the relation between EMGs and the generated muscle forces and joint moments is not linear, the neuromusculoskeletal model is indeed needed to replicate step-by-step all the internal transformations which occur from the excitation of the muscle to the joint movement.

Estimation of the emerging interaction, during the human-robot cooperation, can be performed through an interaction model which is basically a set of contact models. Due to the specific rehabilitation purpose of our work, this contact model needs special attention. I introduced and validated a procedure to calibrate the contact models to improve the accuracy of the estimated interaction forces.

One of the problems of using EMG signals is that, in order to acquire them in a non-invasive way, surface electrodes must be used; however, this means that the collected data quality is quite susceptible to the electrodes placements and decay, and to electric and magnetic interferences. In many contexts, such as home rehabilitation, this could be a limitation. An alternative solution to avoid the direct EMG measurement is presented in this work. The idea is that for some repetitive tasks, which are most interesting for rehabilitation, it is possible to substitute the direct data collection with a subject specific model of EMGs.

The objective of this work is to provide an effective approach to estimate the emerging interaction during the human-robot movement cooperation. The Multi-Level Modeling approach, presented in this thesis, decomposes this complex problem allowing to find all the required components to realize a whole system able to reach this objective.

SOMMARIO

Negli ultimi anni, la riabilitazione sfrutta sempre di più dispositivi robotici al fine di ridurre i costi e velocizzare il processo di recupero dei pazienti. Finora però, la maggior parte dei dispositivi disponibili sul mercato porta il soggetto a comportarsi in modo passivo, imponendo traiettorie preprogrammate ai pazienti. Un'ulteriore limitazione delle attuali tecnologie è l'incapacità di valutare accuratamente la dinamica dell'interazione tra il paziente e il dispositivo robotico. Tale interazione gioca un ruolo centrale nella mutua modulazione del comportamento dell'essere umano e del sistema robotico, che risulerà diverso rispetto a quello indipendente. In particolare, la predizione di questa interazione può fornire informazioni utili per migliorare sia il design dell'esoscheletro che il processo di riabilitazione.

Questa tesi presenta la soluzione che propongo per lo sviluppo di un simulatore in grado di simulare dinamicamente il movimento che risulta dalla cooperazione dell'essere umano e del dispositivo robotico. L'idea principale su cui si basa questa soluzione è di decomporre il sistema in diversi livelli. La soluzione proposta è stata chiamata *Multi-Level modeling approach* ed è l'argomento principale di questa tesi.

La decomposizione proposta si articola in tre livelli: Human, Robot, e Boundary. I livelli sono poi integrati in un unico sistema in cui ogni livello si occupa di rispondere a specifici problemi. Il livello Human rappresenta il soggetto che sta indossando il sistema robotico, ad esempio un esoscheletro per gli arti inferiori. Per raggiungere una collaborazione simbiotica tra il soggetto e l'esoscheletro, l'approccio deve includere le intenzioni del soggetto e monitorare i suoi sforzi per raggiungere il movimento desiderato. Conoscere le trasformazioni interne all'utente possono fornire importanti informazioni sulla modulazione dei parametri dinamici interni dovuti al dispositivo esterno. Il livello Robot si concentra sul sistema robotico indossabile che supporta i movimenti. L'approccio si propone di modellare sia i meccanismi del dispositivo che le strategie di controllo. Questo permette di testare diverse strategie di controllo per trovare quella che meglio si adatta agli specifici bisogni del paziente e alle sue caratteristiche. L'ultimo livello è il Boundary, che ha come obiettivo principale quello di modellare il meccanismo di trasferimento di energia meccanica, includendo anche le non idealità (come le forze dissipative), per riuscire a stimare accuratamente l'interazioni risultante.

Diverse sfide sono emerse durante lo sviluppo del sistema complessivo, che sono state affrontate investigando diverse soluzioni, selezionando e validando la più promettente.

Il primo problema è stato individuare una piattaforma software comune ai tre livelli in grado di riprodurre simultaneamente il loro comportamento dinamico. Tra i diversi software disponibili ho selezionato OpenSim perché molto conosciuto e già usato per lo studio della dinamica del movimento umano. Anche se OpenSim è già testato nell'ambito biomeccanico, era necessaria un'ulteriore valutazione come simulatore per i livelli Robot e Boundary. In questo lavoro sono stati presentati quali analisi sono state compiute e i risultati ottenuti.

I parametri dinamici interni dell'essere umano sono modulati ed influenzati dei dispositivi esterni. Ho quindi proposto di monitorare queste variazioni, prendendo in considerazione il comando neurale che viene inviato ai muscoli. Questo può essere eseguito misurando l'attività elettromiografica dei muscoli, cioè il potenziale elettrico generato dal muscolo quando viene attivato, prima della contrazione muscolare. Questi segnali possono essere usati come ingresso per un modello dell'apparato muscoloscheletrico umano al fine di calcolare il contributo del soggetto al movimento. L'uso di questo modello si rende necessario a causa delle relazioni non lineari tra gli EMG e le forze muscolari generate e quindi i momenti ai giunti.

La stima delle forze di interazione che emergono durante la cooperazione uomo-robot può essere effettuata attraverso un modello di interazione che è fondamentalmente un insieme di modelli di contatto. A causa delle specifiche caratteristiche del nostro lavoro dedicato alla riabilitazione, questo modello di contatto richiede maggiori attenzioni. Per questo ho introdotto e validato una procedura per calibrare i modelli di contatto e migliorare l'accuratezza delle forze di interazione stimate.

Uno dei problemi nell'usare i segnali EMG è che è necessario utilizzare degli elettrodi di superficie per acquisirli in modo non invasivo; questo però significa che la qualità dei dati raccolti è molto sensibile alla disposizione degli elettrodi e al loro decadimento, oltre che alle interferenze magnetiche e elettriche. In molti contesti, come la riabilitazione a casa, questo può costituire una forte limitazione. Una soluzione alternativa per evitare la misura diretta degli EMG è presentata in questo lavoro. L'idea è che per azioni ripetitive, che sono spesso di grande interesse nella riabilitazione, sia possibile sostituire la raccolta dati diretta con un modello degli EMG calibrato sul soggetto.

L'obiettivo di questo lavoro è stato di proporre un approccio efficace per la stima delle iterazioni che emergono durante il movimento cooperativo uomo-robot. L'approccio Multi-Level Modeling, che è stato presentato in questa tesi, decompone questo problema complesso permettendo di sviluppare tutti i componenti necessari alla realizzazione di un sistema completo che sia in grado di raggiungere l'obiettivo finale.

CONTENTS

1 INTRODUCTION

Gait recovery treatment requires a great effort during the rehabilitation therapy. In many cases, such as post spinal cord injuries or post stroke rehabilitation, at least three therapists has to be involved in the process to manually assist the patient's legs and torso to retrain his walking [23]. This results in an increasing demand of qualified persons and of treatment cost. Moreover, considering the increased life expectancy of people, a larger demand of high quality care for gait disorders is expected. All these factors lead the research activity in rehabilitation to propose new solutions which aim to more affordable, and available to more patients and for a longer time period.

In this context, robotic assistive devices able to support the human movement, became an important focus in the robotics research field. The main objectives of the robotic rehabilitation devices are to replace the physical training of therapists, providing support for repetitive and intensive movement at lower costs, and to evaluate the actual patient's motor recovery. Biomechatronics is the application of mechatronics (study, analysis, design and implementation of hybrid systems comprising mechanical, electrical and control components or subsystems) to biological motor systems [14, 79, 70]. Biomechatronic plays a central role in the design of robots which can actually improve human performance and, more specifically the rehabilitation treatment effectiveness.

Among the rehabilitation robotic devices, wearable robots involve a wide range of devices that provide compensation or therapy for the disabled users. In the last decade, several robots for the lower-limbs rehabilitation were developed to restore the functionality of the affected legs.

Passive robotic assistive devices are the less complex and cheaper example of wearable robots. Humans, such as other animals, use their body elastic elements (ligaments and tendons), to minimize impact losses and to reuse a quantity of energy as propulsion during the final striking in walking, running, and jumping. This biological strategy has inspired researchers to design and develop wearable devices without actuation [30, 39]. However, passive robotic rehabilitation devices cannot supply energy to the affected limbs, hence their effectiveness in treatment is quite limited compared to active devices.

Despite a part of robotic rehabilitation still investigates and develops passive devices, nowadays active devices represent the big topic of the research field. According to the rehabilitation principle, these systems can be classified as follows [29]. The first group are treadmill gait

(a) (b)

Figure 1: Examples of passive wearable assistive device (a) The Knee Ankle Foot Orthosis (picture courtesy of Artificial Limb), (b) Ankle Foot Orthotics (picture courtesy of The Leg and Foot Clinic).

trainers, which are usually focused in treadmill training to improve functional mobility [106, 19]. These systems [19, 38, 101] are based on exoskeleton type robots in combination with a treadmill, following a rehabilitation technique known as partial body-weight support treadmill training (Fig. 2a).

Other rehabilitation machines are design with programmable foot plates [50]. Patient's feet are positioned on separate robotic foot plates, which are controlled to reproduce different gait patterns (Fig. 2b).

Overground gait trainer systems [75, 10, 57] are robotic devices that support the patient's overground motion walking (Fig. 2c). They actually allow the patients to move under their own control by a pre-programmed set of movement patterns.

The last group of rehabilitation devices is developed specifically to restore or enforce ankle or knee motion and they can be subdivided into two group: stationary systems and active foot exoskeletons. The objective of the stationary gait trainers is to achieve an efficient muscles strengthening and endurance performance, as well as joints mobility and coordination (Fig.2d). These systems [88, 41] are mainly focused on guided movements to optimize the therapeutic and functional effectiveness. Stationary gait trainers are designed to train knee or ankle motion without walking; so, being always in the same place, the target limb is exercised [11, 84]. They are a subset of the stationary gait trainers. On the contrary, active foot exoskeletons are actuated devices that the user can wear during an overground walking [83, 35]. They are an evolution of passive lower limbs orthoses, with additional capabilities to improve the gait recovery (Fig. 2e).

Nowadays, the great challenge in the rehabilitation robotic research field is to include the subject in the control loop. In other words, the main objective is the development of robotic assistive devices able to

(a) (b) (c)

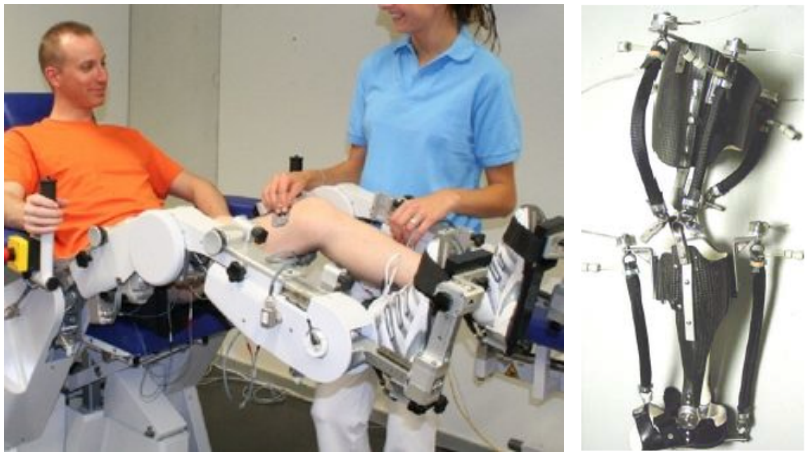

(d) (e)

Figure 2: Robotic Assistive Devices for lower limbs rehabilitation: (a) treadmill gait trainers (Lokomat picture courtesy of Hocoma); (b) footplate based gait trainers (The Gangtrainer pictur courtesy of Reha-Stim); (c) overground gait trainers (KineAssist picture courtesy of Kinea Design, LLC); (d) stationary gait and ankle trainers (The MotionMaker picture courtesy of Swortec SA), and (e) active foot orthoses (KAFO picture courtesy of Prof. Ferris, University of Michigan).

understand the subject intention and specific motor skills, adapting its behavior on them. Furthermore, the possibility of monitoring the subject internal dynamic parameters and their modulation due to the external device during the rehabilitation process would result in an optimization of the recovery process. Several research groups are developing a new generation of robotic assistive devices, that could solve this challenge using the neurological activities of the users. Biological signals collected from the user, such as electromyographic (EMG) signals, are used to control actively the robotic device [35, 36, 48]. Although these systems are quite promising, they are still prototypes.

An additional problem of including of the subject as an active component in the control of a wearable robot is the need of considering the emerging interactions during the human robot movement cooperation. Physical and cognitive interactions [70, 79] are to be known, aiming to build systems in which human and robot symbiotically participate to perform a task. Symbiotic interaction can be achieved by combining computation, sensing technology, and interaction design to realize deep perception, awareness, and understanding between humans and robots [55]. The study of these interactions plays a central role in the development of the next generation of active wearable devices. In particular, the possibility to predict these interactions could result in a better design of both the devices and the motor recovery treatment. Moreover, once the robotic assistive device is realized, the interactions prediction could be used to adjust the robotic system and the rehabilitation treatment on the subject-specific characheristic and motor skills. Finally, the interactions estimation could be integrated in the control chain in order to achieve a symbiosis during the movement cooperation. The possibility to develop a system able to estimate the emerging interactions between a subject and a wearable robot during the movement cooperation is the main objective of this work.

In this thesis, we propose a Multi-Level Modelling Approach to predict the emerging interactions between the subject and the robotic assistive. The main objective is to develop the componenets required to build a system able to accurately simulate the subject-specific neuromusculoskeletal function as well as the mechanical behavior of the robotic device, and the interactions emerging for the human machine movement cooperation.

1.1 PLAN OF THESIS

The thesis is organized as follows:

IN CHAPTER 2 , a description of the main idea of the Multi-Level Modeling approach is provided. The proposed approach aims to simulate the emerging interaction between the human robot cooperating movement. The three main tools, used in the devel-

opment of the proposed framework, are shortly introduced, and following chapters will provide a detailed explanation.

IN CHAPTER 3 , we presented the software used as common platform for the dynamic simulation of the two main frame, human and robotic. Since the selected software was not assessed as mechanical simulator, this chapter also reports its evaluation as multibody system simulator.

IN CHAPTER 4 , a neurumusculoskeletal model, the second tool required for our proposed approach, is described in details.

IN CHAPTER 5 we introduce the last tool for the Multi-Level Modeling framework: the contact model. This tool will be used to predict the emerging interaction between human and robotic assistive devices. The chapter present results on a simper setuo including an humanoid robot.

IN CHAPTER 6 a complementary research is presented: aiming at simplifying the required setup during a robotic rehabilitation session at home.

IN CHAPTER 7 reports the integration of the different tools in our Multi-Level Modeling framework. The development of the system required to overcome some challenges which were introduced, with possible solutions in the previous chapters. A case study is used as an example to show the required procedure.

2 MULTI-LEVEL MODELING APPROACH

2.1 THE PROBLEM

Wearable robots are a wide category of devices which support the human movement improving the performance both of healthy and disabled users. Usually, these are mechatronic devices have a correspondence between their segments and joints and those of the human. Nowadays, despite the fact that the use of robotic exoskeletons in rehabilitation is quite accepted, there are still few commercialized products and still not used in daily life. The main reason is a missing effective strategies for interfacing the wearable robot to its user and this drives a lot of efforts from the research community. For example, currently there are several active projects founded by the European Community on this topic [5, 7, 22, 33, 81, 92]

A solution to this problem could come from the buomechatronics, i.e. the application of mechatronics to biological motor systems [14, 70, 79]. The main concept is that the human becomes a part of the system. In that way, during the rehabilitation treatment, a quantitative evaluation of the recovery process current state of the patient can be performed, allowing the optimization of the training. Moreover, assistive robotic device can provide the mechanical power to perform a movement basing its contribution on the subject intention and motor skills.

In this context, one of the most important aspect is the emerging interaction between human and robot during the movement cooperation [79]. Two different interactions can be defined [70]: cognitive interaction and physical interaction. The former can be defined as the possibility for the user to control the device, while it provides some kind of feedback. The cognitive interaction is critical to realize systems in which human and robot work in a symbiotic way, actually realizing a symbiotic movement cooperation. So far the physical interaction has mainly concerned the user safety. Nevertheless, integrating the prediction of the physical interaction between robot and the user neuromuscularskeletal system in the control loop could led to the development of a more effective strategy to support the movement especially during a rehabilitation treatment.

These emerging dynamics physical interactions play a central role in the mutual modulation of both human and robot system behavior with respect of their standalone behaviors. In particular, the prediction of these interactions can provide useful information to better design the exoskeleton as well as the rehabilitation treatment. Indeed, the simulation of robotic systems behavior, before actual development,

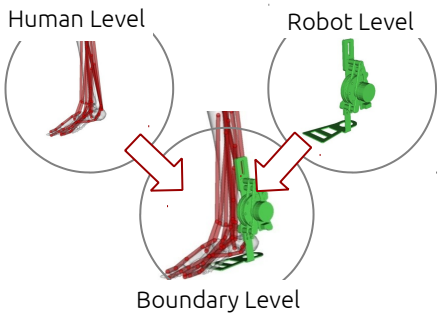

Figure 3: Multi-Level Model approach schema with the three sub-levels.

represents a safer, faster, and cheapest way to try alternative solutions [24]. This became particularly true for wearable robots which actively interact with the human body. Moreover, once the interactions prediction demonstrates a good accuracy and reliability in its results, it could be integrated in the control chain.

In the past, few works have presented some combined human-robot simulation [1, 16], but a systematic framework for the evaluation of different solutions and a parametric design of the mechanisms are still missisng. Other investigations were mainly concentrated in passive devices [2] or in devices in-built with the human body in which the physical interaction is mainly due to in-ground walking locomotion [45]. However, despite their limitations or different principal aims, these works demonstrated the relevance of this research topic as well as its complexity.

In this work our proposed solution aims to develop an approach to dynamically simulate at the same time the actuated robot device, the human body, and their emerging physical interaction during the movement cooperation. The main idea behind this solution is to decompose the main system in different levels. The separation allows to find a simpler solution, even easier to validate, underlining the specific required features. Then the levels will be integrated in a whole system to reach the main objective. We called the proposed solution Multi-Level Modeling Approach, and its development is the main topic of this thesis.

2.2 MULTI-LEVEL MODELING APPROACH

The main objective of our work is to develop an instrument which is actually able to simultaneously model the behavior of both the human neuromusculoskeletal system and the robotic assistive device. Only connecting these two separate systems in a single modeling tool can allow to understand how their interactions modify their standalone behavior. Our proposed solution is based on a Multi-Level Modeling

approach: the main problem is separated in different levels, each one is expected to be simpler to develop and validate. The first step is to define a consistent distribution of sub-levels (Fig.3), then levels will be integrated in an whole system in which each on them will cover specific challenges. We proposed the following decomposition:

- Humal Level
- Robot Level
- Boundary Level

The Human Level represents the subject wearing the robotic device, in Fig. 3 an exoskeleton for the lower limbs. The external manifestation of his own contribution to the movement is the joint moment. However, to reach a symbiotic collaboration between the subject and the exoskeleton, the proposed approach has to include the subject's intentions and efforts. In other word, the Human Level starts from the human neurological system ending, through all the human internal transformations, at joint moments production. Moreover, these internal transformations provides important information about the internal dynamic parameters modulation due to the external device. That is actually an essential feature since the possibility of monitoring and assessing the effectiveness of the robotic rehabilitation treatment is required to improve subject motor skills recovery.

The Robot Level includes the wearable robot system which supports the movements. Design and tuning of a wearable exoskeleton could benefit from a simulated environment in which different solutions can be tested to better fit the specific patient needs and characteristics. Thus, our propose approach needs that both the device mechanical and the control strategy are modelled in an accurate and reliable way.

The last level is the Boundary Level and, probably, whose objective is less intuitive than the previous two. The human-robot movement cooperation can be achieved only through a mechanical power transfer between them. The Boundary Level has the main objective to model this mechanical power transfer, including also the non-idealities (such as forces waste), to achieve an accurate and reliable estimation of the physical interaction. The definition and implementation of this level became the most characterizing point of our proposed work, and it play a central role in the integration of the three presented level in a single system able to dynamically simulate the human-robot movement cooperation.

Design and development of such complex a system required to solve some quite challenging problems: First, a simultaneous simulation of the dynamic behavior of Human, Robot, and Boundary Lever requires a common software platform. Indeed, using the same software could result in a more flexible solution in which different alternatives can be easily applied separately at each level assessing their effects on the whole system.

A common tool would simplify the assessment of the final system simulating the reaction of the subject in term of safety, comfort and treatment effectiveness. That means the human neurological activities must to be included in our system, allowing an in-deep monitoring of the human internal dynamic parameters modulation due to external devices. The same human monitoring can be included in the control loop, realizing a new generation of robot controllers actually based on the specific-subject characteristics, intentions, and motor skills.

Movement cooperation means human and device should be quite synchronous thus emerging interaction forces may be small in magnitude and quite instantaneous. The device control strategies must consider the amount of losses in the Boundary Level also in these particular situations. Therefore our proposed system needs to be able to reproduce also this particular situation in which a low precision in the modeling of the Boundary Level can result in an incorrect interpretation of the movement cooperation.

All these problem were faced, investigating different solutions, and selecting and validating the most promise one. The next section presents the proposed solutions, also explaining how they are integrated inside the Multi-Level Modeling Approach. A comprehensive analysis of each components will be reported in the following chapters of the thesis.

2.3 COMPONENTS

2.3.1 *OpenSim: Common Software Platform*

Our proposed approach aims to develop a tool able to estimate the complex dynamic interactions emerging during the human-robot movement cooperation. The possibility of simulating Human, Robotic and Boundary Level at the same time, inside the same software platform become essential. In particular, the common software platform has to be accurate and reliable, being quite flexible, and provide high level tools to easily modify one or more model parameters to evaluate different solutions. Therefore, the first challenge of this project was the selection and validation of a common software platform. Different available solutions were evaluated, such as ADAMS [90], PhysX [20], Gazebo [40], Simbody [89], and OpenSim [73]. Our final choice to develop our system was OpenSim [27] (Fig. 4). The first motivation is its software architecture. Indeed, it is based on Simbody, a powerful tool, entirely written in C/C++, to create and dynamically simulate multibody systems, supporting different contact model. In addition, OpenSim provides high level tools, built upon Simbody, to allow complex simulation of biomechanical model, including complicated actuators, as the muscles. Thanks to the Simbody and OpenSim integration, the OpenSim models are directly and automatic transposed

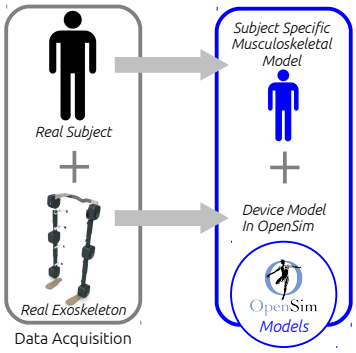

Figure 4: Using OpenSim as common software platform for the proposed appraoch. The human level is simulating till the muculoskeletal system while an analysis of the subject neurological activities is still missing.

to the dynamic equations systems to be solved by Simbody. While OpenSim is largely used and validated in biomechanical field, a complete evaluation of its performance as mechanical simulator was still missing. Actually, since it is based on Simbody, a good behavior as mechanical simulator was expected. However, the suitability of the OpenSim APIs, developed only for biomechanical purposes, and the reachable accuracy and reliability on mechanical simulations needed to be tested.

A comprehensive explanation about the selected common software platform, and the perfomed tests to evaluate its accuracy, reliability and flexibility is presented on Ch. 3 and on works [102, 104].

Fig. 4 shows OpenSim used as common software platform for the development of our proposed approach. However, the analysis of the subject neurological activities is still not available in OpenSim, so the subject monitoring is not possible without an additional tool which is introduced in the next section.

2.3.2 *Subject Monitoring*

While the common software platform can successfully simulate the musculoskeletal system movement, an analysis on the neurological involvement of the user is still missing. This is possible only including an experimental measurement of the neural drive sent to the muscles. After that, the measurements have to be used, combined with a physiologically accurate human musculoskeletal model, to calculate the subject contribution to the movement. This process is called neuromusculoskeletal (NMS) modeling. In our work, electromyographic (EMG) signals are used as input for NMS modeling, since they indirectly reflect the neural drive to muscles. The final result is an EMG-driven NMS model. Using an EMG-driven NMS model allows to determine

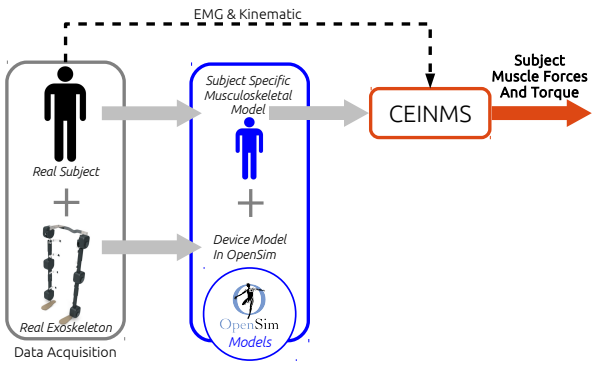

Figure 5: Including an EMG-driven NMS model in our approach allows to evaluate the subject real effort, intention and motor skills in our system.

the subject-specific relationship between patterns of muscle excitation and the resulting muscle dynamics without making any assumption on how muscles activate. In other words, the ankle joint moments of our example can be estimated reproducing the internal steps from the neural activities to the estimated muscle forces and joint moment. Our proposed approach includes in the Calibrated EMG-Informed Neuromusculoskeletal modeling Toolbox (CEINMS) software (Fig.5). CEINMS is a state-of-the-art toolkit that implements an EMG-driven neuromusculoskeletal model, able to estimate joints torque and muscle forces, from the only inputs of kinematic and electromyographic (EMG) signals which are a direct representation of the specific-subject intentions to activate muscles.

Ch. 4 introduces the main concepts of NMS modeling and, in particular, about its development inside CEINMS.

2.3.3 *Estimation of the Emerging Interaction*

Estimation of the emerging interaction, during the human-robot cooperation, can be performed through an interaction model which is basically a contact model.

Due to the specific rehabilitation purpose of our work, this contact model needs special attention. Contact models are already available in OpenSim and aim at reproduce the contact forces among two modelled bodies, but one of them is generally static, such as the floor. Instead, our cases aiming at reproducing rehabilitation processes can require movement of two dynamics bodies. In these cases small changes in the torques lead to large accelerations [36]. Human and robot movements should be synchronous which means that the contact model has to be able to estimate interaction forces even if very small in magnitude and quite instantaneous.

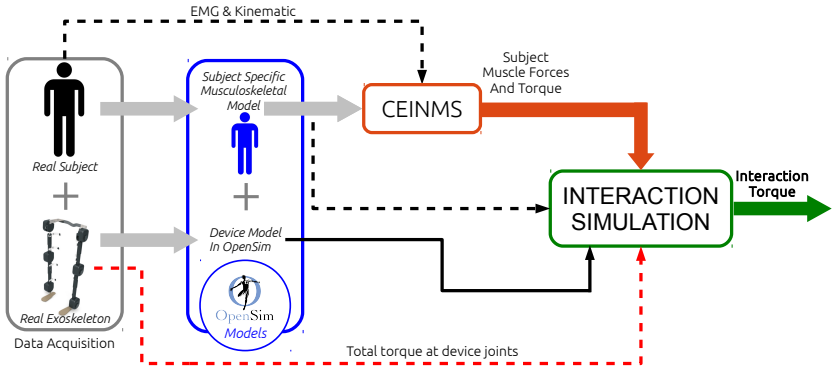

Figure 6: Interaction Simulation block requires special attentions in the definition of the contact model: contact forces may be small in magnitude and quite instantaneous require a further evaluation of it. After that, our system can integrate all the tools to dynamically simulated together all the level.

According these specific needs, Ch. 5 reports a test performed on the calibration of the contact model for a particular case in which the contact forces are also small and quite instantaneous. The work investigates the possibility to implement and to accurately calibrate a contact model in OpenSim to dynamically reproduce the gait movement of a small humanoid robot [103].

Inclusion of the contact model in our proposed framework completes the system development (Fig. 6), resulting in an interaction model which could be actually able to dynamically estimate the human-robot movement cooperation.

2.4 MULTI-LEVEL MODELING SYSTEM

The development of the entire proposed approach, implemented using the tools described in previous sections, results in the whole system shown in Fig.6. A validation procedure, to be ensure about its accuracy and reliability after the integration of the three level in an unique complex system has to be done.

Summarizing, the proposed Multi-Level Modeling System aims at being a solution for the following challenges:

- monitoring the user, from the neural activities to muscle forcesa and joint moments including all his internal neuromusculoskeletal dynamic parameters, to provide an in-deep quantitative evaluation on the effectiveness of the training and of the entire rehabilitation treatment, assessing the correctness of muscles recruitment during the therapy sessions;

- monitoring the human robot interaction, such as interaction forces, to tune the device on the specific characteristics and

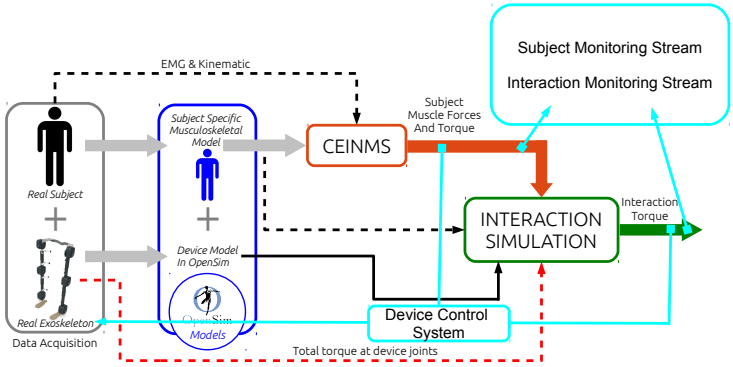

Figure 7: The entire system results from the integration of the level proposed in the Multi-Level Model approach, and it can be useful for subject monitoring, interaction monitoring and device controlling.

condition and to monitor how the device control could improve the motor skill recovery procedure;

- providing environment information to a device control stream which could actually consider the subject efforts and needs, basing its control signals also on the information coming from the interaction model, for example to minimize the losses in it.

Fig. 7 graphically represents all the possibility of our proposed Multi-Level Model approach.

3

A COMMON SOFTWARE PLATFORM: OPENSIM

3.1 INTRODUCTION

Sec. 2.3.1 explains why the possibility of simulating Human, Robotic and Boundary Level at the same time, inside the same software platform become essential. In particularly, the common software platform has to be accurate and reliable, being quite flexible to provide high level tools to simply modify one or more model parameters to try different solutions.

This chapter reports all the followed steps to demonstrate the possibility of using OpenSim as common software platform for our proposed Multi-Level Modelling Approach.

The goal of this chapter is two folds. On one hand we want provide a practical brief introduction to show the path to successfully implement a simulator of a generic robotic device using OpenSim. On the other hand we want to demonstrate that OpenSim is a tool suitable for robotics research, proving a set of well tested instruments that can speed up the process of creation of a simulation.

Three main section compose this chapter. The first one describes in details the motivations of using OpenSim for our purposes. The main tools available in OpenSim, which allow to successfully implement a dynamic simulation, are also described.

The following two main sections report the results obtained using OpenSim as mechanical simulator for implementing solution to problems. First, we developed five benchmark problems for multibody system simulation to formally and completely evaluate OpenSim behavior. Then we implemented a dynamic simulator of a real robotic assistive device to include in our model a the implementation of a controller. The reported results show that OpenSim is able to reproduce the mechanical behavior of a robotic assistive device and its strategy for the control of movement, which is a crucial task for the implementation of our final Multi-Level Model.

3.1.1 *Motivation for a Common software Platform*

In recent years, robotic assistive devices have been increasingly used in rehabilitation to speed up and reduce cost of the recovery process. Robotic manipulators, automated treadmills, and passive or active orthoses are just a few examples of the current state of research. Nowadays the main challenge is to move from passive devices to active ones, able to understand patient's intentions and adapt to his current

neuromuscular capabilities. This adaptation requires to be able to predict the emerging interaction between the patient and the rehabilitation device. The motion cooperation can be measured or estimated when the subject is wearing the real device, giving helpful information to adapt the system to the characteristics and needs of the patients to pursue a personalized rehabilitation treatment. But the design of an effective rehabilitation requires the availability of these variables before the actual construction of the real device. Indeed, knowledge about the human-device interaction allows to compare different design solutions and evaluate which is the most likely to maximize the impact of the rehabilitation treatment. However the prediction of this motion cooperation requires a simulator tool able to accurately predict the behavior of the human body and of the robotics device and their complex interaction. The availability of such a tool would have a huge impact on the design of a new generation of rehabilitation devices. If we are able to predict this interaction, this could provide useful to design better devices and increase rehabilitation treatment effectiveness.

The main idea is to implement a system able to accurately simulate the subject-specific neuromusculoskeletal function as well as the mechanical behavior of the robotic device, and the interaction emerging for the human machine cooperation. We believe that a Multi-Level model simulation could be effectively implemented using as common software platform OpenSim, a well known dynamic simulator, largely used and validated in biomechanical field.

3.2 OPENSIM

OpenSim [27, 73] has been mainly developed by the Neuromuscular Biomechanics Lab, the research group of Prof. Scott Delp at the University of Stanford. OpenSim is an open source software system for biomechanical modeling, simulation and analysis. Its purpose is to provide free and widely accessible tools for biomechanics research and motor control science. OpenSim enables a wide range of studies, including analysis of walking dynamics, studies of sports performance, simulations of surgical procedures, analysis of joint loads, design of medical devices, and animation of human and animal movement [97, 98]. OpenSim is used in hundreds of biomechanics laboratories around the world to study movement and has a community of software developers contributing new features.

The large diffusion of this software is significant on two fronts, both important but different. On one hand, OpenSim structures and algorithms, especially mathematics and physics related, are widely used, tested, and accepted. The large number of available solutions speed up the design and implementation of new dynamic simulator. Additionally, their large use reduce the time required to test and

validate the mechanical model. On the other hand, a software project with such a widespread use is unlikely to be closed. This guarantees the continuity of support and debugging and therefore, the longevity of the projects based on OpenSim.

The library available within the OpenSim tool offers several algorithms also needed in the simulation of robotic systems. The software performs inverse dynamics analysis and forward dynamics simulations. OpenSim suits particularly the latest generation of devices, whose goal is to get more efficient locomotion inspired by biological system studies. This motivates the idea of using OpenSim to produce dynamic simulations of robotic assistive devices.

3.2.1 *Workflow to implement a multibody system model in OpenSim*

This section explains the steps required to create a dynamic simulation of a multibody system, such as a robot device, in OpenSim. We want to demonstrate that OpenSim is a tool suitable for robotics research, proving a set of well tested procedures that can speed up the process of creation of a simulation. The workflow requires three step: the creation of a kinematic model, the creation of a dynamic model and then the simualtion of the implemented system.

Kinematic model

The kinematic model aims at defining the kinematic chain composed of rigid bodies connected through joints. The best way to describe the kinematic in OpenSim is through the use of OSIM file. An OSIM file is an XML file that describe the model properties. This file describes every joint movement and allows to associate a graphical representation to each body.

The addition of a new *body* can be obtained specifying its name and dynamic proprieties (mass, center of mass, and inertial matrix) in the OSIM file. Before the creation of the bodies composing the kinematic chain, the special body *ground* must be created. The required body ground represents the floor which is *father* of every body added to the model. The *joint* definition is required to specify a position of a body.

Fig. 8 represents the joint reference system between two body. The body P is the parent body while the body B is the child body. They are linked with a joint. P_0 is the system reference for the parent body as B_0 is the same but for the child body. P and B are the position of the system reference of the joint in, respectively, body P and body B. In the OSIM file the roto-translation from P_0 to P is described respectively by the tags *location in parent* and *orientation in parent*. In the same way, the tags *location* and *orientation* represent the roto-translation from B_0 to B. OpenSim provides different joints such as: Free Joint, Custom Joint, Weld Joint, Pin Joint, Slider Joint, Ball Joint, Ellipsoid Joint, Joint.

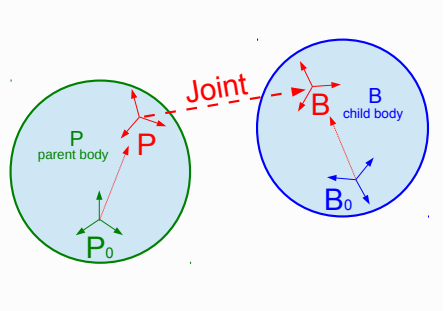

Figure 8: Joint reference system in OpenSim: B specified by location and orientation, P specified by joint location and orientation in parent, Joint coordinates specify the kinematic of B relative to P.

OpenSim allows to add a mesh file to each body for its *visualization*. This provides the users with a 3D visualization of the system and of the simulation result.

Dynamic model

The definition of the properties of the dynamic model requires to direct use of the OpenSim APIs. To successfully implement a dynamic mode, the following three task must be developed:

- creation of the contact model and contact force;
- setup of the splines to control the coordinates;
- addition of actuators and related controllers;

The creation of a *contact model* is required only when there is contact among objects. Each body involved in the description of the contact force requires a contact geometry, i.e. a contact surface. In our works we used the OpenSim API that implements an elastic foundation force as a "bed of springs" contact model [73]. The contact model also requires the definition of the following dynamic parameters to describe the contact: stiffness, dissipation, static friction, dynamic friction, and viscous friction.

To move a dynamic model the developers must implement a *spline function* for each coordinate whose kinematic movement is available because it is known or measurable. As only discrete values are available, the spline reconstructs the evolution of the each coordinate to produce the desired movement.

When the exact trajectory is not known the coordinate movement can be driven by *actuators*. Each actuator in the model calculates and applies loads to its associated bodies based on its control value and the state variables at any time step. OpenSim provides classes that described base actuators such as torque actuator and force actuator. For each actuator is mandatory to associate at least one controller.

Dynamic simulation

To successfully achieve a dynamic simulation of the desired multibody model, two additional tools are required.

- an integrator to solve the simulation.
- a force reporter;

The *integrator* is the tool that actually solve the dynamic simulation. Several integrator algorithms available in OpenSim. For our tests, we choose the Runge-Kutta-Feldberg Integrator. It is a trade off between precision and computational time. All the algorithms are customizable through the definition of parameters as size step, accuracy, and tolerance.

The forces and the moments are the result of a dynamic simulation. To extract values from the simulation a *force reporter* must be added. OpenSim provides a class to record in a storage the forces applied to a model during a simulation. At the end of the simulation a force reporter storage is available.

After the simulation, results are stored in an OSIM file with the model after the integration and two MOT files. The first one contains the evolution of the movement of each coordinate. The second one reports the added reporter force storage. All these data can be plotted and shown by the OpenSim Graphical User Interface.

3.3 OPENSIM AS MULTIBODY SYSTEM SIMULATOR

To achieve our final goal, the simulation of the interaction between a human and a robotic assistive device, we need a tool highly accurate in both the simulation of human and of robotic systems. OpenSim is definitely recognized as an highly reliable tool for the dynamic simulation of movements of human body. However, an in-depth evaluation of OpenSim as a mechanical simulation tool is still missing. To validate OpenSim and evaluate its reliability we used a Multi-Body System (MBS) Benchmark, proposed by Prof. Gonzàlez of the University De La Coruña [43, 44], and implemented the five problems proposed in this benchmark suite. MBS Benchmark is a collaborative project dedicated to develop and maintain a standardized set of problems to evaluate multibody systems simulation software. Each problem target a specific challenge in MBS simulations, such as such as stiffness, singularities, constrains redundancy, etc (Tab. 1). The following of this section introduces the five problems and presents their implementation in OpenSim. OpenSim was able to implement each problem, obtaining simulations matching the reference solutions and thus demonstrating the feasibility of using OpenSim as a dynamic simulator for multibody systems. Description of the problems, implementations, full results, and videos can be found at `http://goo.gl/8KecLt`.

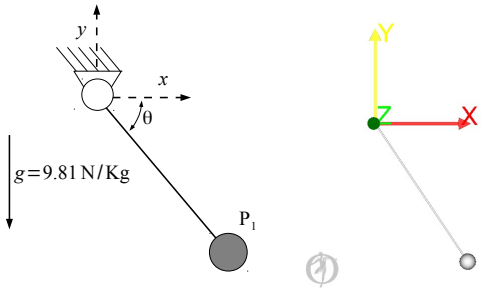

P_1 mass	1.0 kg
Bar length	1.0 m
Bar mass	0.0 kg
$\theta(0)$	0.0 rad
$\dot{\theta}(0)$	0.0 rad/ s

(a) (b) (c)

Figure 9: (a) Simple pendulum: (a) sketch, (b) model in OpenSim and (c) System Properties and Configuration.

A01: Simple Pendulum

The **A01** MBS benchmark problem is a simple planar pendulum, proposed as a demonstration example. The simple pendulum (Fig. 9a) is a planar mechanism composed of a point mass linked to the ground through a rigid massless bar. Tab. 9c reports the system configuration. Gravity is the only force applied to the mechanism. Fig. 9b shows the simple pendulum model implemented in OpenSim.

A02: N-Four-Bar Mechanism

The **A02** MBS benchmark problem, N-four-bar mechanism (Fig. 10), is a common example of a mechanism which undergoes singular configuration [43]. The system has N-four-bar windows composed of 2N+1 links. It is an extension of the two-four-bar mechanism proposed in [6]. When the mechanism reaches the horizontal position, the number of the degrees of freedom instantaneously increase from 1 to N+1. Grav-

Table 1: MBS Benchmark problems and their challenges.

Problem name	MTB simulation challenge
Simple pendulum	Dynamic simulation
N-four bar mechanism	Singular position
Andrew's mechanism	Small time scale
Bricard's mechanism	Redundant constrains
Stiff flyball governor	Stiff system

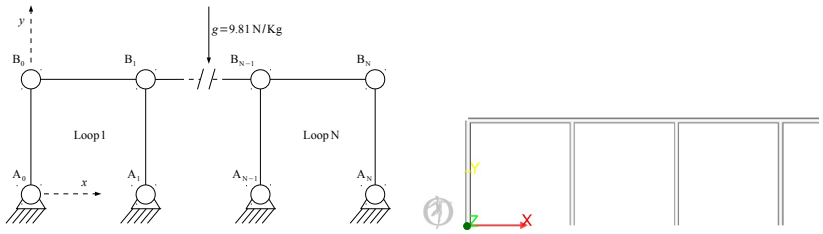

(a) (b)

Figure 10: (a) N-four-bar mechanism: (a) sketch and (b) model in OpenSim (only the first three windows are shown).

Table 2: N-four-bar Mechanism: System Properties and Configuration

N	40
Link mass	1.0 kg
Link length	1.0 m
$\dot{B_0}x(0)$	1.0 m/s

ity is on the negative y direction. Tab. 2 reports the system properties.

A03: Andrew's Mechanism

The **A03** MBS benchmark problem, Andrew's mechanism [87] (Fig. 11), requires a very small time scale, thus making it difficult to simulate for solvers that cannot reach small time steps [43]. The simulated mechanism is a planar system composed of seven bodies interconnected through revolution joints and driven by a motor located in O. Detailed information about the mechanical structure of each body is reported in Tabs. 3–6. Positions of reference systems are presented in Fig. 12a.

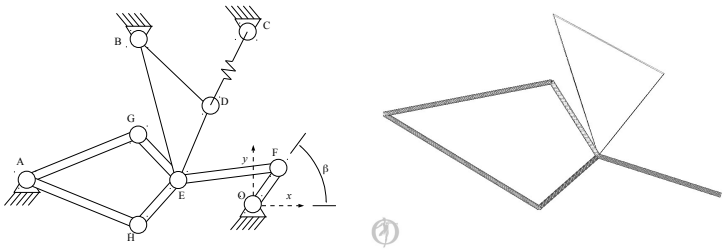

(a) (b)

Figure 11: Andrew's mechanism: (a) sketch and (b) model in OpenSim.

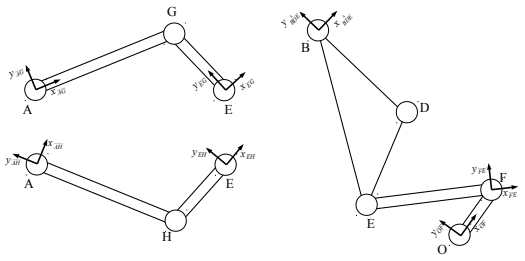

(a)

	Angle [rad]
β	-0.0620
$O\hat{F}E$	0
$F\hat{E}B$	2.088
$F\hat{E}G$	2.341
$E\hat{G}A$	1.792
$E\hat{H}A$	1.348

(b)

Figure 12: Andrew's mechanism: (a) Systems of Reference defined for each body of the mechanism and (b) initial angles value.

Table 3: Andrew's mechanism: Rod Elements Properties

	Center of Mass (CoM)		Mass	Inertia (CoM)	Length
	X [m]	Y [m]	[Kg]	[Kgm^2]	[m]
OF	0.00092	0	0.04325	$2.194e^{-6}$	0.007
FE	-0.0115	0	0.00365	$4.41e^{-7}$	0.028
EG	0	0.01421	0.00706	$5.667e^{-7}$	0.02
AG	0.02308	0.00916	0.0705	$1.169e^{-5}$	0.04
AH	-0.00449	-0.01228	0.05498	$1.912e^{-5}$	0.04
HE	-0.01421	0	0.00706	$5.667e^{-7}$	0.02

Table 4: Andrew's mechanism: Triangular Element Properties, points defined in X_{BDE}-Y_{BDE} RS

Center of Mass (CoM)		Mass	Inertia
X [m]	Y [m]	[Kg]	[Kgm^2]
0.01043	−0.01874	0.02373	$5.255e^{-6}$

Point	X [m]	Y [m]
B	0	0
D	0.02	-0.018
E	0	-0.035

Table 5: Andrew's mechanism: Points in ground X-Y Reference System

Point	X [m]	Y[m]
O	0	0
A	-0.06934	-0.00227
B	0.03635	0.03273
C	0.014	0.072

Table 6: Andrew's mechanism: System Properties and Configuration

Spring coefficient	4530 N/ m
Spring rest length	0.077 85 m
Motor torque	0.033 N m^{-1}

A04: Bricard's Mechanism

Bricard's mechanism (**A04** benchmark problem) [12] is an example of over-constrained system. Grübler's formula [46] results in no degrees of freedom, however, the particular orientation of the revolute pairs results in a system with one degree of freedom. The system is composed of five rods (1 meter length and 1 kilogram weight) and six revolute joints (Fig. 13). Gravity is acting in the negative y direction.

A05: Flyball Governor

The **A05** MBS benchmark problem is an example of a stiff mechanical system. The **A05** benchmark problem is also known as flyball governor (Fig. 14) and was invented by J. Watt in the 18th century. In this stiff mechanical system, coupler rods are substituted by spring-damper

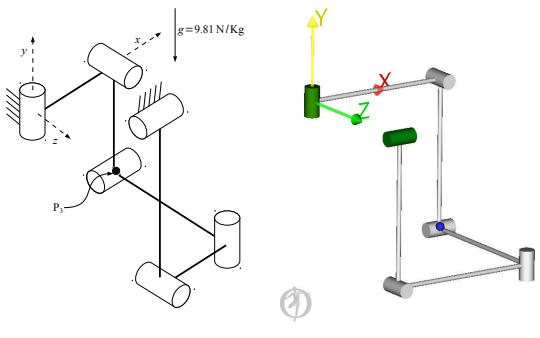

(a) (b)

Figure 13: Bricard's mechanism: (a) sketch and (b) model in OpenSim.

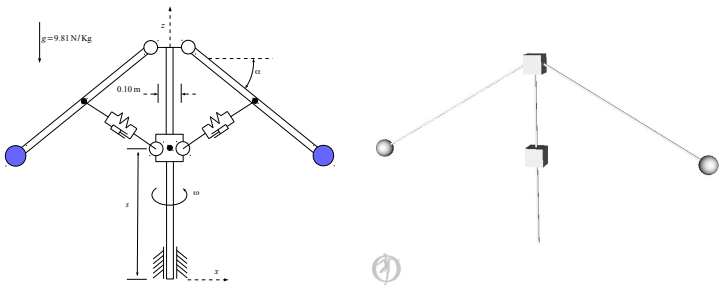

(a) (b)

Figure 14: Flyball Governor: (a) sketch and (b) model in OpenSim.

Table 7: Flyball Governor: System Properties and Configuration

Axis, Rods	$1.0\,\mathrm{m} \times 0.001\,\mathrm{m} \times 0.01\,\mathrm{m}$
Base	$0.01\,\mathrm{m} \times 0.01\,\mathrm{m} \times 0.1\,\mathrm{m}$
Density ρ	$3000\,\mathrm{kg/m^3}$
Spring stiffness K	$8 \times 10^5\,\mathrm{N/m}$
Spring damping C	$4 \times 10^4\,\mathrm{Ns/m}$
Spring rest length	$0.5\,\mathrm{m}$
s	$0.5\,\mathrm{m}$
α	$30°$
$\dot{\omega}$	$2\pi\,\mathrm{rad/s}$

elements. Gravity acts in the negative y direction and the system moves under its effect. Tab. 7 reports system properties.

3.3.1 *MBS Results*

To evaluation the accuracy of OpenSim as a dynamic simulator for mechanical multi-body systems we followed the guidelines presented by the MBS benchmark authors in [43] and compared the results with the provided reference solutions. For each problem, the authors provided the 3-dimensional displacements of one or more reference points that are used to compare the outcomes of the simulations. The precision of the simulations on all the coordinates was evaluated computing the maximum normalized error between the reference solution and the simulated one.. For each time sample t_i, the error at coordinate j is defined by Eq. 3.1, where y is the simulation output and y^{ref} is the reference. The threshold value was introduced to avoid a singularity when the reference values approach zero. The threshold

Table 8: Global error of OpenSim simulation.

	A01	A02	A03	A04	A05
Total Error [%]	3.6E-3	9.8E-4	4.7E-2	6.4E-4	7.3E-5

Table 9: RMS and Peak errors of OpenSim simulation results.

	A01	A02	A03	A04	A05
RMSE X [m]	2.8E-5	7.9E-5	7.0E-6	2.1E-5	4.0E-5
RMSE Y [m]	2.9E-5	5.4E-5	8.0E-6	2.0E-6	
RMSE Z [m]				4.0E-6	
Peak Error X [m]	5.6E-5	2.1E-4	1.6E-5	1.9E-4	1.8E-3
Peak Error Y [m]	5.9E-5	1.8E-4	1.9E-5	5.1E-6	
Peak Error Z [m]				5.3E-5	

value was set to 10^{-5} for problem A03, since it tested small time scale requiring an higher precision, and to 10^{-3} for the others.

$$e_j(t_i) = \frac{|y_i(t_i) - y_i^{ref}(t_i)|}{max\left\{|y_j^{ref}(t_i)|, y_j^{threshold}\right\}} \tag{3.1}$$

Eq. 3.2 define the total error (e_{Total}) on problem composed of m coordinates and with n samples as reference values.

$$e_{Total} = \sqrt{\frac{1}{m}\sum_{i=1}^{m}\frac{1}{n}\sum_{j=1}^{n}(e_j(t_i))^2} \tag{3.2}$$

The first important result was the successful simulation of all the five problems: OpenSim was able to face all the challenges proposed by the MBS benchmark.

Tab. 8 reports the total errors for the five problems. Error values for all the problems are quite low. The highest value for A03 is justified by the small time step and the high complexity of the motion required by the problem. Tab 9 reports the Root Mean Square Error (RMSE) and the Peak Error (PE) for each coordinate. Again the results demonstrate the high precision of the simulations and justify the use of OpenSim as multi-body system simulators. R^2 values were also computed but not reported because very close to the unit value ($R^2 > 0.999$) for all the problems. This almost perfect match is also shown by Fig.15 behavior of reference and OpenSim simulation.

The very good results obtained using OpenSim to simulatethe the problems proposed in MBS benchmark lead us to conclude that OpenSim can be successfully used to achieve accurate simulation of these type of mechanisms.

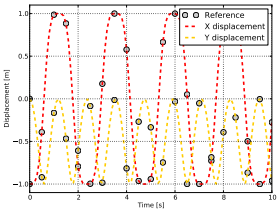

(a) A01 Simple pendulum

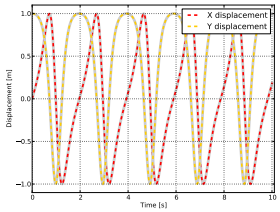

(b) A02 N-Four-bar mechanism

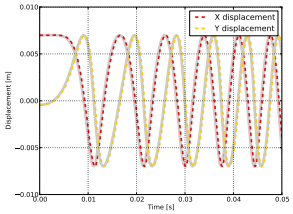

(c) A03 Andrew's mechanism

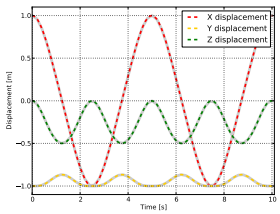

(d) A04 Bricard's mechanism

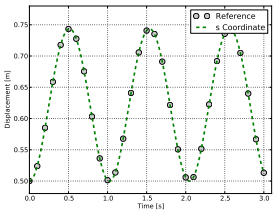

(e) A05 Flyball governor

Figure 15: Comparison of reference point between OpenSim simulation (dashed lines) and MBS benchmark reference (gray lines or dots)

3.4 CONTROLLERS IN OPENSIM

In this section we present our preliminary work in the development of an accurate mechatronics model of a motorized ankle-foot orthosis (i.e. MAFO) [9, 69]. To move the device, an actuator was placed in coorespondence of the real motor joint. The actuator controller was developed miming the real controller, in order to reproduce the real device behavior. The movement of the simulated device was compared and validated with the real device moving under the same conditions. Being able to reproduce the MAFO mechatronics (i.e. the mechanical and the control systems) is crucial for the future integration of the Human, Robot, and Boundary Level in the same simulation software.

3.4.1 *A Motorized Ankle-Foot Orthosis (MAFO)*

The MAFO device used in this study is shown in Fig. 16a. This system was designed and developed by the Bioengineering group of the Spanish Council for Scientific Research (CSIC) [9, 69]. The MAFO has one degree of freedom (DOF) driven by a brushless motor (i.e. 50 W and 94.3 $\mathrm{mN \cdot m}$, Maxon) connected to a reduction gear (i.e. maximal torque of 232.38 $\mathrm{N \cdot m}$). The device is equipped with a torque-force sensor and a joint angular position sensor. The data from the two sensors are used as inputs for the proportional integrative derivative (PID) speed controller. The hardware of the underlying controller is a PC/104 based on x86 architecture. This allowed implementing the control software using xPC Target (MATLAB, MathWorks, US). The range of motion (ROM) of the device joint allowed for a maximal plantar flexion of $-20°$, and for a maximal dorsi flexion of $15°$, with a maximal plantar-dorsi flexion speed of $40°/s$.

3.4.2 *MAFO Simulation with OpenSim*

The MAFO was modelled in OpenSim following the same approach described in Sec. 3.2.1. First, we defined the kinematic chain describing the MAFO rigid bodies interconnected through mechanical joints. Then, we associated dynamic properties to each rigid body of the model. Properties include: rigid body mass, center of mass position, and mass moment of inertia. A model of the ankle joint rotary motor controlled by a PID controller was then developed. This allows actuating the MAFO joint as a function of the selected plantar-dorsi flexion speed and range of motion (ROM). A Runge-Kutta-Feldberg integration algorithm [34] was then used to integrate the dynamic equation of motion and produce joint torque, acceleration, velocity, and position estimates for the next frame in time. The predicted joint displacement was then controlled by the underlying simulated PID controller at each frame.

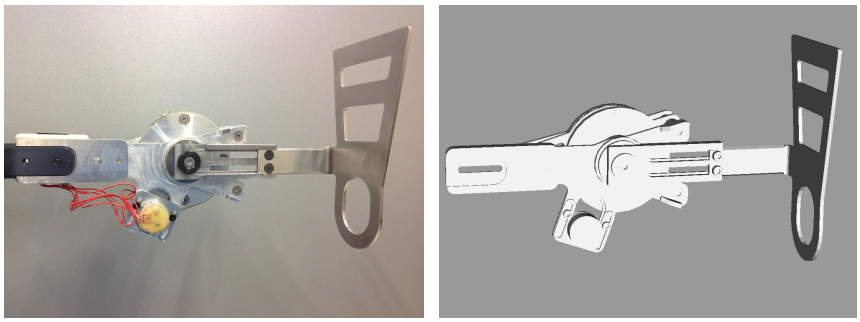

(a) (b)

Figure 16: Motorized Ankle Foot Orthosis (MAFO): (a) Real device (b) Simulated model in OpenSim.

3.4.3 *Data Acquisition for the Validation*

Our proposed MAFO model was validated against experimentally measured data collected from the real MAFO device. The comparison between the measured and the simulated data provided a validation of our proposed model. We performed repeated trials during which both simulated and experimental MAFOs operated under the same conditions of ROM and plantar-dorsi flexion velocity. Each repeated trial had a fixed ROM, which was set to the maximal available range corresponding to a plantar flexion value of $-20°$ and to a dorsi flexion value of $15°$. The device movement started from a rest position that was fixed to $0°$ of plantar-dorsi flexion. A fixed duration of 20s was used throughout the whole set of trials. This resulted in a number of complete plantar-dorsi flexion cycles across trials. The reference plantar-dorsi flexion velocity was changed across trials. This allowed specifically testing the simulated PID controller and multi-body dynamics under different working conditions. We performed tests at three constant velocities: $5°/s$, $10°/s$, $40°/s$. In addition we performed two tests where the velocity was continuously changed between two reference values. Furthermore, velocity changes are common in motor tasks such as gait. In this context, the joint velocity reference was automatically changed after 10s. Being able to reproduce joint velocity changes is fundamental to effectively test the PID controller behavior as well as the mechanical response of the simulated rigid bodies. We performed a first trial with a linear acceleration from $10°/s$ to $20°/s$, and then a second trial with a linear deceleration from $20°/s$ to $10°/s$. In Tab. 10 we summarized all the operating conditions for both the real and simulated MAFOs for each trial. The simulated and experimentally measured values of joint position and velocity were compared for each trial (Fig. 17, and Tab. 11). The Root Mean Squared Error (RMSE) was used for each trial to provide a measure of the difference between the values produced by the simulator and

Table 10: Experimental trial specifications

Trial	Movement Range	Speed	Complete flexion-extension
1	−20° - 15°	5°/s	1
2	−20° - 15°	10°/s	2
3	−20° - 15°	20°/s	5
4	−20° - 15°	10°/s (10 s) 20°/s (10 s)	4
5	−20° - 15°	20°/s (10 s) 10°/s (10 s)	4

Table 11: Experimental results for the different trials described in Tab. 11.

	Position		Speed	
Trial	RMSE [°]	R^2	RMSE [°]	R^2
1	1.09	0.98	2.10	0.82
2	1.98	0.96	4.25	0.80
3	2.96	0.91	9.82	0.73
4	2.14	0.95	6.20	0.83
5	2.23	0.94	7.27	0.76

those experimentally observed. We also calculated the coefficient of determination (R^2) to obtain a measure of how well the trend in the observed values corresponded to those predicted by the simulation.

3.4.4 *MAFO Results*

We reported the results calculated for each trial in Tab. 11. The maximum RMSE value between predicted and experimental position was 2.96°, which was obtained in trial 3. The minimum R^2 value between predicted and experimental position was 0.91, which was obtained in the same trial. In the velocity domain, RMSE reached a maximum value of 9.82°, while R^2 reached a minimum value of 0.73, in the trial 3. The mean values calculated over all performed trials were RMSE $= 2.08° \pm \sigma = 0.60$ and $R^2 = 0.95 \pm \sigma = 0.02$. In the joint velocity domain, they corresponded to RMSE $= 5.93° \pm \sigma = 2.62$ and $R^2 = 0.79 \pm \sigma = 0.04$. A generic index of the simulation could be obtained by the RMSE and R^2 mean values calculated on all trials

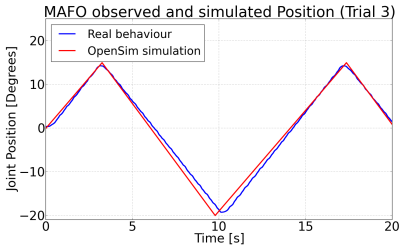

(a)

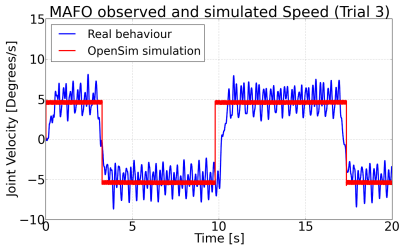

(b)

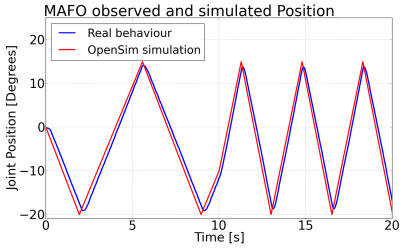

(c)

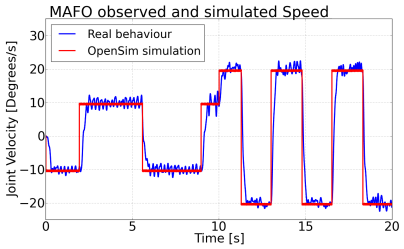

(d)

Figure 17: Experimentally measured and simulated MAFO joint positions and velocities are compared for Trial 3 (a) and (b) and Trial 4 (c) and (d). See Tab. 10 for trial specifications.

without a distinction between position and speed. In this case we obtained RMSE $= 4.00^{\circ} \pm \sigma = 2.70$ and $R^2 = 0.86 \pm \sigma = 0.09$.

3.5 CONLUSION

The proposed Multi-Level Modeling Approach in Ch. 2 required a common software platform to simultaneously simulate Human, Robotic and Boundary Level at the same time 2.3.1. OpenSim was selected as common software platform and this chapter provided an explanation which shows the path to implement a robotic devices using OpenSim. Sec. 3.3 and Sec. 3.4 investigated how OpenSim can be used to dynamically reproduce the behavior of a robotic devices, also including in the model a control system.

All the presented results ensured about the use of OpenSim, demonstrating that it has all the software tool to integrate Human, Robot and Boundary Level in a single simulation.

4

SUBJECT MONITORING

This Chapter presents the tool which allows to monitor the subject intentions and motor skills in our Multi-Level Model approach required to estimated the interaction emerging during the human robot movement cooperation.

The analysis of the joint moment results in a specific movement provide a first measure of the subject contribution but it is often not enough. Indeed, an analysis on the neurological involvement of the user is still missing but it is mandatory to evaluate the modulation of the human internal dynamics parameters due to the influence of the external device.

Our approach proposes to overcome this limitation including in the framework a tool for the neuromusculoskeletal (NMS) modeling: Calibrated EMG-Informed Neuromusculoskeletal Modelling Toolbox (CEINMS) [62]. CEINMS is a state-of-the-art toolkit that implements an EMG-driven neuromusculoskeletal model, able to estimate joints torque and the muscle forces, from the only inputs of kinematic and electromyographic (EMG) signals which are a direct representation of the subject intentions to activate muscles. Moreover, CEINMS allows to build subject-specific model with parameters tuned to the subject characteristics.

The Chapter is composed of three main sections. Sec. 4.1 provides a general overview on the available methods to dynamically described the human movement in terms of joint moments and muscle forces. For the sake of completeness, this overview includes also the methods in which the subject neural involvement is not, or only partially, considered. Sec. 4.2 describes the steps followed by the EMG-driven NMS, implemented in CEINMS, to estimate the joint moments from the EMG signals and the joints kinematics. Finally, Sec. 4.3 shortly introduces the CEINMS software organization, briefly explaining its use and reporting some considerations about its flexibility and modularity.

4.1 DYNAMICS MODELING OF THE HUMAN MOVEMENT

The knowledge of the muscle forces during human movement can result in a better evaluation of the neural control and tissue loading, improving both the diagnosis and treatment of orthopaedic or neurological condition. Since the direct measurement of the muscle force is generally not feasible, or limited to minimally invasive measurements in superficial tendons [58, 28, 37, 82], another non-invasive approach, based on the musculoskeletal modeling, has to be used.

Inverse dynamics and forward dynamics are the two different approach used for estimating joints moments during movements.

Inverse dynamics approach begin with a measure of the body position and the external forces, for example in a gait laboratory [100, 96, 107]. Joints angle can be calculated using the relative position and orientation of the body segments, obtaining also speed and acceleration through derivative operations. The muscle forces can be estimated from the joint moments, including a mescuoskeletal model. However, as multiple muscles are involved in driving each joint, defining the force partition between them result in many possible solutions. Assumptions about how the muscles act must be done before to compute muscle forces. While this approach does not include the actual neural activation in the model, it can be useful to calibrate and validate forward dynamic approaches.

Forward dynamics approach to the study of human movement take as input the neural command. The neural command specifies the actual magnitude and timing of the muscle activation. The neural command can be obtain directly from electromyograms (EMGs) or it can be estimated through optimization or neural networks model. In the optimization procedure initial values for muscle excitations are used to calculate muscle forces and joint kinematics using forward dynamics satisfying additional constrains [68]. Optimization procedures involve an objective function which aims to minimize tracking error between experimental data and model predictions iteratively updating muscle excitations [95]. Alternatively, the objective can be a function of muscle force and kinematics. For example it can be related to task performance, such as a maximum height jumping, or to physiologically evaluation, such as metabolic energy consumption [108, 74]. In these case, kinematics and EMGs data are needed for evaluation of results. However, the objective function selection can be sensitive to the investigators' assumptions, especially for the movement without a clear optimal performance task, such as walking, or related to physiological function target. Thus, this methodology cannot account for differences in an individual's neuromuscular control system, which may be impaired and characterized by abnormalities in the muscle activations patterns. Morever, testing different criteria is not always feasible, particularly due to long computational time. Another approach is the inclusion of the EMG data into the forward dynamics calculation [53, 59, 77, 78]. The muscle activations can be directly extracted from the experimental EMGs and provided to the model. In this case a calibration of the musculoskeletal model and of the muscular gains is required to minimize the differences between the measured joint moments and the ones estimated by the model [4, 17, 21, 63, 66, 67].

Our work uses an EMG-driven NMS modeling approach proposed in [63] and extended in [65, 85, 86]. This chapter, such as our work, mainly refers to the EMG-driven NMS model proposed in [63] and

its extension. Four main steps to complete the process Sec. 4.2. The first step is the *muscle activation dynamics* which transforms the neural signal to a measure of muscle activation. The muscle activation is normalized in the range 0 to 1. Then the *muscle contraction dynamics* describes how the muscle activation becomes muscle forces. In the third step a musculoskeletal geometry model is used to calculate the joint moment from the muscle forces. Finally, the equation of motion calculate the joint moments taking the joint kinematics as inputs.

4.2 EMG-DRIVEN NMS MODELING

The NMS model described was initially proposed by Lloyd et al. [63, 65]. This model has been extensively validated in the past as an anatomically and physiologically accurate representation of the internal dynamics transformation occurring in the human body during a movement. Moreover, it represents the state of the art of the EMG-driven NMS models for the lower limbs. Lloyd's EMG-driven NMS model can be described with four fundamental components: Anatomical Musculoskeletal model, Muscle Activation model, Muscle Dynamics model, Calibration 18. The model uses raw EMG and joint kinematics, recorded during static and dynamic trials, as input to estimate individual muscle forces and joint moments. The model can be regarded as generic as it can be adapted to any joint, given the appropriate anatomical and physiological data.

4.2.1 *Musculoskeletal Modeling*

OpenSim is used to create a musculoskeletal model of the subject's lower limb. The case study use a musculoskeletal model with seven musculotendon actuators (MTAs), each one represented as a line segment that wraps around bones and other muscles. These included MTAs are: gastrocnemius lateralis (GASL), gastrocnemius medialis (GASM), soleus (SOL), tibialis anterior (TIB), peroneus longus (PERL), peroneus brevis (PERB), and peroneus tertius (PERT). The actual subject's body size is used to linear scale the model, in particular the lengths of the bones and MTAs. This scaled musculoskeletal model is then used in OpenSim to perform a kinematic driven simulation. The results are muscletendon lengths (l^{mt}), velocities (v^{mt}), and moment arms (r) during the movement. All thes values are used as input for the Muscle Dynamics, together with the muscle activation to produce a muscle force estimation.

4.2.2 *Muscle Activation*

The normalized linear envelopes are obtained processing the raw EMG signals as described in [63] and summarizing in first blocs of

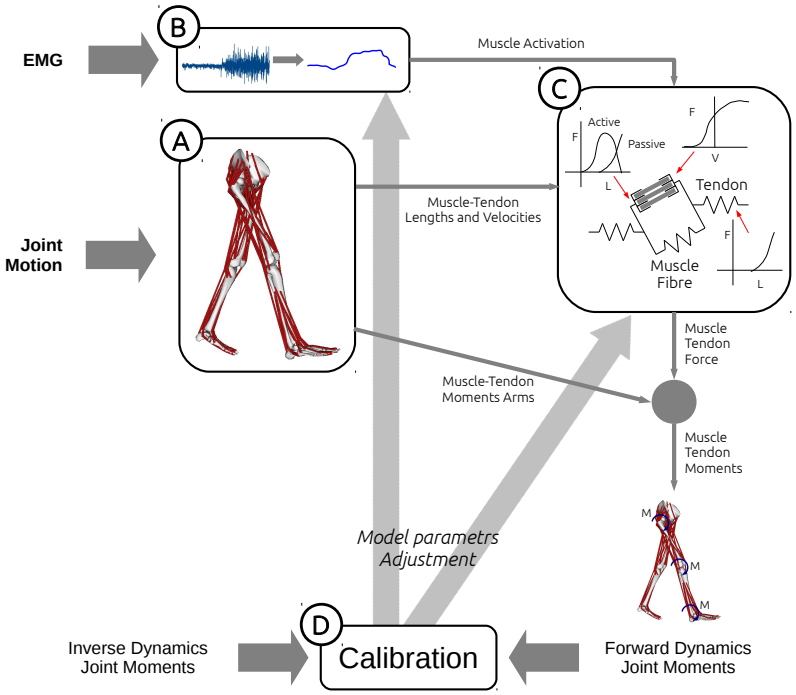

Figure 18: Flow chart of the EMG-Driven NMS model [63, 65]. Four main steps can be defined: (A) musculotendon lengths, velocities, and moment arms are obtained from the OpenSim anatomical musculoskeletal model which, together to the processed EMG (B), are inputs for Hill-Type muscle model (C) to estimate muscle forces and resultant joint moments. The calibration process (D) adjusts selected parameters to minimize the difference between these estimated joint moments and the experimental ones which are, in this case, obtained from inverse dynamics.

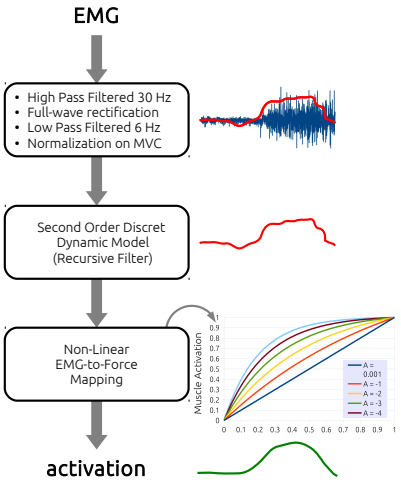

Figure 19: To obtain a normalized envelope the raw EMGs are low-lass filtered (30 Hz), full-wave rectified and low-pass filtered (6 Hz). Signals are then normalized to maximal voluntary contraction (MVC) to normalize the linear envelope. A second order recursive filter is applied to consider the electromechanical delay and also to include the muscle twitch response [63]. Signals are then non-linearly mapped to account for the non-linear relationship between EMG amplitude and muscle force [63].

schema in Fig. 19. These envelopes are filtered through a second order recursive filter to model a muscle electromechanical delay and twitch response characterization obtaining the processed signal $u(t)$. Then, a non-linear map is used to reproduce the non-linear relation between the amplitude of the EMGs and the muscle forces [63] (Fig. 19). Eq. 4.1 described this exponential relationship [13], where A is the non-linear shape parameter which is constrained to $-5 < A < 0$, where 0 is a linear relation.

$$a(u(t)) = \frac{e^{A(u(t))-1}}{e^{A}-1} \tag{4.1}$$

4.2.3 *Muscle Dynamics*

The muscle dynamics calculates the forces produced by the musculotendon actuators (MTA) in the model. Each MTA is represent using a Hill-type muscle model [109, 51]. It consists of an active force generating component coupled with two passive elastic components (Fig. 21). An exponential force-strain curve is used to model the passive component which is the tendon (Fig. 22c). This curve is scaled by tendon slack length (l_s^t) and the maximal isometric force at the optimal fiber length (F_0^m) and it is used to interpolate musculotendon forces.

The muscle fibre is composed of an active force-generating contractile element in parallel with a passive elastic one. The contractile

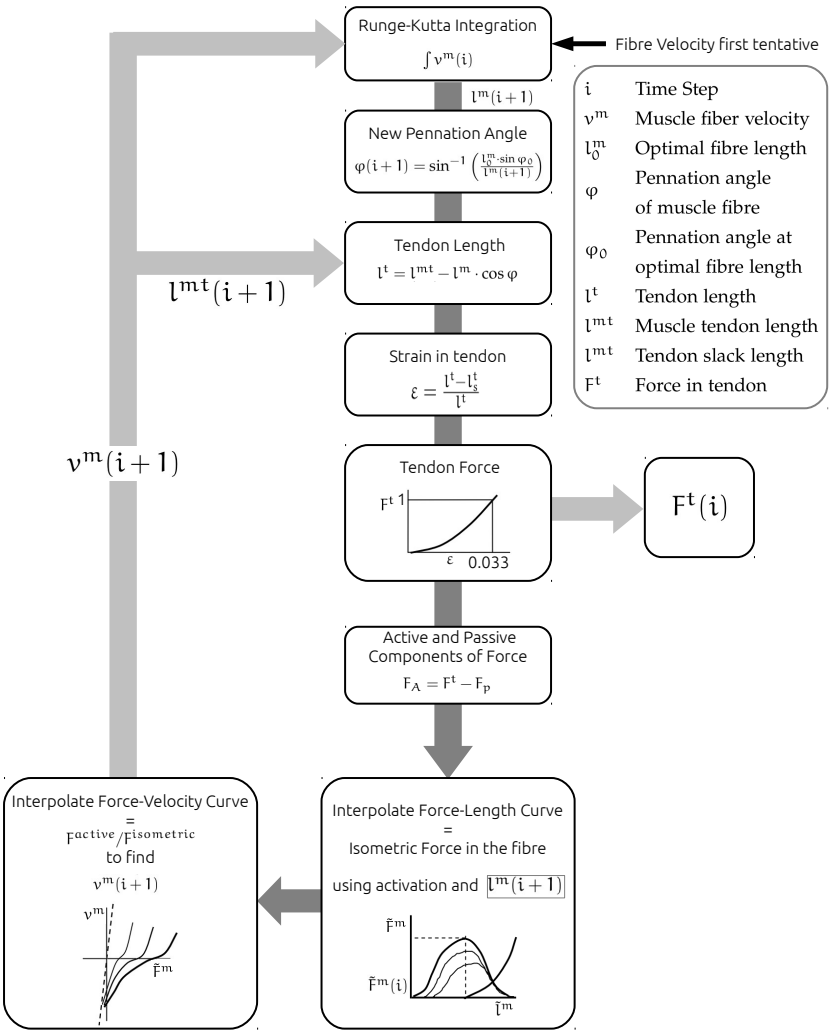

Figure 20: Muscle dynamics flow chart.

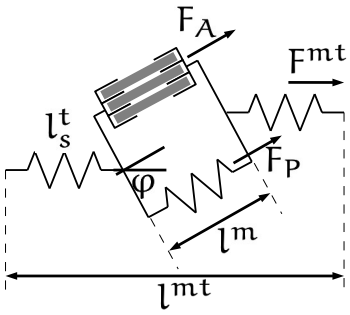

Figure 21: Hill-type elastic-tendon muscle model. The tendons are represented by single elastic passive elements. The fibre is represented by an active contractile element in parallel with a passive element. The two-element fibre is placed between the two tendons. The fibre is oriented with respect to the tendon according to the pennation angle φ. l^{mt} is the musculotendon length. l^m is the fibre length. l_s^t is the tendon slack length. F_A is the force produced by the fibre active element. F_P is the force produced by the fibre passive element. Musculotendon force F^{mt} is the fibre force projected on to the tendon line of action.

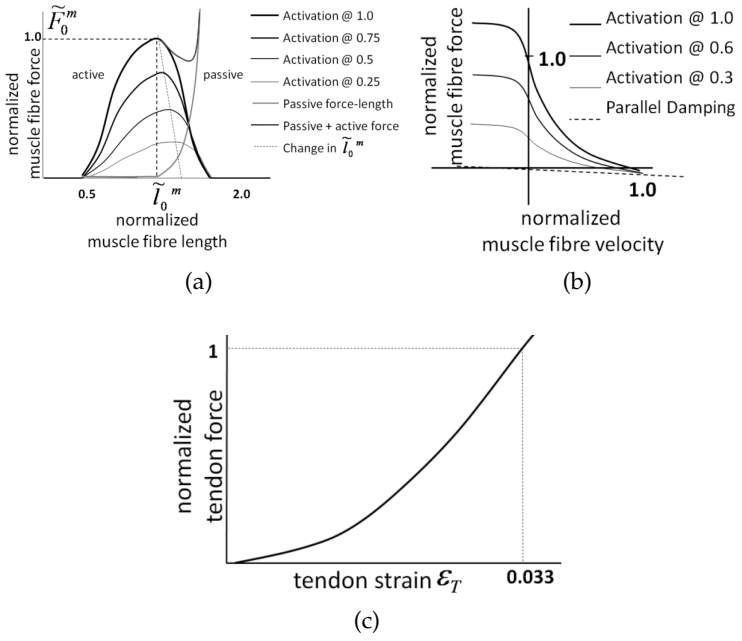

Figure 22: (a) Active and passive force length curves. Values are normalised by F_0^m and l_0^m so 1.0 means 100% activation. Optimal muscle fibre length was scaled with activation by a relationship experimentally determined in [54](b) Normalised force-velocity relationship. Note the parallel damping element added to prevent singularities when activation or isometric force $= 0.0$ of the inverted force-velocity relationship. (c) Exponential tendon force-strain relationship.

element consists of a generic active force-length function $f_A(\tilde{l}^m)$ (active curve in Fig. 22a) and a force-velocity function $f_V(\tilde{l}^m)$ (Fig. 22b). The passive elastic component in the muscle fibre is modeled using the exponential relationship $f_P(\tilde{l}^m)$ (passive curve in Fig. 22a). The final MTA force depends on a number of parameters including: maximum isometric muscle force at optimal fibre length F_0^m, optimal muscle fibre length l_0^m, instantaneous pennation angle φ, instantaneous muscle fibre length l^m, instantaneous fibre contraction velocity v^m, and instantaneous muscle activation $a(u)$. It is the contractile element of the model which is the final component of the EMG-driven NMS model. Thus, the velocities of the muscle can be numerically integrated to estimate the time evolution of the muscle fibre length. Eq. 4.2 describes the dependence of l_0^m on muscle activation [47] trough a linear relationship.

$$l_0^m(t) = l_0^m \cdot (\varphi \cdot (1 - a(t)) + 1) \tag{4.2}$$

In Eq. 4.2 φ is the percentage change in optimal fibre length l_0^m is the current optimal fiber length while $l_0^m(t)$ is the new optimal fiber length and $a(t)$ is the activation at time t.

Fig. 22a shows the effect of this relation. The percentage change in optimal fibre length, φ, is altered in the calibration process between 0 and 20% as a function of activation. Muscle fibre lengths are calculated using a Runge-Kutta-Fehlberg algorithm forward integrating the fibre velocities obtained from the force-velocity and force-length relationships. Initial muscle fibre lengths and fibre velocities are detrmined by calculating the stiffness of the muscle fibre and tendon, and distributing the total muscle tendon velocity to the muscle fibre and tendon based on their relative stiffness. Fig. 20 shows schematic diagram of the complete muscle model. Eq. 4.3 expresses the muscle fibre force, where the term δ is the muscle strength coefficient and all the other terms are the same previously defined.

$$F^m = \left(f_A(\tilde{l}^m) \cdot f_V(v^m) \cdot a(u) + f_P(\tilde{l}^m) + d^m \cdot \tilde{v}^m\right) \cdot F_0^m \cdot \delta \tag{4.3}$$

The force produced by the MTA, F^{mt}, can then be derived by projecting the fiber force F^m onto the tendon line of action as described in Eq. 4.4 where the pennation angle φ defines the angle orientation of the fibers with respect to the tendon (Fig. 21).

$$F^{mt} = F^m \cdot \cos(\varphi) \tag{4.4}$$

The joint moment, such as the ankle joint plantar-dorsiflexion moment, are produced summing the contribution due to the product of each estimated MTA force and its related moment arm r, as described in Eq. 4.5 where $r_i F_i^{mt}$ is the moment joint contribution due to the i^{th} muscle.

$$M = \sum_{N}^{i=1} r_i F_i^{mt} \tag{4.5}$$

4.2.4 *Model Calibration*

Model calibration process aims to define a set of subject-specif model parameters that allow to accurately estimate the joints moments. A set of experimentally measured joint moments is required to achieve a consistent model calibration to avoid wrong estimations which result in truly representative of the real joint dynamics. Alternatively, a standard Inverse Dynamics can be used to calculate the joint moments [63].

In the calibration process, a set of trials are chosen to correctly reproduce the muscle dynamics. A simulated annealing algorithm [42] alters a set of initially uncalibrated parameters to obtain estimated moments by the NMS model which actually fit the experimental joints moments. Indeed, the optimization algorithm uses an objective function that minimize the sum of squared difference between the estimated and experimental moments. If the calibration process is successful it is possible to use the subject-specific calibrated parameters to estimate muscle forces and joint moments. It is important to underline that, once the NMS model is calibrated, it only required EMG signals and joint angles as input and it can be executed in open-loop. No tracking is require to reproduce the experimental joint moments. In other words, only the calibration process required to track the experimental moments, then the model will track new data without further optimizations. That means a remarkable increasing of the run-time execution of the NMS model allowing by a reduced amount of required information. The set of parameter adjusted during the calibration procedure are divided in two main subset. The first includes the activation parameters which are selected from the Muscle Activation model. The second group involves muscle parameters chosen from the Muscle Dynamics model. Other parameters constrained during the calibration procedure are the activation filtering coefficients. These parameters, which are dimensionless and included between 1 and -1, are used to obtain a stable positive solution to the discrete linear dynamic model and to determine the gain and recursive coefficients of the recursive filter. They can take in account changes in muscle excitation due to different EMG electrode placement, skin preparation, and impedance and they may be different between subjects, muscles, and experimental sessions. Also the non-linear muscle activation shape factor A (Sec. 4.1) is altered during the calibration between -5 and 0. The non-linearity of the EMG to force relationship has been well documented and has shown that the inclusion of this parameter within a transfer function improves model estimates of stress from EMG data [80]. The adjusted parameters of the Hill-type model are muscles strength coefficient, resting tendon slack, and muscle optimal fiber length. The strength coefficients scale the relative maximum isometric force allowing each muscle to produce a contribution dependent on the individual differences in muscle strength, such as

difference in strength between different muscles and physiological cross-sectional area. The relative strength across all muscles is ensured by global gains which are opposed to individual muscle gains. Muscle dependent force coefficients are physiologically valid since they take in account the strength difference between individuals. Moreover, they are already used in previously in EMG-Driven models.

However, increasing the number of the parameters involved in the calibration process may compromise the physiological consistency of the model. To avoid unrealistic estimated muscle force, constrains on the muscle gains are applied, limiting their value between 0.5 and 1.5.

Resting tendon slack length l_s^t defines the length of the fiber and the related force they can produce. Literature provides only little information regarding lower limb musculature tendon slack length. This is manly due to the difficulty in measuring these values and the ill-defined junction between muscle and tendon. This motivates the inclusion in the calibration process of this parameter, with initial values $l_s^{t\prime}$ taken from [64] and constrained to $l_s^t = l_s 0^t \pm 5\%$. Optimal fibre length l_0^m is calibrated as it has been demonstrate to vary among individuals and to have a strong impact on the behavior of each muscle [64]. Initial values $l_0^{m\prime}$ were obtained from [64] and constrained as $l_0^m = l_0^{m\prime} \pm 2.5\%$.

The objective function used in the calibration algorithm is defined in Eq. 4.6.

$$\min \sum_{N_t} \frac{\frac{M^2 - \hat{M}^2}{var(\hat{M})} + \text{Penalty}}{N_t} \tag{4.6}$$

$$\text{Penalty} = \sum_{i=1}^{N_t} \sum_{j=1}^{N_m} P(i,j) \tag{4.7}$$

$$P(i,j) = \begin{cases} 0, & \text{if } 0.5 < \tilde{l}^m(i,j) < 1.5 \\ 0.5, & \text{otherwise} \end{cases} \tag{4.8}$$

In Eq. 4.6 M and $\hat{M}$ are the experimental and estimated joint moments respectively. The N_m term is the number of the muscles included in the NMS model. A penalty term is included in the objective to avoid solutions from the algorithm which actually describe muscles operating in a not physiologically range. For this reason the penalty prevents cases of $\tilde{l}^m$ outer the range between 0.5 and 1.5. For each time point which presents any muscle outside the range $0.5 < \tilde{l}^m < 1.5$, the penalty factor is incremented. The magnitude of this increment can approximately double the cost function value for a muscle operating outside the range for the entire trial.

4.3 CEINMS

Our proposed Multi-Level Modeling approach required an evaluation the modulation of the human internal dynamics parameters due to the influence of the external device required an additional tool. This is possible including an experimental measurement of the neural drive sent to the muscles. An EMG-driven NMS model allows to determine the subject-specific relationship between patterns of muscle excitation and the resulting muscle dynamics without making any assumption on how muscles activate. The tool used in the development of our Multi-Level Model of the human robot movement cooperation is the Calibrated EMG-Informed Neuromusculoskeletal modelling toolbox (CEINMS). CEINMS is the result of an interdisciplinary collaboration among the biomechanics and the computer science worlds. EMG-driven neuromusculoskeletal model presented in this chapter [63], and its extensions [85, 86], consists of a set of algorithms and software implementations, partly based on previous proposed EMG-driven NMS model, which aim to calibrate the internal model parameters to match each specific-subject characteristics. All these calibrated methods need a validation on the output data on a further set of experimental data which were not included in the calibration routine.

CEINMS is actually the result of the integration of all these algorithms and software. It was designed and implement to be a flexible and generic software. This results in a tool which can actually operate with any number MTU and any number of degree of freedom (DOF) once the appropriate anatomical and physiological data are available. Furthermore, the modularity of CEINMS allows the user to select different operation modes:

1. *Full-predictive open-loop mode*. Acquired EMG signals and three dimensional (3D) joint angles are used as input for the NMS model to drive the computations of the musculotendon forces.

2. *Hybrid mode*. An optimization algorithm builds the muscle excitation patterns for the muscle EMG signals which are not possible or easy to collect, such for as deep muscles. These constructed excitations are used, together with the experimental EMGs and the 3D joint angle, as innput for the NMS model.

3. *EMG-assisted mode*. This mode is a more generaziable form of the Hybrid mode. The optimization algorithm try to adjust both the excitations determined from experimental EMGs and the excitations of muscle with no acquired EMGs. Finally, the muscle excitations coupled with 3D joint angles, are used as input to the neuromusculoskeletal model.

4. *Full optimization-driven closed-loop mode*. This mode allows to construct all the muscle excitations to drive the NMS model without the aid of experimental EMD data.

The different modes correspond to different neural solutions which can be compared executing them on the same neuromusculoskeletal model.

The calibration of the EMG-driven NMS model to the specific-subject characteristics in CEINMS is not mandatory, and it can run uncalibrated or calibrated state.

4.3.1 *Calibration in CEINMS*

CEINMS provides a specific executale file *CEINMScalibrate* to perfom the subject calibration procedure presented in Sec. 4.2.4. Even if the NMS model could work on a generic way avoiding the calibration, this step plays a central role in the monitoring of a specific subject, ensuring a quite realistic representation of him intentions and motor skills. As described in 4.2.4, CEINMS uses an optimization algorithm to minimizes the error between the estimated and the measured joint moments during a set of tasks.

Before running the CEINMScalibrate software, experimental data files and calibration setup files have to be prepared. Experimentally Joint kinematics data is not directly used as input for the CEINMS software. Sec. 4.2.3 and Fig. 21 explained how the muscle-tendon length affects the force generation in Hill-type muscle models. The moment arm of a muscle insertion with respect to an anatomical joint rotation axis determines how that muscle force contribution influences the joint moment (Eq. 4.5). Thus a preprocessing steps are required to compute the geometrical state of each muscle during the subject's motion. This preprocessing step can be done through an anatomical modeling tool such as OpenSim. Summarizing , the input values to run a CEINMS from experimental data are:

- musculo-tendon lengths for the muscles in the model, calculated by means of an anatomical musculoskeletal model of the subject;
- moment arms for the muscles that insist on each joint, calculated by means of an anatomical musculoskeletal model of the subject;
- muscle excitations usually estimated from experimentally collected EMG signals;
- joint moments at the joints of interest, experimentally measured or calculated through Inverse Dynamics.

CEINMS setup configuration is entirely described in XML files, each one explained in a proper XML schema (XSD). Most of the setup files are related to the model definition and the interpretation

of input data. The file that is most critical and is the Calibration configuration file. Indeed, modifying this file might yield to very different results in terms of calibrated parameters. The definition of the calibration properties requires attention because it is strictly related both to the subject description and the specific application. Parameters of the optimization algorithm can be modified to reduce computation time but convergence to the global minimum becomes less likely. The general idea is that an increasing in the number of variables in an optimization problem means a computational time increase and less reliable solution. Therefore, when it is possible, other techniques should be used to estimated some parameters values and their reliability. An example is the use of imaging techiniques to appropriately scale generic models.

4.3.2 *Execution of CEINMS*

Once the CEINMS calibration procedure (Sec. 4.3.1) is successfully done, the executable file CEINMSexecute can be run using a NMS model specific for the subject of the trial. As discussed in Sec. 4.3, the CEINMS executable allows to run neuromusculoskeletal simulations in different operation modes Operation mode selection depends depending on application and available data.

If setup and data files can be correctly found, the execution will run and some information on current results will be reported to screen. Upon completion a set of storage files containing all the quantities that are calculated during the simulation of each muscle behaviour, such as activation, lenght and contraction velocity of the fibres, and ultimately muscle forces. Furthermore, joint moments are computed, that can be compared to experimental ones. While it is generally difficult to compare single muscles quantities against experimental data, these files are useful to get a better insight at how each muscle is behaving, and to verify that there are no errors or artifacts in the input data or in the model parameter.

5

EMERGING INTERACTION ESTIMATION: CONTACT MODELLING

Since the Multi Level model Approach aims to estimate the emerging interaction between a subject and a robotic assistive device during the movement cooperation, we need an accurate and reliable methodology to reproduce it. Then, the main idea involves a contact model between the subject musculoskeletal model and the robotic device model to reproduce that.

This Chapter reports a test on the contact model available in OpenSim in order to asses its accuracy,reliability, and flexibility to reproduce actual contact forces. The case study is the dynamic movement of a small humanoid robot. That means that the simulation has to reproduce the forces between the humanoid feet and the ground. Due to the dimension and the movement evolution the robot, this work results in a very difficult test for the contact model. Indeed, the forces were quite instantaneous and quite small in magnitude and definitely challenge to be reproduced in a simulated environment.

The Chapter is organized in four main sections which described the experimental process followed to results demonstrate that it is possible to calibrate contact model parameters and reproduce the ground reaction forces (GRFs) of the robot foot during its walking.

5.1 CONTACT MODEL PARAMETERS CALIBRATION

The main objective of this study is to present a methodology that allows determining the values of the contact model parameters used for the robot movement simulation. While the robot internal parameters can be measured and are invariant properties of the robot (i.e. weight, height,segmental center of mass, segmental moment of inertia), it is often hard to preliminary define the internal parameters of the simulation that influence the interaction between the mechanical system and the environment. In the dynamic simulation of a walking robot, the interaction is limited to the foot-ground contact. Therefore, in this study we focused on the estimation of the parameters of the contact model between feet and ground The objective of the overall procedure is to adjust the values of the parameters so that the dynamic simulation reproduces the experimentally observed foot-ground contact forces. Inputs of the proposed methodology are the experimental kinematics and the measured ground reaction forces during a robot walking. At the beginning, the dynamic simulator runs with randomly chosen values for the contact parameters. The simulated robot is moved ac-

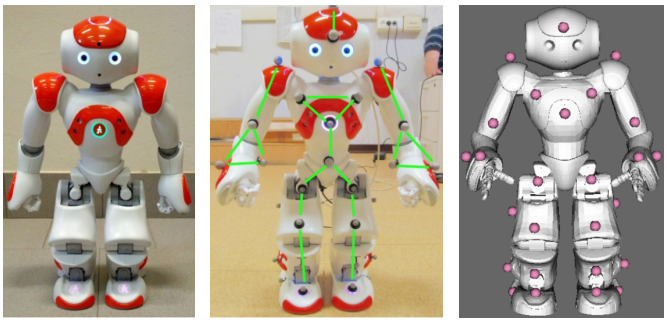

(a) (b) (c)

Figure 23: Nao robotics platform: (a) Real robot, (b) Real robot with reflective markers, and (c) Simulated model in OpenSim with virtual markers.

Table 12: Nao Mechanical Characteristics

Dimension (HxDxW)	$573 \times 275 \times 311$mm
Weight	5.8 kg
Degrees of freedom	25

cording to the experimentally recorded kinematics computed with the inverse kinematic tool provided by OpenSim. We used the experimental inverse kinematics to drive the simulated robot as we want to replicate the movement of the real robot as captured by the motion capture system.

The simulated model generates the resulting GRFs as a function of the current parameters. The predicted GRFs are compared with the GRFs experimentally measured through the force plates. The optimization procedures iteratively adjusts the contact model parameters until the root mean square error (RMSE) between the captured and the predicted forces is minimized throughout the motion trial. This cycle is repeated until one of the following events occurs: the prediction has an acceptable accuracy or the number of cycles reached a maximum value.

5.2 MAIN TOOLS

5.2.1 *Nao Humanoid Robot*

In this study we used the autonomous, programmable Nao robotics platform - Aldebaran Robotics [3], France (Fig. 23 and Tab. 12). The Nao platform has 25 degrees of freedom (DOFs) that provide enough mechanical dexterity to execute complex movements. Its dexterity, together with the small size, reasonable price, good autonomy, and several programming environments made Nao a successful and widespread

robotics platform for research purposes. However, its low weight does not allow collecting ground reaction forces data with high signal-to-noise ratios using conventional in-ground plates used for human gait analysis. While we present results on the Nao humanoid, the proposed procedure is platform independent and it can be applied to other humanoids with similar results.

5.2.2 *Laboratory of Movement Analysis*

The robot movement data were collected at the Laboratory of Movement Analysis of the Department of Information Engineering of the University of Padua, Italy. The three-dimensional kinematics of the robot was recorded at 60 Hz using a six camera motion capture system (BTS, Italy). A set of reflective markers was placed on the robot body and used to reconstruct the actual trial-specific whole-body segmental kinematics. The robot GRFs were collected at 960 Hz, synchronously to the kinematics data, using two in-ground force plates (Bertec,USA). The data collection procedure was controlled through the BTS SMART Analyzer software. While the hardware devices are capable of higher frequency, the software is only able to exports data (kinematics, video, and analog) downsampling them at the camera frequency of 60 Hz.

5.3 NAO SIMULATION WITH OPENSIM

The development of the kinematics and dynamics simulator of the Nao robot is based on the specifications of the Nao available from the Aldeabaran web site [3] and on the tools provided by OpenSim. The mechanical structure - the kinematic chain of rigid bodies connected through joints - is based on the primitives for the description of the complex human kinematics already available in OpenSim. Therefore, the definition of the kinematics only requires to write a simple XML file according to the OpenSim input format. More information can be found in the OpenSim User's Guide [98]. Starting from the kinematic model we extended the simulation with dynamic properties. Together with mass and inertial properties of the robot bodies [3], we added a contact model between the robot's feet and the ground. The model of the Nao robot is controlled through a set of time functions - each function continuously computes the value for one of the robot's degree of freedom. The functions are splines interpolating a sequence of DOF configurations computed at discrete steps. Spline interpolation is already included in OpenSim and current implementation uses Natural Cubic Splines. An integrator executes the dynamic simulation based on the input provided by the splines. Among the several integrator algorithms provided by OpenSim, we selected the Runge-Kutta-Feldberg. This algorithm solves the dynamic problem, i.e. is a numerical analysis algorithm for the solution of ordinary differential

equations. Our algorithm choice is motivated by the accuracy of the solution and the achievable computational speed.

5.3.1 *Contact Model*

During the walking, the only objects in contact with each others are the feet and the ground surface. This interaction is defined using the model of the contact elastic foundation force provided by OpenSim. As described in the OpenSim Developers' Guide [98], in this model each contact surface is associated to an additional mesh, not used for display purpose. The surface of each mesh is divided into triangular surfaces, and a spring is placed at the center of each surface. Each spring acts independently from the others and determines the dynamics of contact between two bodies. The point of contact is defined as the closest to the surface in the displacement direction. The forces exerted by two surfaces in contact are then calculated separately, giving a control on the simulation result (they must be equal and opposite). Finally, the resulted elastic force for each spring is given by 5.1 in the displacement direction.

$$f = k \cdot a \cdot x \cdot (1 + c \cdot v) \tag{5.1}$$

In 5.1, k is the spring stiffness, a is the surface, c is the spring dissipation, and v is the displacement speed directly calculated by $v = dx/dt$ The contact elastic foundation force model also provides a way to include the friction forces effects. For each spring that replaces the elastic contact surface, the exerted friction force is represented using the Hollars' Model [27] 5.2.

$$f = f_n \cdot \left[\min\left(\frac{v_s}{v_t}, 1\right) \cdot \left(u_d + 2\frac{u_s - u_d}{1 + \left(\frac{v_s}{v_t}\right)^2} \right) + u_v \cdot v_s \right] \tag{5.2}$$

In 5.2 where f_n is the contact point normal force, v_t is the transition velocity, u_s the static friction, u_d the dynamic friction, v_s is the slip (tangential) velocity of the two bodies at the contact point, and u_v the viscous friction. This formulation depends on the speed, therefore, it does not describe correctly the static friction. If there is a tangential force, two bodies in contact can move relatively. The presence of transition velocity limits this problem to setting an upper limit to drift velocity. The parameters of restoring force, dissipation in the material, and surface friction should be as close as possible to the real world values as they highly affect the success of the simulation. The objective of the proposed methodology is to evaluate the parameters of this contact model, i.e.stiffness, dissipation, static friction, dynamic friction, and viscous friction.

5.3.2 *Experimental Inputs*

The instrumentation used in this study is setup and optimized to record data from human subjects. As a result, the GRFs and the inverse kinematics recorded from the movement of a small and light weight humanoid robot were negatively affected by a low signal-to-noise ratio. For the difficulty of reducing the noise without affecting the information content, we decided to avoidgenovese2005improved filtering the data in our study. This choice is particularly important in movement acquisition with the cameras.

1) Ground Reaction Forces: We chose to target only the vertical component of the ground reaction forces during the procedure to estimate the contact parameters. The main reason is that the most meaningful information, in terms of both amplitude and waveform, is in the vertical force during a walking. Moreover, the low amplitude of the other forces (less than 10 N) does not permit to correctly identify the noise contribution. Due to software limitations of the motion capture system, exported data from force plates are downsampled at the camera frequency (60 Hz), much lower than the achievable hardware frequency (960 Hz).

2) Experimental Kinematics: The experimental kinematics is the sequence of joint angles that best reproduce the real robot movement. It is computed through the Inverse Kinematics (IK) tool available in OpenSim [98]. At each time step, the IK algorithm computes the coordinates values to minimize the difference between the experimental markers and the virtual ones in the model. This is a weighted least squares problem. The aim is to minimize markers errors. The markers error is the difference between the position in the model and the one experimentally computed. The position in the model is defined using the generalized coordinate computed by the IK solver. It is possible to include a weight for the error of each marker to define priority in the minimization process. The problem formulation is 5.3 where q is the generalized coordinates vector, x_i^{exp} is the experimental position of the marker i, $x_i(q)$ is the position of marker i on the model and w_i are the weights.

$$\min_{q} = \left[\sum_{i \in markers} w_i \left\| \mathbf{x}_i^{exp} - \mathbf{x}_i \right\|^2 \right] \tag{5.3}$$

Thirty eight markers were applied on the robot as shown in Fig. 23b. The number and placement of the markers were based on kinematic considerations and to simplify their identification. Thirty eight virtual markers were also applied to the OpenSim model (Fig. 23c). As there is no automatic protocol that ensures the perfect correspondence between real and virtual markers, their placement can be tricky. Usually the inverse kinematics tool must be executed multiple time with changes in virtual marker placement until an acceptable match is found. In bio-

engineering a residual error is considered acceptable when it does not influence the goodness of the acquisition [15]. The guidelines on when a solution is acceptable depends on the application and the examined motion. In our application with a small-size robot, minimal differences in the placement of virtual markers resulted in large differences of the final kinematics. Therefore, we had to manually execute multiple times the inverse kinematics tool with a gradual improvement on the matching before reaching satisfactory results.

5.3.2.1 *Optimization Algorithm: Simulated Annealing*

The objective of the optimization algorithm is to compute a new set of contact parameters that allow the simulation to improve the matching between the measured and simulated ground reaction forces. Formally, we want to minimize the following objective function 5.4

$$f(X) = \sqrt{\sum_{i=1}^{n} \left(F_y^{exp} - F_y^{sim}\right)^2} \tag{5.4}$$

where X is vector of contact parameters: five values for *stiffness*, *dissipation*, *static friction*, *dynamic friction*, and *viscous friction* that are required to be identified. At the beginning of our research we tried traditional (gradient-based) local optimization methods but they failed to arrive at satisfactory solutions. Therefore, we decided to use the Simulated Annealing (SA) algorithm, a global optimization alternative to overcome previous difficulties. This method is well known for its flexibility and performance as it is able to find the best solution in many challenging problems. We have implemented this stochastic optimization technique following the algorithm proposed and clearly described in [42].

5.4 EXPERIMENTAL RESULTS

The experimental results are comprised of two analysis. The first analysis evaluates the estimation of the contact model parameters and the resulting fitting of the experimental vertical ground reaction forces. The second analysis assesses whether the estimated contact model parameters can be employed to predict the robot movement during a novel set of validation trials that are not used for calibration.

During our experiments, the actual Nao robot was operated in the real world using the set of joint coordinates provided by the factory. However, it is worth stressing the fact that the simulated robot was operated using the inverse kinematics generated angles. This allowed reproducing the kinematics of the joints as well as the kinematics of additional degrees of freedom that are the result of the joint actuation such as the trunk three-dimensional movement. This is crucial to ensure that the simulated robot movement reproduces the actual

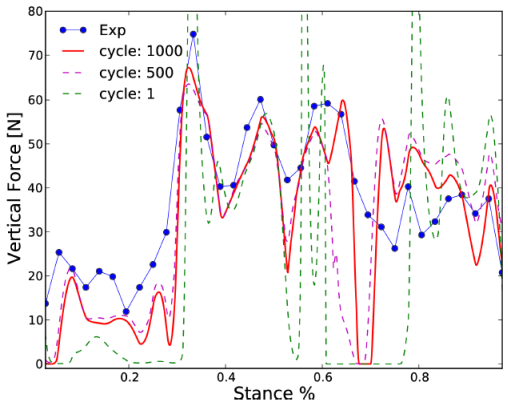

Figure 24: Estimation process of internal contact parameters. During the first few cycles of optimization, the objective function assumes high values, i.e.RMSE $\equiv f_Opt = 161.688$. After further 500 cycles the objective function value could be reduced to RMSE $\equiv f_Opt = 79.675$. The optimal parameter set was found after a total of 1000 cycles, RMSE $\equiv f_Opt = 72.454$.

movement that was observed in the motion capture laboratory and that underlies the generation of the measured GRFs.

5.4.1 *Evaluation of Contact Parameters*

This section reports the main results of our research. We demonstrate that it is possible to experimentally evaluate environmental contact parameters for the dynamic simulations of a robot based on experimentally recorded robot motion data. As previously described, we identified the parameters of the elastic foundation contact model including: *stiffness*, *dissipation*, and *static*, *dynamic* and *viscous frictions*. The identification procedure was based on an optimization procedure. Several choices are possible for the objective function 5.4. We decided to include only the vertical ground reaction forces available for both the right and left feet. To reduce the computation time required for the evaluation of the parameters we identified the most informative phase of the robot gait cycle to be used for calibration. Our findings demonstrated that good results could be achieved considering only the vertical GRF of a single foot stance (i.e. from heel strike to toe-off). This was done by evaluating the contact parameters over different phases of the gait cycle of increasing length. In this scenario, the 32 frames associated to the foot stance (around 0.6 s) were used for calculating iteratively the proposed objective function 5.4. A short simulation interval (less than 1 s) is important to reduce the convergence time. At each cycle, indeed, an integrator is solved to evaluate the dynamic simulation. The average execution time for a single integration of the robot stance phase is 1′ 39″ 764 ms (worst case 5′ 28″ 210 ms) on a Intel Core i5-2410, 2.5 GHz processor, 4 GB. The initial values chosen

Table 13: Average Values For Estimated Parameters Over Six Different Evaluation Procedures

	Initial Values Range	**Optimized Values**
Stifness	$10^4 - 10^6$	896838 ± 34348.69
Dissipation	$10 - 600$	106.39 ± 5.83
Static Friction	$0.1 - 15$	3.30 ± 1.40
Dynamic Friction	$0.1 - 15$	6.30 ± 1.98
Viscous Friction	$0.1 - 15$	4.83 ± 1.57

for the contact parameters do not influence the final solution of the optimization procedure: the value of the optimal parameters always converge to a specific solution as shown in Tab. 13. The only discrepancy is due to a short (less than 0.06 s) loss of contact between the foot and the ground occourring at 0.67% of the stance phase. This difference corresponds with the beginning of the other foot's stance. The new contact could have a limited influence on left foot forces. We expect to have a similar behavior in the real forces but the low sample frequency (60 Hz) of the force plates may not be able to catch this sharp peak.

5.4.2 *Validation of optimized parameters*

The motion capture system was used to capture a novel set of trials that were not used for calibration purposes. The novel trials were only used to validate ability of the calibrated contact model to reproduce experimentally observed robot motion data. Figure 5(a) shows the experimental and simulated vertical ground reaction forces for the right foot during the same walking trial. The RMSE function value between the real values and the ones obtained with a dynamic simulation using the previously evaluated contact parameters is equal to 70.012 N suggesting a substantially good match. The optimal parameter set was also used to simulate the robot movement on two additional gait trails (Figure 5(b) and 5(c) Again, we were able to obtain low RMSE errors between experimental and predicted GRFs with values of 68.490 N and 52.178 N on the two trials, respectively. The really close behavior of simulated and real forces shown in the Figure 5 demonstrate the correctness of the parameters estimated in the previous step.

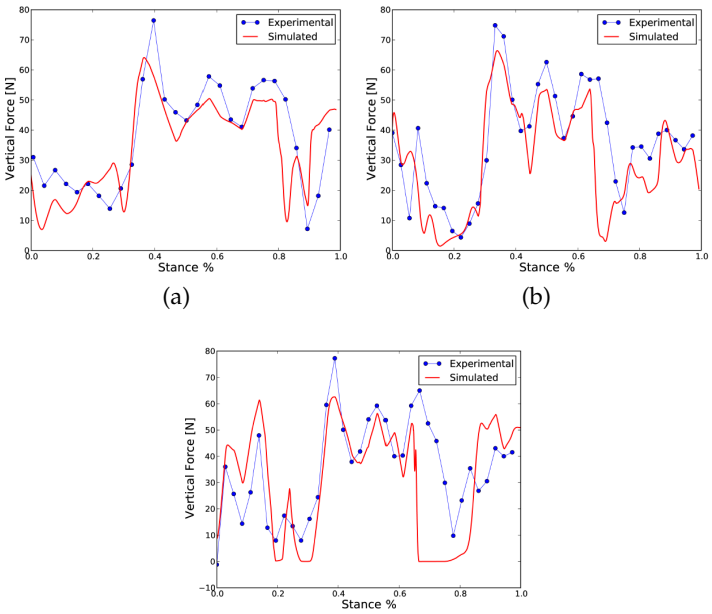

Figure 25: Validations results on different stance phase: (a) right foot stance on the same trial (RMSE of 70.012 N) (b) and (c) left foot stances on different trial acquisitions (RMSE of 68.490 N and 52.178 N, respectively).

6

SUBJECT MONITORING IN HOME REHABILITATION: EMG MODEL

6.1 INTRODUCTION

In this chapter a new approach to estimate muscle forces and the joint torque, during training or rehabilitation assisted by robotic devices, is presented.

Although good results in the motor relearning can be achieved using preprogrammed robotic assistive device, a better knowledge of the patient intentions and efforts could represent a great improvement in the treatment and device design. A promising approach to capture the interanl dynamics of the user is the use of a neuromusculoskeletal (NMS) model, which is able to reproduce, step by step, the no linear relation between the electromyographic (EMG) signals and its external manifestation such as anatomical muscle forces and joints torque. The critical point is the acquisition of the EMG signals that requires a complex setup. In this chapter we peopose a procedure to avoid direct measurement of EMG signals during cyclic movement.

The chapter contains a comprehensive explanation about the hypothesis and methodologies followed to produce a Subject and Task Specific EMG Model which could be useful in the robotic rehabilitation. Experimental setup and the procedure used to evaluate the obtained results are described.

At the end of the chapter, the obtained results are presented to reinforce and complete the proposed solution.

6.2 MOTIVATION FOR EMG MODEL USE

Every year alterations in locomotion afflict an increasing number of people. Population aging and neurological disorders or injuries are the main causes [105, 76]. Personalized rehabilitation treatment, actually designed on the anatomical, physiological, and neurological patient characteristics, can restore motor functionalities [99, 60, 91]. Traditional rehabilitation relies on therapists to personalize the treatment. Effectiveness of this approach is very high, but also its cost due to the required number of therapists and sessions. Beside the cost, recovery time and achievable results are strictly correlated on the therapists skills. In order to decrease the cost and speed up the recovery process, robotic technologies have been increasingly introduced in rehabilitation to assist the patient in the repetition of exercises. Examples are automated treadmill assisting the gait rehabilitation through

pre-programmed gait patterns [56, 101] or orthoses that support over-ground locomotion with the objective of relearning gait [52, 8, 35]. The major limitation is that all these devices could push the patient to behave in a passive way, and there is no evaluation about his real efforts and improvements during the exercise. The current research challenge is to move from passive to active devices, able to understand patient's intention and adapt to the current state of the specific subject. Moreover the knowledge of internal forces, moments, and dynamic variables during movement could improve the designed of rehabilitation. Since in vivo muscle force measurements are not practical optimization techniques are used to predict muscle forces using differen cost functions [71, 18]. Forward dynamics simulations optimize muscle excitation patterns to reproduce movement kinematics estimating the muscle forces are also used [72, 94]. However, they use cost functions which may wrongly predict co-contraction and cannot account for different muscle synergy patterns during various tasks. Actually, effective control strategies for rehabilitation robot can be design using this approaches but still missing a monitoring about real subject condition, intention and improvement during the treatment.

A promising approach is the use of electromyographic (EMG) signals, which are electrical potential generated in the muscles cells due to a neurological activation. Since EMGs has a strong relation with human motion, their non-invasive acquisition, through surface electrodes, is used as control on many robot systems such as power assit exoskeleton, intelligent wheelchair, rehabilitation robot, and prosthesis. Each system try to interpreter the subject active motion intention from EMG signals in terms of angle, motion patterns, muscles force, and joint torques.

Our research group uses Calibrated EMG-Informed Neuromusculoskeletal Modelling (CEINMS) (see Ch. 4) which is a state-of-art toolkit, which implement an EMG driven neuromusculoskeletal model able to compute muscle dynamics and joint torques [63, 85, 86]. This model takes EMG signals as inputs rather than attempting to predict how muscles are activated to produce a given movement. EMG signals also provide important information about metabolic energy consumption, muscles activities and compliance in the muscles and joints. However, collection of EMG data is still not a simple task as placement of electrodes requires professional skills and EMG data can be affected by electric and magnetic noise. It would be much easier to skip the direct measurement and predict EMG values based on other external observable variables and then use these predicted EMG data to drive the neuromusculoskeletal model. Albeit this prediction would be usually impossible for the complex relation between muscle activations and resulting movement, it could be instead feasible for the simpler, repetitive movements that are used in rehabilitation treatments. Since the used NMS model is known and deeply tested, our

efforts were focused on finding the best way to design a reliable and accurate subject and task specific EMG model. This work presents a first effort to investigate the possibility to predict EMG values during plantar-dorsiflexion (P-DF) cyclic movements, often used to rehabilitate common ankle injuries such as sprains or fractures. Based on an experimental database of EMG data collected when a subject performs P-DF movements at six different speeds, an EMG model was developed to predict electromyographic data for P-DF movements executed at arbitrary speeds. The presented results are a step in the direction of investigating the accuracy and reliability of EMG prediction for its use in driving neuromusculoskeletal models. The main advantage of the proposed approach is that, once an Subject and Task Specific EMG Model has been defined, no EMG recordings are needed for the joint torque estimation. In particular the EMG acquisition could be limited only to periodically adjust the model and asses patients improvements. This might have substantial implications in the development of novel neurorehabilitation technologies to be used in home and self treatments. Despite its applicability limited to repetitive movements it would greatly simplify the use of rehabilitation devices and still keeping their possibility to be driven by patient's intention and monitoring the real patient's movement recovery.

6.3 METHODS

6.3.1 *Participants*

Five voluntary subjects (1 female and 5 males) participated to our experiments. Their age was 25.6 ± 2.9 years (mean *pm* STD), their body weight was 66.8 ± 11.9 kg, and their height was 1.73 ± 0.12 m. The participants had no neurological or muscular disorder that could influence their movements. Participants provided written informed consent prior to participation.

6.3.2 *Equipments and setup*

Anthropometric of the subjects were obtained through a static acquisition using a motion analysis system with eight infrared digital video cameras at 256 Hz (Oqus 300, Qualisys, Gothenburg, Sweden). During the static acquisition the three-dimension location of 12 retro-reflective markers placed on the subjects' body was recorded. The markers were placed on the right leg at anatomical landmarks of thigh, shrank, and foot [32, 61]. The markers placement (Fig. 26 followed the protocol used in [26]

EMG signals were collected with a EMG-USB2 System (OT Bioelettronica, Turin, Italy) at a sample rate of 2048 Hz from the following muscles: Gastrocnemius Lateralis (GASL), Gastrocnemius Medialis

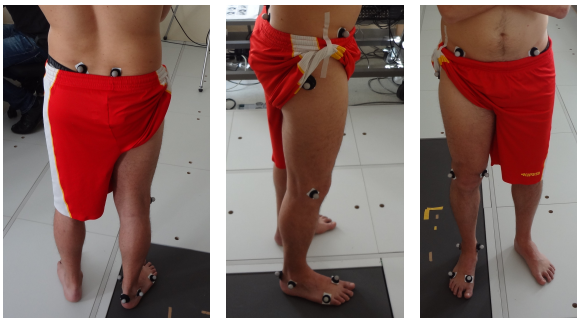

(a) (b) (c)

Figure 26: Subject with markers placed according to the adopted protocol: (a) back, (b) sagital, and (c) front view.

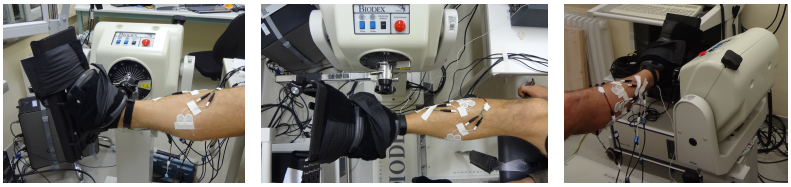

(a) (b) (c)

Figure 27: EMG electrodes placement on the subjects [49]

(GASM), Soleus (SOL), Peroneus Longus (PER), Tibialis Anterior (TIB). Bipolar electrodes sites were determined following the SENIAM [49] recommendation.

Planta-dorsi flexion (P-DF) movement of the ankle and speed were driven and recorded by a dynamometer System 3 Pro (Biodex, Corp., Shirley, NY). System 3 Pro (S3P) provides different modes of operation. In this experiment we used the *Isokinetic Mode* which allows to impose a defined trajectory and speed to the subjects. During the experiment, S3P recorded measure of the motor joint torque as result of the subject-machine movement cooperation. Kinematic data and motor joint torque from the S3P were acquired through the EMG signals amplifier to obtained synchronized data.

6.3.3 *Experimental Procedure*

The acquisition procedure was performed at the Motor physiology and Biomechanics (MBL) and the Electromyography and Motor Control (EML) Laboratories of the Department of Neurorehabilitation Engeneering of the University of Medical Center Göttingen Georg-August University (Germany). The static acquisitions were performed at the MBL while acquisition with the S3P took place at EML. Partecipants were asked to sit comfortably on the S3P keeping the right knee in a fixed position of 40° and laying the right foot on the Biodex ankle sup-

(a) (b)

Figure 28: (a) All the subjects performed the P-DF movement sitting on a S3P system and modifying their effort to track a torque visual feedback (b).

port. Before the collection of the experimental data, they were shortly instructed on the procedure and they practiced on P-DF movements with the right leg already instrumented. Then, they were asked to perform P-DF movements of the right ankle following in a passive way the movement imposed by the S3P. This task provided a torque measurement limited to the S3P movement contribution to compensate the subject foot weight. This torque was then used to correctly estimate the subject torque contribution.

Afterwords the subjects were instructed to repetitively span the whole range of motion, starting at the maximum plantarflexion angle, reaching the maximum value for dorsiflexion and then going back to the starting position. Since the speed was always imposed by the S3P, the subjects could produce different efforts, trying to speed-up or, alternatively, speed-down the ankle support movement. In this work the subjects were asked to follow the movement trying to speed-up it while they were producing their maximum effort. A visual feedback, developed using Matlab (MathWorks, Natick, MA), helped the subjects in keeping their maximum effort. The feedback was calibrated for each speed and it provided a mean torque curve obtained from their first maximal effort trial.

Tests were executed at six different speeds, chosen for feasibility and safeness for the subject: 30 °/s, 45 °/s, 60 °/s, 75 °/s, 90 °/s, 120 °/s. For each trial the subject performed at least five P-DF repeating the acquisition four times for each speed.

The collection of the movement data at different speed was aimed at obtaining a subject-specific EMG Model covering the whole range of variability of the ankle movement during rehabilitation exercises.

6.3.4 *EMG Data Processing*

Raw *EMG signals* were processed by high-pass filtering (Butterworth, IV order, 300 Hz), rectification, and low-pass filtering (Butterworth, IV order, 8 Hz) [63]. The resulting EMG linear envelopes were then normalized using the maximum EMG peak obtained for each muscle during the execution of all trials.

6.4 TOOLS

6.4.1 *EMG Model*

The objective of the proposed EMG model is to use only the plantar-dorsiflexion speed and anle position to predict muscle EMG values during the P-DF cyclic ankle movement.

For each participant, a subject-specific EMG model was built based on the data from the P-DF cyclic movement at six different speed (30 °/s, 45 °/s, 60 °/s, 75 °/s, 90 °/s, 120 °/s). For each speed and muscle, an average EMG mean curve was first computed. EMG data and ankle P-DF of nine cycles for each speeds were used to build the model. Then, for each muscle, the curves at different speeds were time warped over 2000 samples releasing the time dependance, to allow the computation of a single average curve. Eq. 6.1 reports this concept where emg is the measured emg value for the muscle m at speed s. After the warping its value is a function of the sample k.

$$emg_{m,s}(t) \rightarrow emg_{m,s}(k) \tag{6.1}$$

After the warping, each curve could be included in the mean calculation obtaining a mean EMG curve for each muscle.

$$EMG_m(k) = \frac{\sum_s emg_{m,s}(k)}{N_s} \tag{6.2}$$

Equation does not indicate the acquisition trial number to simplify the notation. However, increasing the number of trials ensures to limit the influence of possible errors in EMG measurement. These curves, one for each muscle, can then be used to estimate EMGs at the cadences required in the rehabilitation treatment. Starting from the time required to execute a complete P-DF (input of the model), for each muscle the average EMG curve previously computed is un-warped to match the current task speed thus generating a first prediction of EMG signals. In other words, the EMG model extraction procedure can be described as a linear regression from an experimental EMG data set, measured during subject P-DF movement. Additionally, the model has to consider that the movement speed influences the peak of the EMG curves. Therefore, we introduced a shape factor index to correct the model curve is estimated. The EMG model maximum value for each muscle is compared with the maximum value of the mean curves for each speed calculating a shape factor index that is the ratio between them. These indexes are used to scale the EMG model curves to obtain a better fitting with the experimental data.

6.4.2 *CEINMS*

In this work CEINMS was used to estimate subject individual muscle forces and joint moments [13, 63]. Ch. 4 reports a comprehensive in-

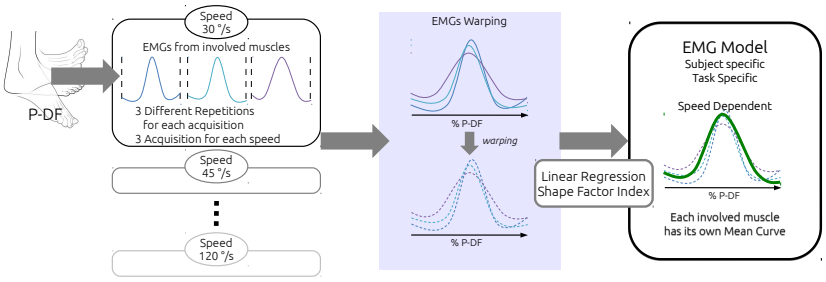

Figure 29: Flow chart of the EMG Model. To extract the EMG model each subject performed P-DF cyclic movements at six different speeds. EMG values were collected from the mainly involved muscles: GASL, GASM, TIB, PER, and SOL. The acquisition was repeated 5 times for each speed. To obtain speed-independent curves, we warped the curves in an average EMG curve. For each muscle, we extracted through a linear regression an average speed-independent EMG curve which is subject and task specific. Moreover, a shape factor index, to correct the model curves, is estimated. An estimation of the real EMGs can then be obtained stretching these curves based on the movement speed.

troduction to the human neuronusculoskeletal modelling. Recorded joint kinematics and EMGs are the main inputs of the model. The EMG-driven model could be explained as three separate and related sub-models: anatomical, muscle activation dynamics, and muscle contraction dynamics. The anatomical model of the lover limbs was developed using OpenSim [73], and its extensions. It was used to determine subject muscle tendon lengths and moment arms for the ankle plantar-dorsiflexors. The muscle activation dynamics model transforms experimental EMG to muscle activation. Raw EMGs were processed (filtered, rectified, and normalized) and then, through a recursive filter, was possible to determine neural activation. Muscle activations and joint kinematics were inputs in a modified Hill-type muscle model to calculate individual muscle forces. Once each single muscle force is calculated, they were multiplied for their specific moment arms obtaining the joint moment. In this work the experimental EMGs was used to calibrate the NMS model parameters. The synthesized EMGs, extracted from the EMG model, was used as input to estimate the ankle joint torque. This was done to directly compare the estimated torque with the experimental one. An additional comparison was done on the estimated torque obtained with the experimental EMGs as input for CEINMS.

6.4.3 *EMG Model Validation*

The ability of the EMG Model to estimate EMGs collected from the subject was tested in two separate validation procedures. The synthe-

sized EMG have to be sufficient accurate and realiable to maintain the possibility of monitor the subject internal parameters. Each analysis of the obtained results was performed calculating the root mean square error (RMSE) and the Pearson product moment correlation R^2 to provide quantitative values for accuracy and reliability of the proposal EMG model. Both the validation procedures were performed using data from trials not included in the model extraction.

In the first validation procedure, synthetic EMGs were compared with experimental ones. This step was necessary to asses the accuracy and reliability of our proposed EMG model for different muscles and speeds. Indeed, muscles location and their different involvement in the selected movement could limit the accuracy of the collected EMG signals in some trials. Since the following step depends on the quality of the synthetic EMG, we provide an analysis of the predicted EMG signals. At first we averaged the obtained values on different speeds but maintaining the muscle separation. Then as the experimental procedure covered a quite wide range of movement speeds, we also report the obtaining values for an analysis of the systhetic EMGs among different speed, but averaged on the muscle.

In the second validation procedure, synthetic EMGs from the model were used as input for CEINMS, to predict muscles forces, joint moments and all the human internal dynamics parameters useful the subject monitoring. Synthesized EMGs were used as input for CEINMS, and the estimated joint moments were evaluated through a comparison with the experimental ones. Experimental EMGs were used as input to CEINMS to check how well it can estimate the joint moment, providing a maximal target for the accuracy and reliability for further evaluation. This evaluation could be the most important because it reproduce the same operating mode for which our proposal EMG Model was developed. CEINMS was calibrated using the experimental EMGs. Finally, a further evaluation was reported in which a comparison between estimated torques by CEINMS, taking as input both synthesized and experimental EMG curves, providing direct measurement on the discrepancies between them.

6.5 RESULTS

The first test evaluated the accuracy of the EMGs from the model through a comparison with experimental values obtained at the same speed but in trials which were not included in the model creation procedure. Results from this analysis are reported in Tab. 14 and Tab. 15.

Table 14: Comparison between estimated and experimental EMGs on different muscles. Results are averaged on 3 trials for each speed.

		Subject ID				
Muscle		S0	S1	S2	S3	S4
Gastrocnemius Lateralis	RMSE ± STD	0.094 ± 0.018	0.091 ± 0.029	0.078 ± 0.022	0.068 ± 0.013	0.063 ± 0.024
	R^2 ± STD	0.819 ± 0.074	0.667 ± 0.211	0.803 ± 0.131	0.876 ± 0.087	0.79 ± 0.098
Gastrocnemius Medialis	RMSE ± STD	0.097 ± 0.020	0.057 ± 0.019	0.103 ± 0.025	0.069 ± 0.015	0.084 ± 0.02
	R^2 ± STD	0.827 ± 0.080	0.733 ± 0.147	0.8 ± 0.112	0.867 ± 0.088	0.828 ± 0.082
Peroneus Longus	RMSE ± STD	0.126 ± 0.023	0.097 ± 0.03	0.083 ± 0.020	0.094 ± 0.017	0.07 ± 0.013
	R^2 ± STD	0.423 ± 0.222	0.754 ± 0.14	0.784 ± 0.099	0.789 ± 0.128	0.776 ± 0.148
Soleus	RMSE ± STD	0.102 ± 0.017	0.104 ± 0.021	0.061 ± 0.014	0.089 ± 0.014	0.083 ± 0.017
	R^2 ± STD	0.722 ± 0.133	0.614 ± 0.17	0.729 ± 0.237	0.806 ± 0.139	0.758 ± 0.105
Tibialis Anterior	RMSE ± STD	0.118 ± 0.036	0.110 ± 0.039	0.087 ± 0.017	0.094 ± 0.023	0.087 ± 0.027
	R^2 ± STD	0.784 ± 0.271	0.723 ± 0.098	0.887 ± 0.016	0.862 ± 0.048	0.873 ± 0.077

Tab. 14 reports the behaviour of the model for the different muscle averaged on all movement speeds. The average RMS error is 0.088 ± 0.017 which means, since the EMGs values are normalized, error usually less than 10%. The overall R^2 is equal to 0.785 ± 0.094 showing that predicted curves have good correlated with the experimental ones. As already said in Sec. 6.4.3 different accuracy obtained for different muscles is manly due to two aspects: electrodes placement and their involvement during the P-DF. For example, Tibialis Anterior, which is the main involved muscle during the dorsiflexion and easy to acquire for its position, shows the better results, both in term of RMSE and R^2. On the opposite side, Peroneous Longus, which is only partially involved in both plantar and dorsiflexion was more difficult to characterize and its performance is the worst one. Subject S0 and Subject S1 exhibit the worst behavior, probably due to their specific anatomical and geometrical body characteristics which required different solutions on the electrodes placement and amplification during the EMG signals recording. Despite this limitation, only the Peroneous Longus of the Subject S0 presents a RMSE and an R^2 which actually could require a new data collection to extract a more accurate model.

Table 15: Comparision between estimated and experimental EMGs on different speeds. Results are averaged on all muscles using 3 trials for each speed.

Speed °/s		Subject ID				
		S0	S1	S2	S3	S4
30	RMSE ± STD	0.125 ± 0.022	0.123 ± 0.033	0.093 ± 0.029	0.09 ± 0.028	0.079 ± 0.024
	R^2 ± STD	0.56 ± 0.184	0.519 ± 0.181	0.704 ± 0.151	0.664 ± 0.146	0.685 ± 0.147
45	RMSE ± STD	0.11 ± 0.025	0.072 ± 0.018	0.088 ± 0.021	0.079 ± 0.02	0.077 ± 0.027
	R^2 ± STD	0.663 ± 0.208	0.646 ± 0.15	0.608 ± 0.183	0.854 ± 0.07	0.789 ± 0.074
60	RMSE ± STD	0.086 ± 0.01	0.074 ± 0.021	0.065 ± 0.015	0.072 ± 0.015	0.064 ± 0.01
	R^2 ± STD	0.851 ± 0.078	0.8 ± 0.07	0.869 ± 0.042	0.882 ± 0.06	0.826 ± 0.075
75	RMSE ± STD	0.1 ± 0.012	0.121 ± 0.033	0.099 ± 0.014	0.078 ± 0.018	0.088 ± 0.019
	R^2 ± STD	0.776 ± 0.114	0.624 ± 0.153	0.847 ± 0.044	0.9 ± 0.043	0.785 ± 0.096
90	RMSE ± STD	0.096 ± 0.036	0.092 ± 0.023	0.062 ± 0.014	0.083 ± 0.016	0.075 ± 0.028
	R^2 ± STD	0.745 ± 0.271	0.787 ± 0.098	0.921 ± 0.016	0.879 ± 0.048	0.858 ± 0.077
120	RMSE ± STD	0.127 ± 0.017	0.069 ± 0.019	0.088 ± 0.019	0.096 ± 0.012	0.08 ± 0.015
	R^2 ± STD	0.694 ± 0.181	0.812 ± 0.07	0.854 ± 0.05	0.861 ± 0.047	0.887 ± 0.044

Probably, they were not able to correctly coordinate their movement with the one imposed by the dynanometer, producing EMG signals not reproducible across different trial acquisition. Better results are obtained at the other speeds, which were easy to perform to the subjects, where we could observe the subjects had no difficult to execute the movement. This is confirmed by the Biodex Manual Reference, that suggests $60\,^{\circ}/s$ as the lowest speed for reliable acquisitions of a P-DF movement. However, we decide to include these data to asses the behavior of CEINMS on the joint moment estimation when synthetic EMGs with high error are used. Again Subjects S0 and S1 show the worst behavior, which again confirms possible errors in data collection procedure,

Amore detailed analysis is resented for subject S3. For Subject S3, Fig. 30 - 35 report the plots detailing results about EMG model prediction among different muscle and speed.

The second part of the proposal EMG model validation involved also CEINMS. The objective was evaluate the synthesized EMGs as input for CEINMS, and the obtained performance values are reported in Tab. 18. This validation aims to assess the CEINMS muscle force and joint moments prediction when it takes synthetic EMGs from the model as input. First, the experimental ankle torques are used as reference to asses the joint moments estimated by CEINMS with experimental EMGs (Tab. 16). This step was required to obtain a maximum reachable accuracy. An overall $R^2 = 0.885 \pm 0.042$ confirms a good correlation between the estimated joint moments and the experimental ones despite the RMSE of 11.595 ± 2.813 indicating a remarkable error. However, this error is mainly concentrated in the prediction of the first moment peak related to change movement from dorsi to plantar flexion. This was partly expected because all the subject, have difficulty in synchronously follow the S3P support in this phase resulting in a experimental torque mainly due to the S3 contribution. Fig. 36 shows this effect and represent the best reachable fitting from the experimental data set used for the calibration.

The second step evaluated the effect of using the synthesized EMGs as input for CEINMS. Tab. 18 summarized the obtained results. Overall RMSE of 12.595 ± 2.876 and R^2 of 0.857 ± 0.053 are really close to ones obtained using as input the experimental EMGs. This is an important result because it indicates that the accuracy of our EMG model allows to use the synthetized EMG signals instead of the experimental one, without losing too much accuracy in the prediction. This is also show by Fig. 37 that have quite similar behavior of the one reported in Fig. 36. Moreover, the low influence of the synthetized EMGs in the CEINMS torques estimation is well shown in Fig. 38, where the predicted torque using the synthesized EMGs are almost inside the range of the the torque which are predicted using the experimental EMGs. This graphical observation is strongly confirmed by Tab. 18, where

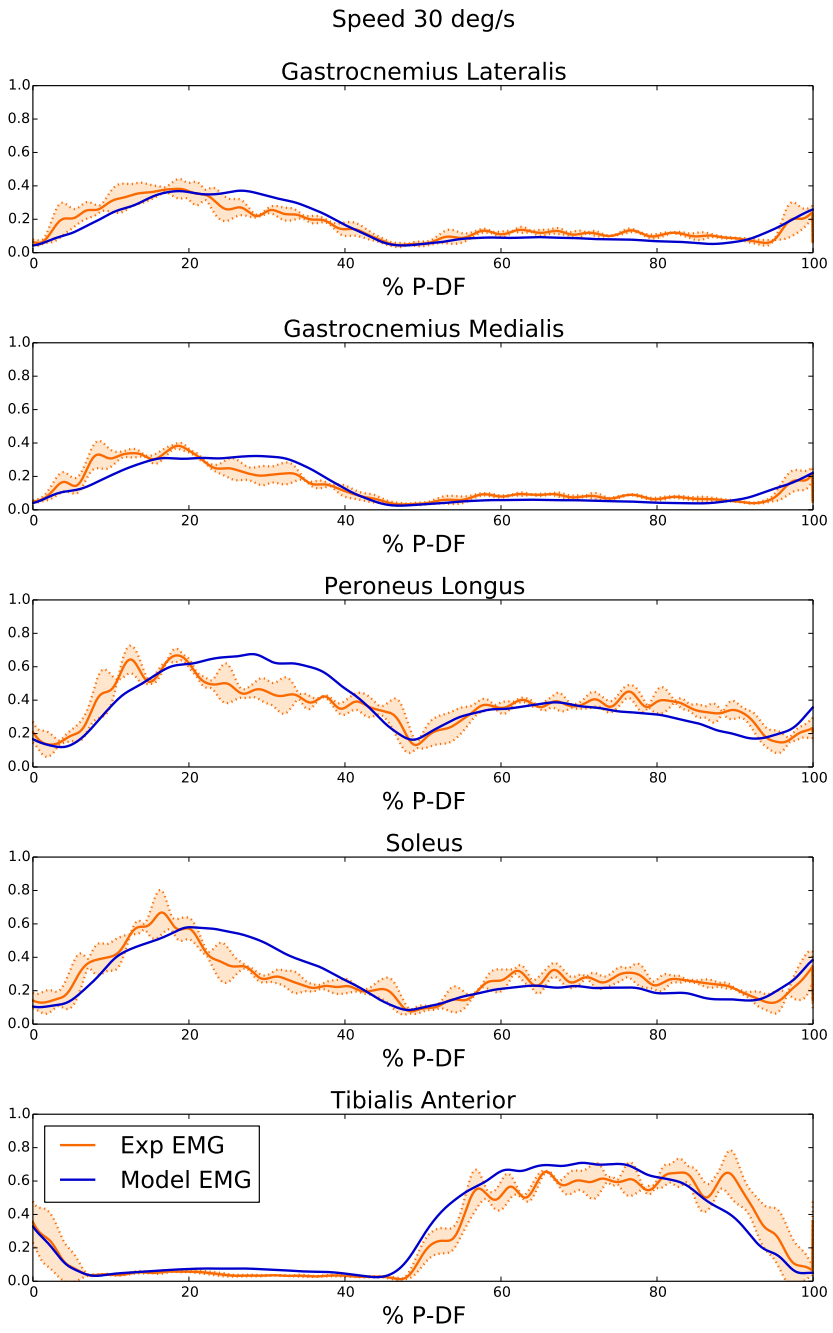

Figure 30: Comparison between estimated EMG signals and measured ones for each muscle of subject S03 reported as a percentage of the P-DF cycle at speed 30 °/s. Gray areas reports the ± STD intervals of the reference

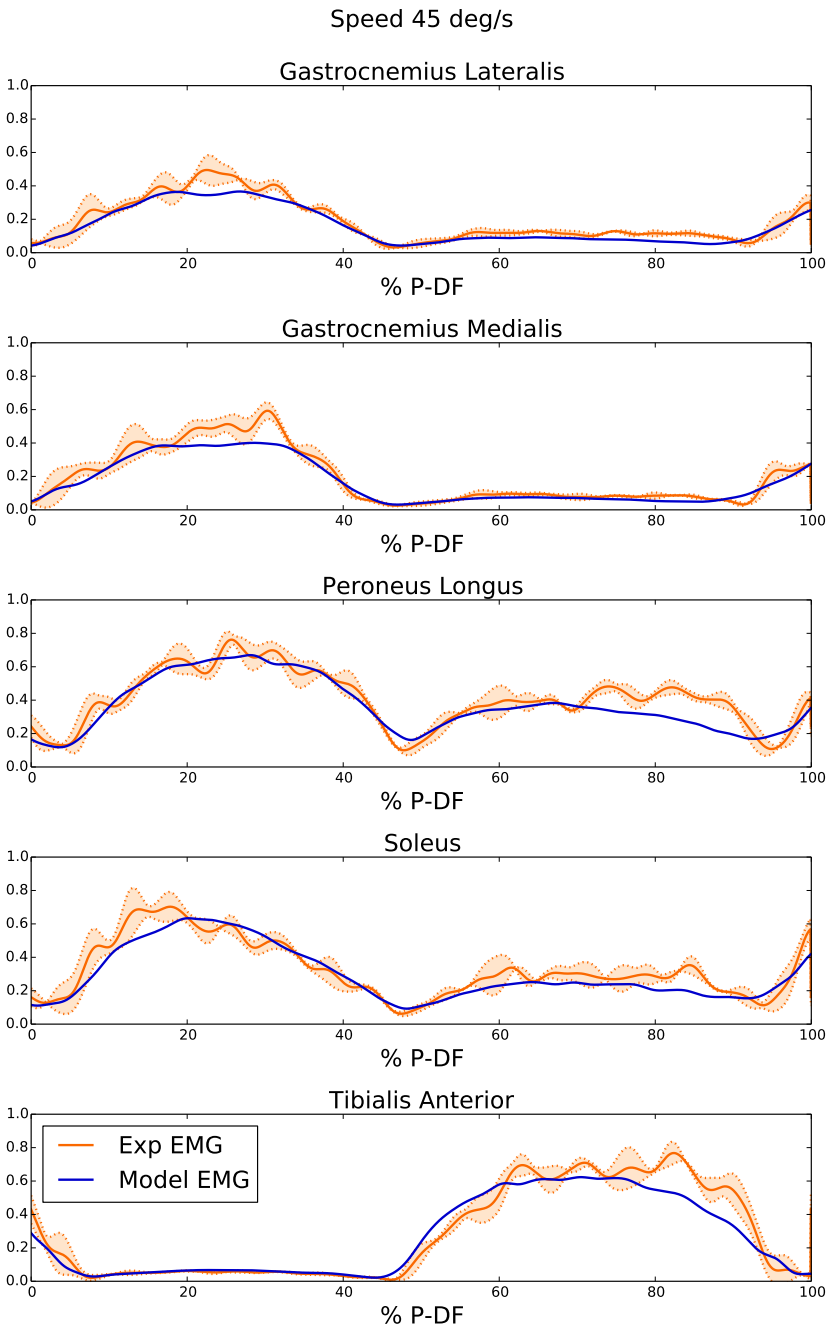

Figure 31: Comparison between estimated EMG signals and measured ones for each muscle of subject S03 reported as a percentage of the P-DF cycle at speed 45 °/s. Gray areas reports the ± STD intervals of the reference

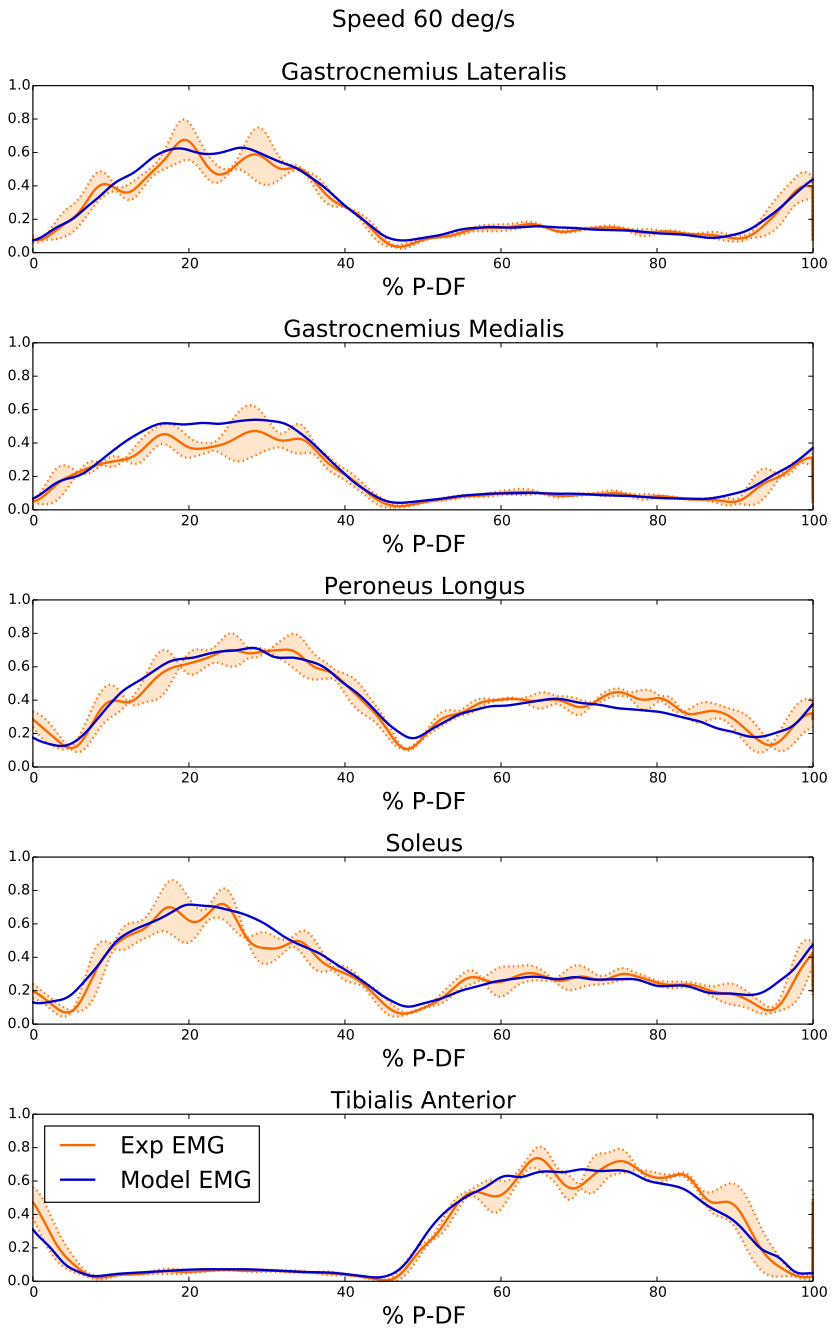

Figure 32: Comparison between estimated EMG signals and measured ones for each muscle of subject S03 reported as a percentage of the P-DF cycle at speed 60 °/s. Gray areas reports the ± STD intervals of the reference

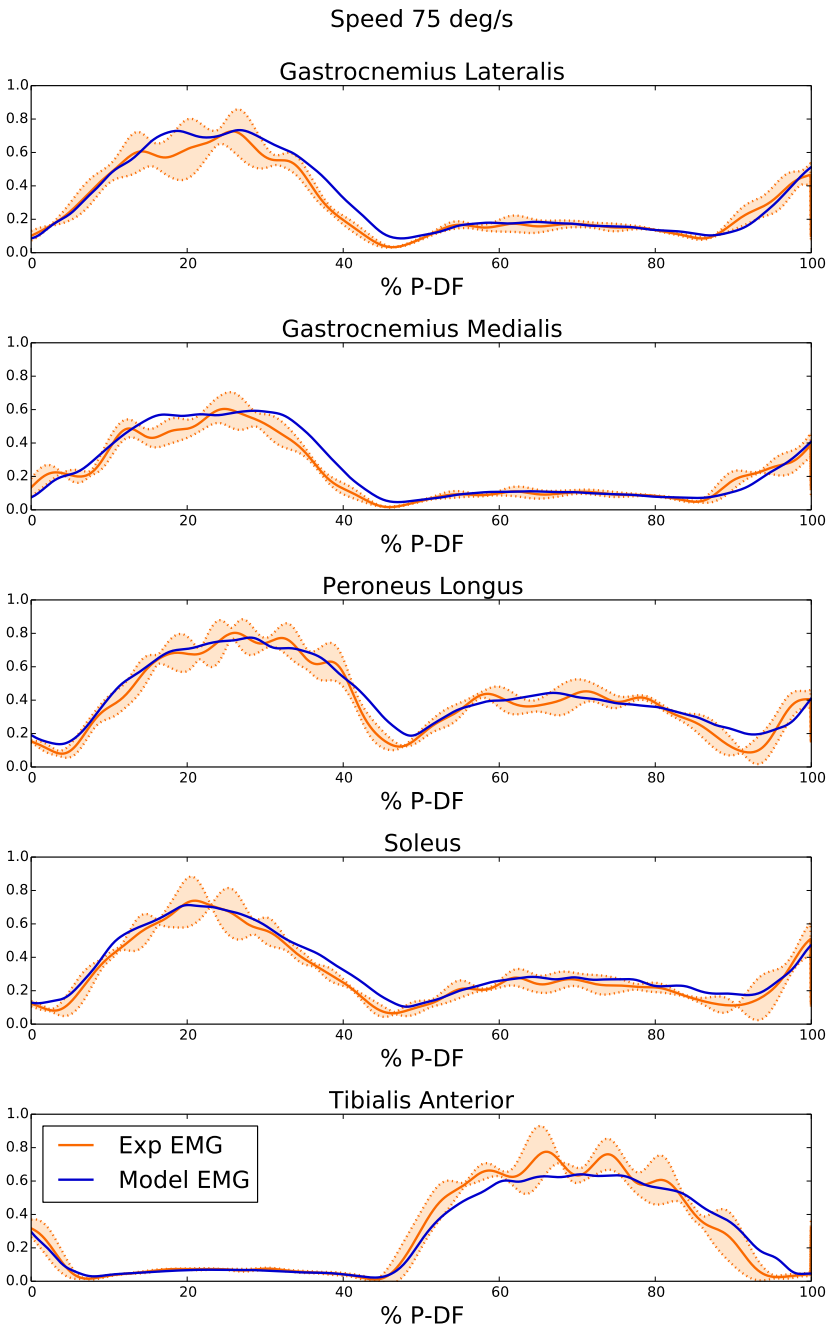

Figure 33: Comparison between estimated EMG signals and measured ones for each muscle of subject S03 reported as a percentage of the P-DF cycle at speed 75 °/s. Gray areas reports the ± STD intervals of the reference

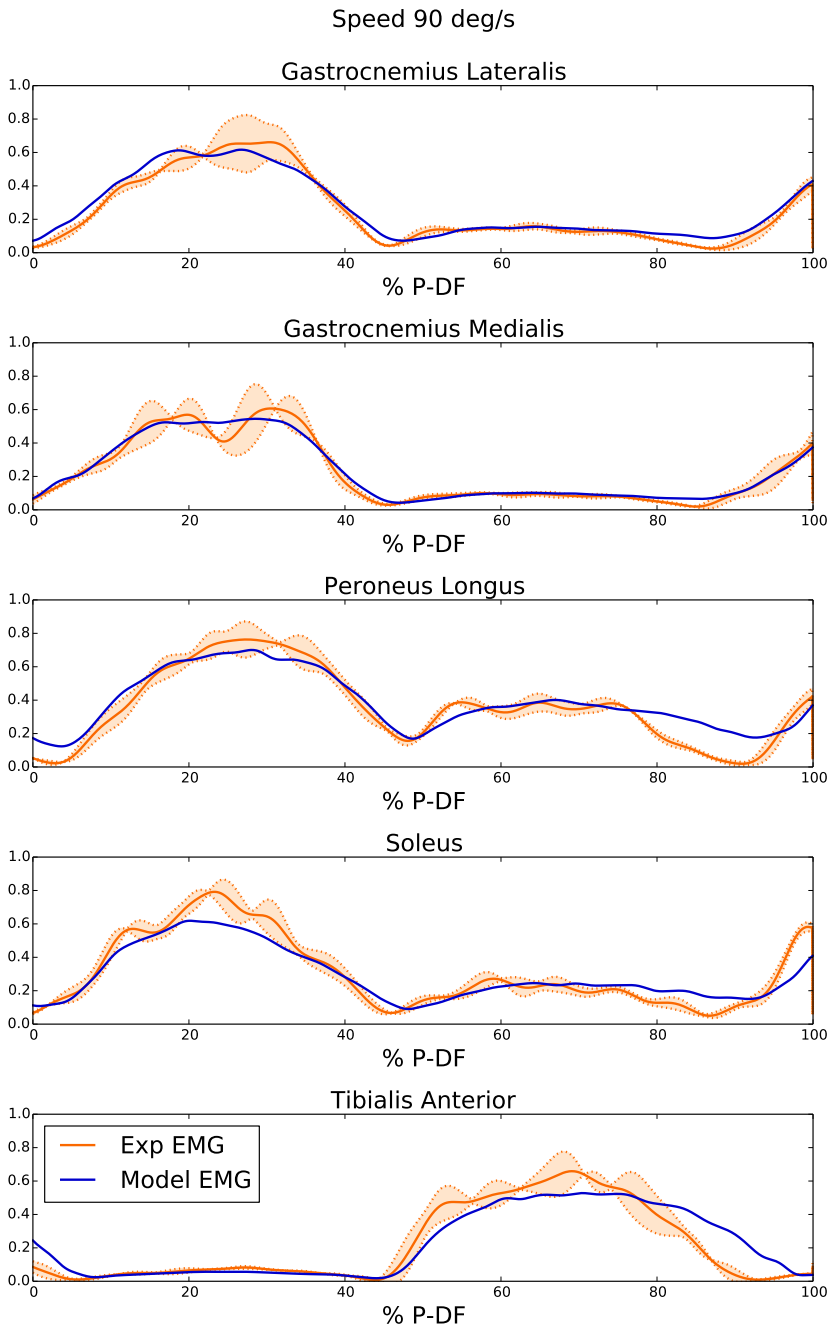

Figure 34: Comparison between estimated EMG signals and measured ones for each muscle of subject S03 reported as a percentage of the P-DF cycle at speed 90 °/s. Gray areas reports the ± STD intervals of the reference

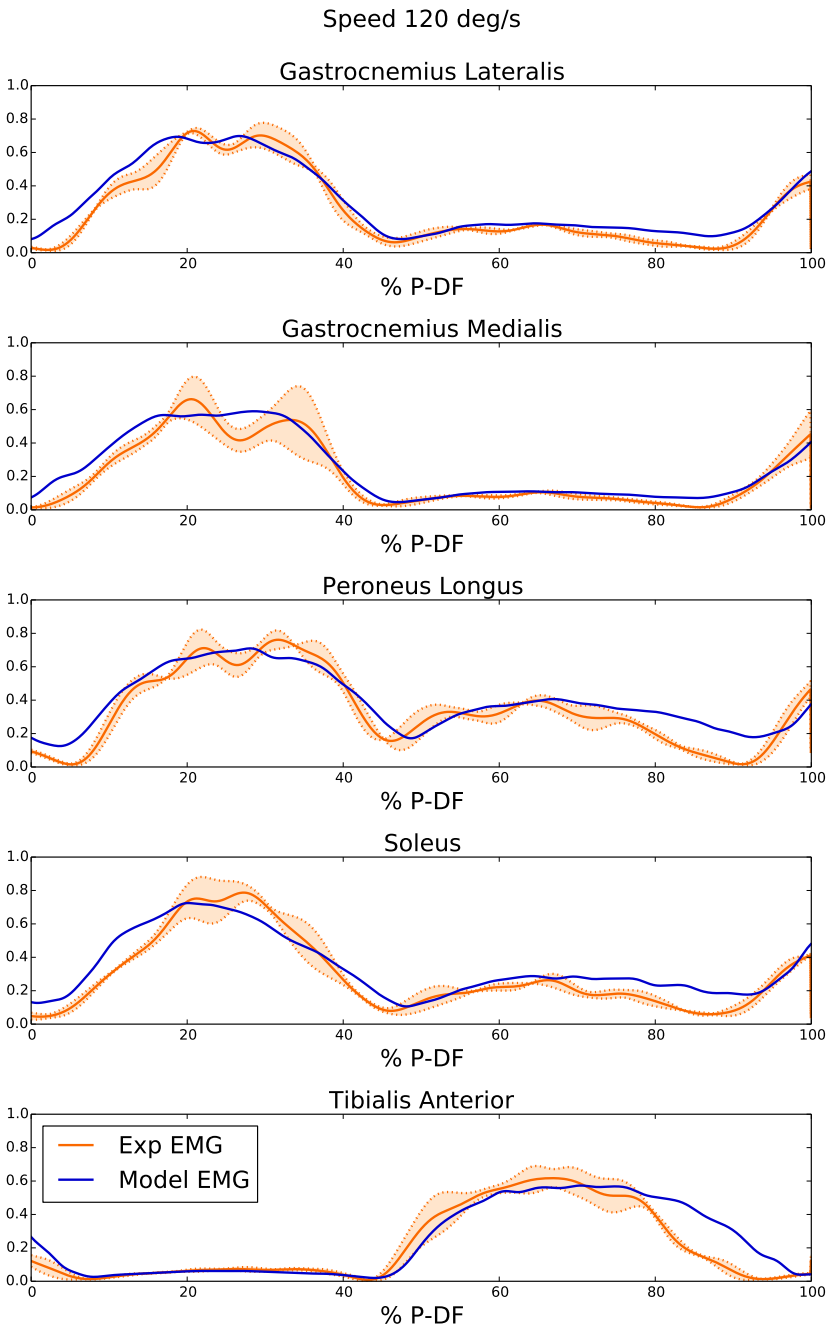

Figure 35: Comparison between estimated EMG signals and measured ones for each muscle of subject S03 reported as a percentage of the P-DF cycle at speed 120 °/s. Gray areas reports the ± STD intervals of the reference

the RMSE values is very low among each subject and speed and R^2 is really close to 1 for each speed. Actually, a worst behavior can be found for the speed $30\,°/s$, but as said before, the EMG model was not very accurate for this speed. However, despite the lower precision, the result are still acceptable.. As our first objective was to provide an alternative solution to the direct EMGs measurement, the overall RMSE of 5.930 ± 1.595 and $R^2 = 0.963 \pm 0.028$ demonstrated the feasibility of our work.

Table 16: Comparision between experimental torques and the one estimated by CEINMS with the experimental EMGs as input averaged on 9 trials for each speed.

		Subject ID				
Speed °/s		S0	S1	S2	S3	S4
30	RMSE ± STD	10.35 ± 1.645	12.691 ± 0.658	13.861 ± 2.348	14.352 ± 1.818	15.526 ± 3.213
	R^2 ± STD	0.918 ± 0.022	0.879 ± 0.014	0.889 ± 0.02	0.891 ± 0.031	0.921 ± 0.016
45	RMSE ± STD	7.704 ± 0.754	8.434 ± 1.41	13.539 ± 2.174	13.912 ± 1.747	13.412 ± 4.022
	R^2 ± STD	0.921 ± 0.016	0.85 ± 0.037	0.856 ± 0.03	0.85 ± 0.03	0.943 ± 0.019
60	RMSE ± STD	9.544 ± 1.903	9.484 ± 1.606	11.774 ± 0.992	15.055 ± 2.095	11.705 ± 1.995
	R^2 ± STD	0.914 ± 0.021	0.842 ± 0.032	0.889 ± 0.014	0.888 ± 0.019	0.908 ± 0.026
75	RMSE ± STD	7.979 ± 0.801	7.879 ± 1.621	17.968 ± 3.371	12.273 ± 1.33	11.013 ± 1.64
	R^2 ± STD	0.915 ± 0.018	0.838 ± 0.053	0.87 ± 0.019	0.895 ± 0.024	0.927 ± 0.014
90	RMSE ± STD	7.687 ± 0.731	8.443 ± 0.528	14.733 ± 1.852	12.09 ± 0.679	9.303 ± 1.039
	R^2 ± STD	0.932 ± 0.007	0.812 ± 0.031	0.865 ± 0.02	0.878 ± 0.014	0.937 ± 0.016
120	RMSE ± STD	9.161 ± 2.288	8.548 ± 1.099	15.563 ± 2.066	12.302 ± 1.26	11.565 ± 2.801
	R^2 ± STD	0.92 ± 0.016	0.748 ± 0.049	0.852 ± 0.021	0.883 ± 0.023	0.91 ± 0.031

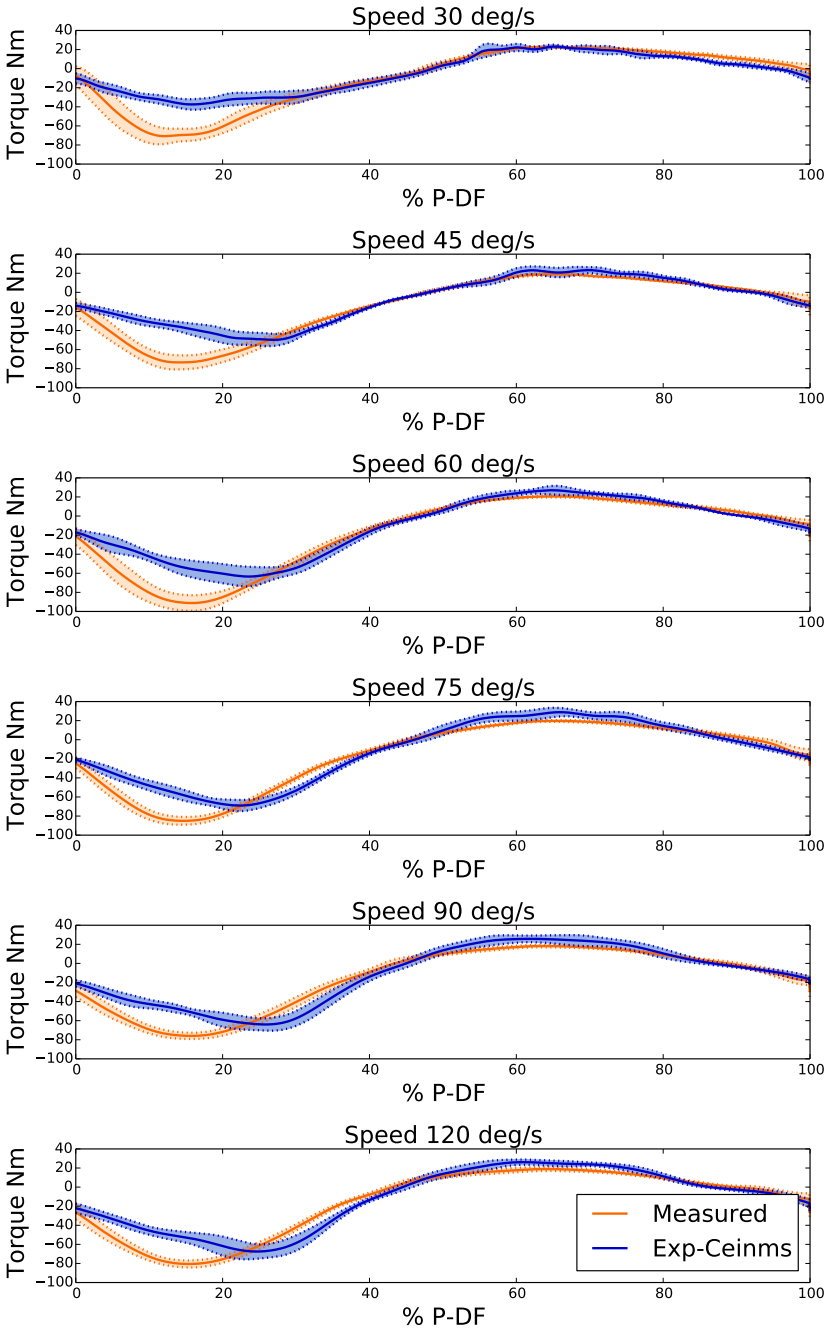

Figure 36: Comparison between estimated torques (blue line) by CEINMS, with experimental EMG signals as input, and measured ones (orange line) for the subject 03 reported as a percentage of the P-DF cycle at each speed. The light areas report the ± STD intervals of the torque values.

Table 17: Comparision between experimental torques and the one estimated by CEINMS with the synthesized EMGs as input averaged on 9 trials for each speed.

		Subject ID				
Speed °/s		S0	S1	S2	S3	S4
30	RMSE ± STD	13.101 ± 2.015	13.582 ± 1.41	15.46 ± 2.663	16.412 ± 2.707	16.331 ± 5.025
	R^2 ± STD	0.786 ± 0.066	0.821 ± 0.039	0.856 ± 0.037	0.783 ± 0.052	0.9 ± 0.048
45	RMSE ± STD	11.536 ± 1.283	10.172 ± 1.936	12.433 ± 1.498	14.637 ± 2.522	15.391 ± 3.943
	R^2 ± STD	0.816 ± 0.042	0.782 ± 0.086	0.873 ± 0.02	0.859 ± 0.029	0.918 ± 0.019
60	RMSE ± STD	10.212 ± 2.703	10.744 ± 2.247	12.067 ± 1.225	15.374 ± 3.127	13.759 ± 2.619
	R^2 ± STD	0.912 ± 0.029	0.778 ± 0.056	0.884 ± 0.023	0.869 ± 0.036	0.88 ± 0.044
75	RMSE ± STD	7.882 ± 1.019	9.09 ± 2.901	19.033 ± 3.453	13.351 ± 1.498	12.952 ± 3.062
	R^2 ± STD	0.914 ± 0.027	0.785 ± 0.114	0.837 ± 0.027	0.858 ± 0.025	0.901 ± 0.042
90	RMSE ± STD	7.706 ± 0.991	9.527 ± 0.699	13.906 ± 2.261	11.242 ± 1.464	11.038 ± 2.815
	R^2 ± STD	0.925 ± 0.014	0.81 ± 0.05	0.878 ± 0.023	0.891 ± 0.032	0.948 ± 0.026
120	RMSE ± STD	8.979 ± 2.62	9.165 ± 1.095	16.776 ± 2.557	11.284 ± 1.319	14.697 ± 2.372
	R^2 ± STD	0.913 ± 0.039	0.744 ± 0.075	0.831 ± 0.024	0.896 ± 0.021	0.876 ± 0.047

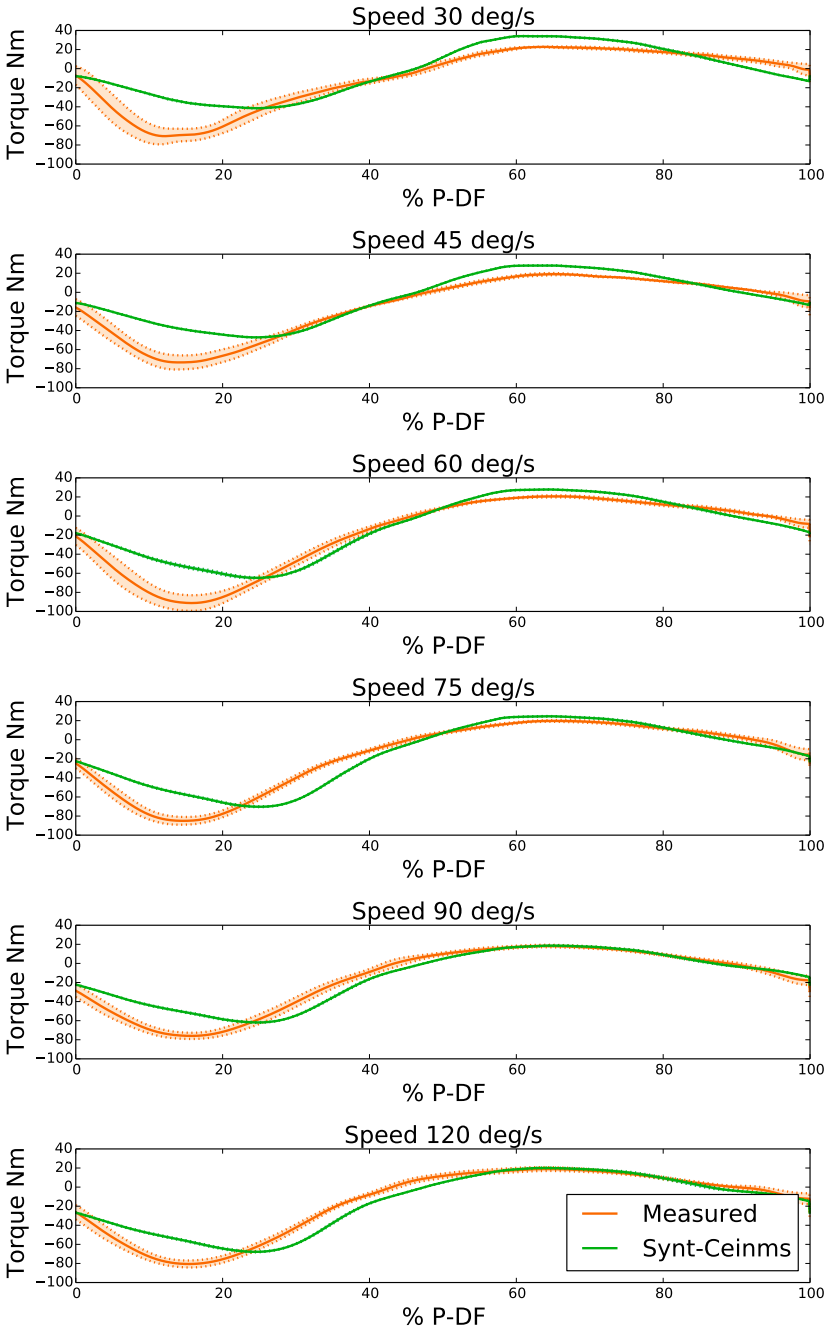

Figure 37: Comparison between estimated torques (green line) by CEINMS, with synthesized EMG signals as input, and measured ones (orange line) for the subject 03 reported as a percentage of the P-DF cycle at each speed. The light areas reports the ± STD of the measured torque values.

Table 18: Comparision between estimated torques by CEINMS with the synthesized and experimental EMGs as input averaged on 9 trials for each speed.

		Subject ID				
Speed °/ s		S0	S1	S2	S3	S4
30	RMSE ± STD	8.652 ± 3.119	7.809 ± 1.893	6.212 ± 1.625	8.667 ± 0.516	8.091 ± 1.766
	R^2 ± STD	0.886 ± 0.079	0.888 ± 0.065	0.966 ± 0.018	0.928 ± 0.013	0.965 ± 0.019
45	RMSE ± STD	7.969 ± 1.435	4.759 ± 1.379	7.828 ± 1.291	5.403 ± 1.169	7.433 ± 1.446
	R^2 ± STD	0.914 ± 0.03	0.946 ± 0.046	0.954 ± 0.012	0.973 ± 0.013	0.975 ± 0.012
60	RMSE ± STD	4.247 ± 1.581	4.133 ± 1.34	4.809 ± 1.698	5.003 ± 1.164	5.429 ± 1.486
	R^2 ± STD	0.981 ± 0.016	0.952 ± 0.031	0.985 ± 0.012	0.981 ± 0.006	0.982 ± 0.01
75	RMSE ± STD	3.902 ± 0.795	4.904 ± 2.517	5.127 ± 2.087	5.645 ± 1.431	6.417 ± 1.784
	R^2 ± STD	0.981 ± 0.011	0.926 ± 0.084	0.988 ± 0.011	0.98 ± 0.008	0.973 ± 0.015
90	RMSE ± STD	4.038 ± 0.75	4.341 ± 1.088	3.946 ± 1.177	6.377 ± 1.536	7.11 ± 2.838
	R^2 ± STD	0.982 ± 0.008	0.98 ± 0.014	0.989 ± 0.006	0.977 ± 0.012	0.972 ± 0.02
120	RMSE ± STD	6.385 ± 1.106	3.131 ± 0.889	6.001 ± 1.486	6.325 ± 1.42	7.143 ± 1.101
	R^2 ± STD	0.952 ± 0.021	0.977 ± 0.008	0.977 ± 0.014	0.981 ± 0.011	0.983 ± 0.008

6.6 DISCUSSION

This chapter presented a proposal subject-specific model able to predict EMG signals of five muscles during the plantar-dorsiflexion ankle movement, often used in rehabilitation treatments. The quite promising results presented in this work on six different healhty subjects underline the importance to calibrate a specific model for each subject. This led us to expect a successful application also for ill-conditioned patients since the model will be calibrated considering their own EMG signals. The good accuracy shown by the experimental results is promising for the future steps of this research. The possibility to use the predicted EMG as input for an EMG-driven neuromusculoskeletal model, that could be used to develop physiological control strategies, removes the need of trained personnel for the placement of EMG sensors. Moreover,including some special session in the patient treatment to recalibrate the EMG model, the possibility of a real subject monitoring is still available. In this context, future work will focus on comparing neuromusculoskeletal model outputs obtained using as input the predicted EMGs for other typical rehabilitation movement such as knee flexion-extension.

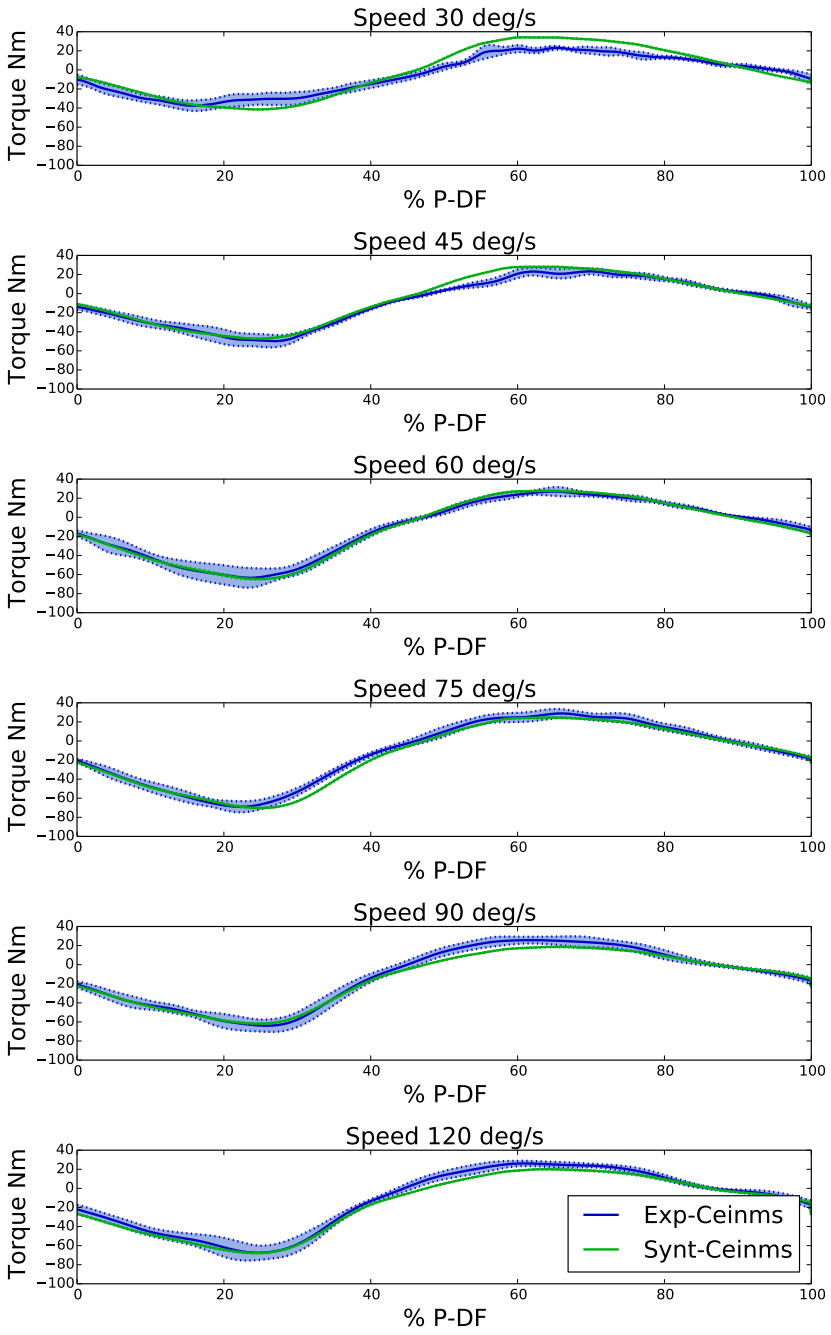

Figure 38: Comparison between estimated torques by CEINMS, with synthesized EMG signals (green line) and experimental EMGs (blue line) as input for the subject 03 reported as a percentage of the P-DF cycle at each speed. The light areas reports the $\pm$ STD of the estimated torque values by CEINMS with the experimental EMGs as input.

7

CONCLUSION

Research on rehabilitation robotic devices has always been a central topic for the robotics research community. The core challenge is to design the wearable system where the user is actively participating in the control loop. This requires the design of effective strategies for interfacing the wearable robot to its user, understanding his/her intentions, in order to realize a symbiotic collaboration. A central problem to be solved to enable this collaboration how to evaluate the emerging interaction during the human-robot movement. Indeed, this emerging dynamic interaction modifies the standalone behavior of both the human and the device, realizing a mutual modulation of their internal parameters. The capability of predicting this interaction would be useful to design better devices and increase rehabilitation treatment effectiveness.

This thesis proposes a new approach to tackle this problem through a Multi-Level Model solution that decomposes the main problem in three cooperation sub-levels: Human level, Robot Level, Boundary Level. Human Level and Robot Level represent, respectively, human and robot contributions to the movement. The Human Level model the internal steps, starting from the neural activities and ending to muscle forces and joint moments. The Robot Level has dinamically reproduces the robot assistive device, including its dynamic properties, such as bodies mass and inertial matrix, actuators characteristics and their control strategy. The Boundary Level models how the mechanical power is transferred between Human and Robot Level, providing an accurate and reliable estimation of the physical interaction. Since the cooperation movement is expressed at the Boundary Level, it has to include also the non-idealities (such as dissipative forces). The Multi-Level Modeling Approach is a general solution, potentially, each human robot movement cooperation can be modeled following the proposed decomposition. In the same way, also the emerging challenges of the approach is quite general and they can be faced and solved using alternative strategies.

The implementation of the Multi-Level Modeling Approach presents several challenges which were faced and solved in this thesis. The first challenge was to define a tool which could effectively implement the dynamic simulation of the three Levels (Ch. 2). OpenSim [73] was the selected option to be the common software platform in which develop our proposed Multi-Level Model of the human robot movement cooperation. While dynamic simulation of human movement was already well validated in OpenSim, simulation of robotic devices needed fur-

ther analysis. OpenSim was demonstrated to be accurate and reliable as multibody system simulator (Sec. 3.3), and also able to reproduce the robotic device control strategy in the simulation (Sec. 3.4).

The second challenge was to include in the system a way to estimate characteristics, intentions, and motor skills specific of the subject. Therefore we implemented the Human Level including a Neuromusculoskeltal (NMS) Model. We chose the Calibrated EMG-Informed Neuromusculoskeletal modeling Toolbox (CEINMS) [62], which is a state-of-the-art toolkit that implements an EMG-driven neuromusculoskeletal model, able to estimate joints torque and muscle forces, from the only inputs of kinematic and electromyographic (EMG) signals. Since EMG signals are a direct representation of the subject-specific intentions to activate his/her muscles, the Human Level movement contribution can be computed tracking user's internal transformations (Sec. 4.2 and Sec. 4).

The last challenge concerned the Boundary Level modeling. An accurate calibration of the contact model is mandatory to reproduce the interaction forces at the Boundary Level. Since these forces could be small in magnitude and quite instantaneous (Sec. 2.3.3) we tested the contact model already implemented in OpenSim individuating a similar situation. Using an optimization algorithm we were able to calibrate the contact model, and then reproduce experimental measured forces (Sec. 5.1).

The integration of these three levels (Human, Robot, and Boundary) using the chosen and tested solutions, results in an unique simulation platform able to reproduce the interactions occurring in a human robot movement cooperation. To better clarify how the proposed solution could be integrated in a Multi-Level Model System, next section present a case study of human robot cooperation to perform an ankle plantar-dorsiflexion (P-DF) that we are currently studying. The human is interacting with a dynanometer system (Fig. 39). The complexity of the problem required to define a first study with a setup simpler than a wearable robot but still representative of the whole problem. Therefore, we designed a experiment where the human is interacting with a dynanometer system to perform a P-DF cyclic movement, acquiring different data to calibrate our proposed simulator system.

7.1 MULTI-LEVEL MODEL APPROACH: A CASE STUDY

Development and application of the proposed Multi-Level Model approach is presented through a case study: modeling the ankle of a user performing a plantar dorsiflexion on a dynanometer device. In the following, we describe the data already collected to reproduce this simplify human robot movement cooperation in our system. The experiment required six healty subject to perform an ankle P-DF on a Biodex dynanometer System 3 Pro (S3P) (Biodex Medical System, USA)

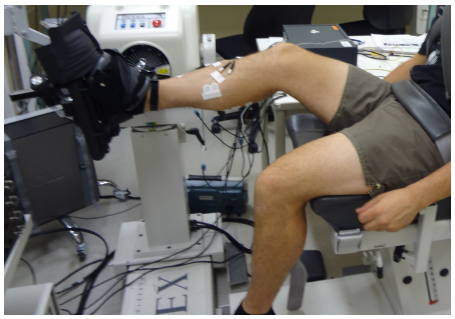

(a)

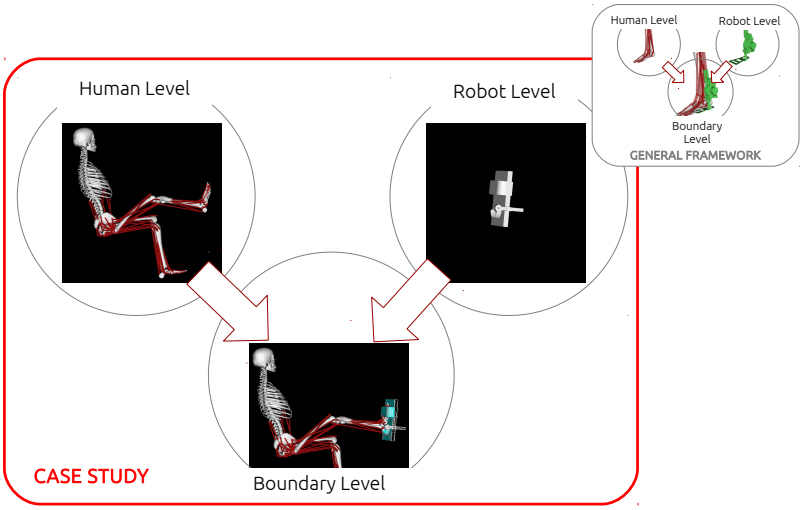

(b)

Figure 39: The integration of the system and its application to reproduce the presented case study: (a) a subject is interacting with a SP3 performing a P-DF. (b) The Multi-Level Model approach models Human and Robot Level separately. Then, modeling the Boundary Level, the integration is able to reproduce the mechanical power transmission during their cooperation.

at six different speeds imposed by the S3P. The subjects performed the movement spanning the 80% of their range of motion while trying to express their maximum ankle torques. EMG signals of five main involved muscle (Gastrocnemius Lateralis (GASL), Gastrocnemius Medialis (GASM), Soleus (SOL), Peroneus Longus (PER), Tibialis Anterior (TIB)) were collected (OT Bioelettronica, Italy), as well as kinematics and torque data (S3P). The target is to simulate this setup following the proposed Multi-level Modeling approach. Additional data were collected to calibrate the system components parameters.

Human Level requires the calibration of CEINMS, which is mandatory to include in our system the specific subject contribution to the movement. Subjects anthropometric data were obtained through a static acquisition performed using a motion analysis system with eight infrared digital video cameras at 256 Hz (Oqus 300, Qualisys, Gothenburg, Sweden). During the static acquisition the three-dimension location of 12 retro-reflective markers placed on the subjects' body was recorded. Markers placement was decided following the protocol used in [26]. We used this set of data in OpenSim to scale a generic human lower limbs model to the subject-specific's geometrical characteristics. After that, CEINMS could be calibrated to match the experimental subject joint moments and obtain an accurate estimation of user's contribution to the movement.

For Robot Level a set of data was collected using the S3P device with only the ankle support attached to the dynanometer system. This data set was used to validate the dynamic model of the attachment and to confirm the precision of the implemented controller.

Finally, Boundary Level needs data for the calibration of the contact model. Dara were acquired during a P-DF movement when the subject is fully passive and the movement is drive by the S3P. Monitory of the EMG signals confirms the passive condition of the user. The S3P measures a torque resulting from three components: torque to move the S3P ankle attachment, torque to move the passive subject's ankle, and interaction torque. The first two component could be estimated by an OpenSim simulation of foot and the ankle attachment. Therefore, an estimation of the interaction torque could be obtained removing the previous two torque, from the measured one. Finally, this interaction torque could be used to calibrate the parameters of the contact model.

These measurement and calibration steps lead to a fully calibrated Multi-Level Modeling system, that should reproduce data from the real experimental setup.

Preliminary investigation on the results coming from the experimental modeling has highligthed the foundamental role of the contact model calibration. Indeed, an accurate and reliable direct measurement of the interaction force is still missing but preliminary results show that it is required to better understand, reproduce, and estimate these emerging forces. With the aim of collecting contact information

to validate the interaction model, Sec. 7.2 introduces our future work on the development of a targeted force sensor able to measure the interaction forces on the supporting cuffs.

7.2 OPEN CHALLENGES AND FUTURE WORKS

The Boundary Level is introduced in our proposed framework to estimate the mechanical power transfer between Human and Robot Level. This is achieved including in the system a contact model. As already highlighted (Sec. 2.3.3) the success of contact modeling the depend on a careful calibration of its parameters that allow an accurate and reliable estimation of the emerging contact forces during the human robot movement cooperation. While preliminary results have been obtained in the test case presented in the previous section, a complete and reliable solution requires to introduce in the experimental setup a force sensors to direct measure the interaction forces.

Some preliminary work in this direction has been done by other research group. In [25] authors introduced a force sensor prototype to monitor pressure distribution on the physical human-robot interface of lower-limb exoskeletons. The sensor was developed to provide useful information for the assessment of safety and comfort of human-robot interaction. At the same time, it can be also provide the interaction forces required to successfully calibrated the Boundary Level contact modeling. An extension of the same work [31] suggests to perform the interaction forces measurement inserting the force sensors in the exoskeleton cuffs. Despite these sensors proved to give accurate, redundant and reliable measurements of the interaction force, they are too complex to be successfully modeled in our system. This is mainly due to the flexible material used for sensor case. Moreover, this kind of sensors are still not commercialized.

These considerations lead us to propose a new interaction forces sensor which is simpler to model. This sensor will be composed of two force sensors (FlexiForce, Tekscan, USA) [93], introduced at the extremity of two rigid plastic supports. An array of these sensors will be insert in the supporting cuffs, providing the interaction data that we need to calibrate the Boundary Level model.

Time limit of this thesis makes impossible to present first data from these sensors. However, the design is already completed and its first implementation is in process. Their successful characterization and validation will allow to calibrate the contact model of the Boundary Level, and finalize the implementation of the Multi-Level Modeling approach to reproduce the experiment data acquired with the exoskeleton and therefore enabling the prediction of the human robot interaction.

BIBLIOGRAPHY

[1] P. Agarwal, M.S. Narayanan, L. Lee, F. Mendel, and V.N. Krovi. Simulation-based design of exoskeletons using musculoskeletal analysis. In *Design Eng. Tech. and Computer and Inf. 2010 ASME Int. Conf. on*, pages 1357 – 1364. ASME, 2010.

[2] P. Agarwal, P. Kuo, R.R. Neptune, and A.D. Deshpande. A novel framework for virtual prototyping of rehabilitation exoskeletons. In *Rehab. Robotics (ICORR), 2013 IEEE Int. Conf. on*, pages 1 – 6. IEEE, 2013.

[3] Aldebaran. Aldebaran Homepage, 2015. URL `https://www.aldebaran.com/`. Online; accessed January 2015.

[4] D. Amarantini and L. Martin. A method to combine numerical optimization and emg data for the estimation of joint moments under dynamic conditions. *J. of Biomech.*, 37(9):1393 – 1404, 2004.

[5] Balance Project. Balance Homepage, 2015. URL `http://www.balance-fp7.eu/`. Online; accessed January 2015.

[6] E. Bayo and A. Avello. Singularity-free augmented lagrangian algorithms for constrained multibody dynamics. *Nonlinear Dyn.*, 5(2):209 – 231, 1994.

[7] BioMot Project. BioMot Homepage, 2015. URL `http://www.biomotproject.eu/`. Online; accessed January 2015.

[8] J.A. Blaya and H. Herr. Adaptive control of a variable-impedance ankle-foot orthosis to assist drop-foot gait. *Neural Sys. and Rehab. Eng., IEEE Trans. on*, 12(1):24 – 31, 2004.

[9] M. Bortole and J.L. Pons. Development of a exoskeleton for lower limb rehabilitation. In *Converging Clinical and Eng. Research on Neurorehab.*, pages 85 – 90. Springer, 2013.

[10] M. Bouri, Y. Stauffer, C. Schmitt, Y. Allemand, S. Gnemmi, R. Clavel, P. Metrailler, and R. Brodard. The walktrainer: a robotic system for walking rehabilitation. In *Robotics and Biomimetics, IEEE Int. Conf. on*, pages 1616 – 1621. IEEE, 2006.

[11] M. Bouzit, G. Burdea, G. Popescu, and R. Boian. The rutgers master ii-new design force-feedback glove. *Mechatronics, IEEE/ASME Trans. on*, 7(2):256 – 263, 2002.

[12] R. Bricard. Mémoire sur la théorie de l'octaèdre articulé. *J. de Mathématiques pures et appliquées*, pages 113 – 148, 1897.

[13] T.S. Buchanan, D.G. Lloyd, K. Manal, and T.F. Besier. Neuromusculoskeletal modeling: estimation of muscle forces and joint moments and movements from measurements of neural command. *J. Applied Biomech.*, 20(4):367, 2004.

[14] M.C. Carrozza, B. Massa, P. Dario, M. Zecca, S. Micera, and P. Pastacaldi. A two dof finger for a biomechatronic artificial hand. *Tech. and Health Care*, 10(2):77 – 89, 2002.

[15] L. Chiari, U.D. Croce, A. Leardini, and A. Cappozzo. Human movement analysis using stereophotogrammetry: Part 2: Instrumental errors. *Gait & Posture*, 21(2):197 – 211, 2005.

[16] K. Cho, Y. Kim, D. Yi, M. Jung, and K. Lee. Analysis and evaluation of a combined human–exoskeleton model under two different constraints condition. *Human Simulation 2012 Int. Summit on*, 2012.

[17] J. Cholewicki, S.M. McGill, and R.W. Norman. Comparison of muscle forces and joint load from an optimization and emg assisted lumbar spine model: towards development of a hybrid approach. *J. of Biomech.*, 28(3):321 – 331, 1995.

[18] J.J. Collins. The redundant nature of locomotor optimization laws. *J. Biomech.*, 28(3):251 – 267, 1995.

[19] Gery Colombo, Matthias Joerg, Reinhard Schreier, Volker Dietz, et al. Treadmill training of paraplegic patients using a robotic orthosis. *J. of Rehab. Research and Revelopment*, 37(6):693 – 700, 2000.

[20] Nvidia Corporation. PhysX Homepage, 2015. URL `http://www.geforce.com/hardware/technology/physx`. Online; accessed January 2015.

[21] R. Cromwell, A.B. Schultz, R. Beck, and D. Warwick. Loads on the lumbar trunk during level walking. *J. of Orthopaedic Research*, 7(3):371 – 377, 1989.

[22] Cyberlegs Project. Cyberlegs Homepage, 2015. URL `http://www.cyberlegs.eu/`. Online; accessed January 2015.

[23] M. Dam, P. Tonin, S. Casson, M. Ermani, G. Pizzolato, V. Iaia, and L. Battistin. The effects of long-term rehabilitation therapy on poststroke hemiplegic patients. *Stroke*, 24(8):1186 – 1191, 1993.

[24] J. de Jalón and E. Bayo. Kinematic and dynamic simulation of multibody systems. *Mech. Eng.*, 1994.

[25] S.MmM. De Rossi, N. Vitiello, T. Lenzi, R. Ronsse, B. Koopman, A. Persichetti, F.abrizio Vecchi, A. Jan Ijspeert, H. Van der Kooij, and M.C. Carrozza. Sensing pressure distribution on a lower-limb exoskeleton physical human-machine interface. *Sensors*, 11 (1):207 – 227, 2010.

[26] S. Del Din, E. Carraro, Z. Sawacha, A. Guiotto, L. Bonaldo, S. Masiero, and C. Cobelli. Impaired gait in ankylosing spondylitis. *Med. & Biological Eng. & Computing*, 49(7):801 – 809, 2011.

[27] S.L. Delp, F.C. Anderson, A.S. Arnold, P. Loan, A. Habib, C.T. John, E. Guendelman, and D.G. Thelen. Opensim: open-source software to create and analyze dynamic simulations of movement. *Biomed. Eng., IEEE Trans. on*, 54(11):1940 – 1950, 2007.

[28] J.T. Dennerlein. Finger flexor tendon forces are a complex function of finger joint motions and fingertip forces. *J. of Hand Therapy*, 18(2):120 – 127, 2005.

[29] I. Díaz, Jorge J. Gil, and E. Sánchez. Lower-limb robotic rehabilitation: literature review and challenges. *J. of Robotics*, 2011, 2011.

[30] G.J. Dick and E.A. Edwards. Human bipedal locomotion device, may 1991. US Patent 5,016,869.

[31] M. Donati, N. Vitiello, S.M.M. De Rossi, T. Lenzi, S. Crea, A.o Persichetti, F. Giovacchini, B. Koopman, J. Podobnik, M. Munih, et al. A flexible sensor technology for the distributed measurement of interaction pressure. *Sensors*, 13(1):1021 – 1045, 2013.

[32] T.W. Dorn, A.G. Schache, and M.G. Pandy. Muscular strategy shift in human running: dependence of running speed on hip and ankle muscle performance. *J. Exp. Biol.*, 215(11):1944 – 1956, 2012.

[33] Exo-Legs Project. Exo-Legs Homepage, 2015. URL `http://www.exo-legs.org`. Online; accessed January 2015.

[34] Erwin Fehlberg. Low-order classical runge-kutta formulas with stepsize control and their application to some heat transfer problems. Nasa Technical Report, 1969.

[35] D.P. Ferris, K.E. Gordon, G.S. Sawicki, and A. Peethambaran. An improved powered ankle-foot orthosis using proportional myoelectric control. *Gait & posture*, 23(4):425 – 428, 2006.

[36] C. Fleischer and G. Hommel. A human-exoskeleton interface utilizing electromyography. *Robotics, IEEE Trans. on*, 24(4):872 – 882, 2008.

[37] B.C. Fleming and B.D. Beynnon. In vivo measurement of ligament tendon strains and forces: a review. *Annals of Biomed. Eng.*, 32(3):318 – 328, 2004.

[38] J. Freivogel, S. Mehrholz, T. Husak-Sotomayor, and D. Schmalohr. Gait training with the newly developed'lokohelp'-system is feasible for non-ambulatory patients after stroke, spinal cord and brain injury. a feasibility study. *Brain Injury*, 22(7 - 8):625 – 632, 2008.

[39] R.I. Gamow and H.M. Herr. Shoe and foot prosthesis with bending beam spring structures, feb 2000. US Patent 6,029,374.

[40] Gazebo Opensource Project. Gazebo Homepage, 2015. URL `http://www.http://gazebosim.org`. Online; accessed January 2015.

[41] R. Gelabert, M. Moreno, J.M. Lluch, A. Lledós, V. Pons, and D.M. Heinekey. Synthesis and properties of compressed dihydride complexes of iridium: Theoretical and spectroscopic investigations. *J. of the American Chem. Soc.*, 126(28):8813 – 8822, 2004.

[42] K. Genovese, L. Lamberti, and C. Pappalettere. Improved global-local simulated annealing formulation for solving non-smooth engineering optimization problems. *Int. J. of Solids and Structures*, 42(1):203 – 237, 2005.

[43] M González, D Dopico, U Lugrís, and J Cuadrado. A benchmarking system for mbs simulation software: Problem standardization and performance measurement. *Multibody System Dynamics*, 16(2):179 – 190, 2006.

[44] M. González, F. González, A. Luaces, and J. Cuadrado. A collaborative benchmarking framework for multibody system dynamics. *Eng. with Computers*, 26(1):1 – 9, 2010.

[45] S. Grosu, P. Cherelle, C. Verheul, B. Vanderborght, and D. Lefeber. Case study on human walking during wearing a powered prosthetic device: Effectiveness of the system human-robot. *Advances in Mech. Eng.*, 2014, 2014.

[46] M. Grübler. *Allgemeine Eigenschaften der zwangläufigen ebenen kinematischen Ketten*. L. Simion, 1884.

[47] A.C. Guimaraes, W. Herzog, M. Hulliger, Y.T. Zhang, and S. Day. Effects of muscle length on the emg-force relationship of the cat soleus muscle studied using non-periodic stimulation of ventral root filaments. *J. of Exp. Biology*, 193(1):49 – 64, 1994.

[48] T. Hayashi, H. Kawamoto, and Y. Sankai. Control method of robot suit hal working as operator's muscle using biological and dynamical information. In *Inte. Robots and Sys. (IROS) 2005 IEEE/RSJ Int. Conf. on*, pages 3063 – 3068. IEEE, 2005.

[49] H.J. Hermens, B. Freriks, R. Merletti, D. Stegeman, J. Blok, G. Rau, C. Disselhorst-Klug, and G. Hägg. *European recommendations for surface electromyography*. Roessingh Research and Development The Netherlands, 1999.

[50] S. Hesse, D. Uhlenbrock, et al. A mechanized gait trainer for restoration of gait. *J. of Rehab. Research and Development*, 37(6): 701 – 708, 2000.

[51] A.V. Hill. The heat of shortening and the dynamic constants of muscle. *Proceedings of the Royal Society of London. Series B, Biological Sciences*, pages 136 – 195, 1938.

[52] J. Hitt, A.M. Oymagil, T. Sugar, K. Hollander, A. Boehler, and J. Fleeger. Dynamically controlled ankle-foot orthosis (DCO) with regenerative kinetics: Incrementally attaining user portability. In *Robotics and Automation, 2007. IEEE Int. Conf. on*, apr. 2007.

[53] A.L. Hof and J.W. Van den Berg. Emg to force processing i: an electrical analogue of the hill muscle model. *J. of Biomech.*, 14 (11):747 – 758, 1981.

[54] P.A. Huijing. Important experimental factors for skeletal muscle modelling: non-linear changes of muscle length force characteristics as a function of degree of activity. *European J. of Morphology*, 34(1):47 – 54, 1995.

[55] G. Jacucci, A. Spagnolli, J. Freeman, and L. Gamberini. Symbiotic interaction: a critical definition and comparison to other human-computer paradigms. In *Symbiotic Interaction*, pages 3 – 20. Springer, 2014.

[56] S. Jezernik, G. Colombo, T. Keller, H. Frueh, and M. Morari. Robotic orthosis lokomat: A rehabilitation and research tool. *Neuromodulation: Tech. at the Neural Interface*, 6(2):108 – 115, 2003.

[57] H. Kawamoto and Y. Sankai. Power assist system HAL-3 for gait disorder person. In *Computers helping people with special needs*, pages 196 – 203. Springer, 2002.

[58] P.V. Komi, S. Fukashiro, and M. Järvinen. Biomechanical loading of achilles tendon during normal locomotion. *Clinics in Sports Medicine*, 11(3):521 – 531, 1992.

[59] T.K.K. Koo and A.F.T. Mak. Feasibility of using emg driven neuromusculoskeletal model for prediction of dynamic movement of the elbow. *J. of Electromyography and Kinesiology*, 15(1):12 – 26, 2005.

[60] G. Kwakkel, R. van Peppen, R.C. Wagenaar, S.W. Dauphinee, C. Richards, A. Ashburn, K. Miller, N. Lincoln, C. Partridge, I. Wellwood, et al. Effects of augmented exercise therapy time after stroke a meta-analysis. *Stroke*, 35(11):2529 – 2539, 2004.

[61] A. Leardini, Z. Sawacha, G. Paolini, S. Ingrosso, R. Nativo, and M.G. Benedetti. A new anatomically based protocol for gait analysis in children. *Gait & posture*, 26(4):560 – 571, 2007.

[62] D. Lloyd, M. Reggiani, C. Pizzolato, E. Ceseracciu, and M. Sartori. CEINMS Project Overview, 2015. URL `https://simtk.org/home/ceinms`. Online; accessed January 2015.

[63] D.G. Lloyd and T.F. Besier. An EMG-driven musculoskeletal model to estimate muscle forces and knee joint moments in vivo. *J. Biomech.*, 36(6):765 – 776, 2003.

[64] D.G Lloyd and T.S Buchanan. A model of load sharing between muscles and soft tissues at the human knee during static tasks. *J. of Biomech. Eng.*, 118(3):367 – 376, 1996.

[65] D.G. Lloyd, T.F. Besier, C.R. Winby, and T.S. Buchanan. Neuromusculoskeletal modelling and simulation of tissue load in the lower extremities. *Handbook Biomech. and Human Movement Science*, pages 3 – 17, 2008.

[66] K. Manal and T.S. Buchanan. A one-parameter neural activation to muscle activation model: estimating isometric joint moments from electromyograms. *J. of Biomech.*, 36(8):1197 – 1202, 2003.

[67] K. Manal, R.V. Gonzalez, D.G. Lloyd, and T.S. Buchanan. A real-time emg-driven virtual arm. *Computers in Biology and Medicine*, 32(1):25 – 36, 2002.

[68] S.G. McLean, A. Su, and A.J. van den Bogert. Development and validation of a 3-d model to predict knee joint loading during dynamic movement. *J. of Biomech. Eng.*, 125(6):864 – 874, 2003.

[69] J.C. Moreno, F. Brunetti, E. Rocon, and J.L. Pons. Immediate effects of a controllable knee ankle foot orthosis for functional compensation of gait in patients with proximal leg weakness. *Medical & biological engineering & computing*, 46(1):43 – 53, 2008.

[70] J.C. Moreno, F. Brunetti, E. Navarro, A. Forner-Cordero, and J.L. Pons. Analysis of the human interaction with a wearable lower-limb exoskeleton. *Appl. Bionics and Biomech.*, 6(2):245 – 256, 2009.

[71] N. Neckel, M. Pelliccio, D. Nichols, and J. Hidler. Quantification of functional weakness and abnormal synergy patterns in the lower limb of individuals with chronic stroke. *J. of NeuroEng. Rehab.*, 3(1):17, 2006.

[72] R.R. Neptune, S.A. Kautz, and F.E. Zajac. Contributions of the individual ankle plantar flexors to support, forward progression and swing initiation during walking. *J. Biomech.*, 34(11):1387 – 1398, 2001.

[73] OpenSim. OpenSim - Supports, Events, and Sources, 2015. URL `http://opensim.stanford.edu/support`. Online; accessed January 2015.

[74] M.G. Pandy. Computer modeling and simulation of human movement. *Annual review of Biomed. Eng.*, 3(1):245–273, 2001.

[75] J. Patton, D.A. Brown, M. Peshkin, J.J. Santos-Munné, A. Makhlin, E. Lewis, E.J. Colgate, and D. Schwandt. Kineassist: design and development of a robotic overground gait and balance therapy device. *Topics in Stroke Rehab.*, 15(2):131 – 139, 2008.

[76] W. Pentland, M.A. McColl, and C. Rosenthal. The effect of aging and duration of disability on long term health outcomes following spinal cord injury. *Spinal Cord*, 33(7):367 – 373, 1995.

[77] S.J. Piazza and S.L. Delp. The influence of muscles on knee flexion during the swing phase of gait. *J. of Biomech.*, 29(6):723 – 733, 1996.

[78] S.J. Piazza and S.L. Delp. Three-dimensional dynamic simulation of total knee replacement motion during a step-up task. *J. of Biomech. Eng.*, 123(6):599 – 606, 2001.

[79] J.L. Pons, A. Forner-Cordero, E. Rocon, and J.C. Moreno. Mechatronics and bioinspiration in actuator design and control. *Appl. Bionics and Biomech.*, 5(3):127 – 133, 2008.

[80] J.R. Potvin, R.W. Norman, and S.M. McGill. Mechanically corrected emg for the continuous estimation of erector spinae muscle loading during repetitive lifting. *European J. of applied Physiology and Occupational Physiology*, 74(1-2):119 – 132, 1996.

[81] H2R Project. H2R Homepage, 2015. URL `http://www.h2rproject.eu/`. Online; accessed January 2015.

[82] B. Ravary, P. Pourcelot, C. Bortolussi, S. Konieczka, and N. Crevier-Denoix. Strain and force transducers used in human and veterinary tendon and ligament biomechanical studies. *Clinical Biomechanics*, 19(5):433 – 447, 2004.

[83] A. Roy, H.I. Krebs, S.L. Patterson, T.N. Judkins, I. Khanna, L.W. Forrester, R.M Macko, and N. Hogan. Measurement of human ankle stiffness using the anklebot. In *Rehab. Robotics (ICORR) 2007 IEEE 10th Int. Conf. on*, pages 356 – 363. IEEE, 2007.

[84] J.A. Saglia, N.G. Tsagarakis, J.S. Dai, and D.G. Caldwell. A high performance redundantly actuated parallel mechanism for ankle rehabilitation. *Int. J. of Robotics Res.*, 2009.

[85] M. Sartori, M. Reggiani, D. Farina, and D.G. Lloyd. EMG-driven forward-dynamic estimation of muscle force and joint moment about multiple degrees of freedom in the human lower extremity. *PloS one*, 7(12):e52618, 2012.

[86] M. Sartori, M. Reggiani, E. Pagello, and D.G. Lloyd. Modeling the human knee for assistive technologies. *IEEE Trans. on Biomedical Eng.*, 59(9):2642–2649, 2012.

[87] W. Schiehlen. Multibody system dynamics: roots and perspectives. *Multibody System Dyn.*, 1(2):149 – 188, 1997.

[88] C. Schmitt and P. Métrailler. The motion maker: a rehabilitation system combining an orthosis with closed-loop electrical muscle stimulation. In *8th Vienna Int. Workshop on Funct. Elect. Stimulation*, pages 117 – 120, 2004.

[89] SimTK Project. Simbody Homepage, 2015. URL `https://simtk.org/home/simbody`. Online; accessed January 2015.

[90] MSC Software. Admas Homepage, 2015. URL `http://www.mscsoftware.com/product/adams`. Online; accessed January 2015.

[91] M. Sumida, M. Fujimoto, A. Tokuhiro, T. Tominaga, A. Magara, and R. Uchida. Early rehabilitation effect for traumatic spinal cord injury. *Arch. Physical Med. and Rehab.*, 82(3):391 – 395, 2001.

[92] Symbitron Project. Symbitron Homepage, 2015. URL `http://www.symbitron.eu/`. Online; accessed January 2015.

[93] Tekscan. FlexiForce Sensors, 2015. URL `http://www.tekscan.com/flexible-force-sensors`. Online; accessed January 2015.

[94] D.G. Thelen and F.C. Anderson. Using computed muscle control to generate forward dynamic simulations of human walking from experimental data. *J. Biomech.*, 39(6):1107 – 1115, 2006.

[95] D.G. Thelen, F.C. Anderson, and S.L. Delp. Generating dynamic simulations of movement using computed muscle control. *J. of Biomech.*, 36(3):321 – 328, 2003.

[96] D. Tsirakos, V. Baltzopoulos, and R. Bartlett. Inverse optimization: functional and physiological considerations related to the force-sharing problem. *Critical Reviews in Biomed. Eng.*, 25(4-5), 1997.

[97] Standford University. OpenSim Developer's Guide, 2015. URL `http://simtk-confluence.stanford.edu:8080/display/OpenSim/Developer%27s+Guide`. Online; accessed January 2015.

[98] Standford University. OpenSim User's Guide, 2015. URL `http://simtk-confluence.stanford.edu:8080/display/OpenSim/User%27s+Guide`. Online; accessed January 2015.

[99] R.P.S. Van Peppen, G. Kwakkel, S. Wood-Dauphinee, H.J.M. Hendriks, P.J. Van der Wees, and J. Dekker. The impact of physical therapy on functional outcomes after stroke: what's the evidence? *Clinical rehabilitation*, 18(8):833 – 862, 2004.

[100] C.L. Vaughan, B.L. Davis, and J.C. O'connor. *Dynamics of human gait*. Human Kinetics Publishers Champaign, Illinois, 1992.

[101] J.F. Veneman, R. Kruidhof, E.E.G. Hekman, R. Ekkelenkamp, E.H.F. Van Asseldonk, and H. van der Kooij. Design and evaluation of the lopes exoskeleton robot for interactive gait rehabilitation. *IEEE Trans. Neural Syst. Rehabil. Eng.*, 15(3):379 – 386, 2007.

[102] M. Vivian, M. Reggiani, J.C. Moreno, J.L. Pons, D. Farina, and M. Sartori. A dynamically consistent model of a motorized ankle-foot orthosis. In *Neural Eng. (NER), 2013 6th Int. IEEE/EMBS Conf. on*, pages 1558 – 1561. IEEE, 2013.

[103] M. Vivian, M. Reggiani, and M Sartori. Experimentally-based optimization of contact parameters in dynamics simulation of humanoid robots. In *ICRA*, pages 1643 – 1648, 2013.

[104] M. Vivian, L. Tagliapietra, M. Sartori, and M. Reggiani. Dynamic simulation of robotic devices using the biomechanical simulator OpenSim. In *Intell. Aut. Sys. (IAS), 2015 13th Int. Conf. on*. IAS, 2014.

[105] D.T. Wade and R. Hewer. Functional abilities after stroke: measurement, natural history and prognosis. *J. Neurology, Neurosurgery & Psychiatry*, 50(2):177 – 182, 1987.

[106] S. Wernig, A. Müller, A. Nanassy, and E. Cagol. Laufband therapy based on rules of spinal locomotion is effective in spinal cord injured persons. *European J. of Neuroscience*, 7(4):823 – 829, 1995.

[107] D.A. Winter. *Kinematics*. Wiley Online Library, 2005.

[108] G.T. Yamaguchi and F.E. Zajac. Restoring unassisted natural gait to paraplegics via functional neuromuscular stimulation: a computer simulation study. *Biomed. Eng., IEEE Trans. on*, 37(9): 886 – 902, 1990.

[109] F.E. Zajac. Muscle and tendon: properties, models, scaling, and application to biomechanics and motor control. *Critical Reviews in Biomed. Eng.*, 17(4):359 – 411, 1988.